

6815

INVESTIGATION OF PARAMETERS
CONTROLLING METAL POWDER PRODUCTION
BY CENTRIFUGAL ATOMIZATION

Ph. D. THESIS
in
Mechanical Engineering
Middle East Technical University

T. C.
TÜRKİYE KÜLTÜR BAKANLIĞI
Dokümantasyon Merkezi

By
Cengiz DOĞAN
September, 1989

Approval of the Graduate School of Natural and Applied Sciences

R. Seve

Prof. Dr. O. Alpay ANKARA

Director

I certify that I have read this thesis and that in my opinion it is fully adequate, in scope and quality, as a dissertation for the degree of Doctor of Philosophy.

Sedat Baysec

Assoc. Prof. Dr. Sedat BAYSEC

Chairman of the Department

We certify that I have read this thesis and that in our opinion it is fully adequate, in scope and quality, as a dissertation for the degree of Doctor of Philosophy.

S. Saritaş

Assoc. Prof. Dr. Süleyman SARITAŞ

Supervisor

Examining Committee in Charge :

Prof. Dr. Eti UYGUR (Chairman)

Prof. Dr. Zeki ÇİZMECİOĞLU

Assoc. Prof. Dr. Süleyman SARITAŞ

S. Saritaş
S. Saritaş
S. Saritaş

ABSTRACT

INVESTIGATION OF PARAMETERS CONTROLLING METAL POWDER PRODUCTION BY CENTRIFUGAL ATOMIZATION

DOGAN, Cengiz

Ph. D. in Mechanical Engineering

Supervisor: Assoc. Prof. Dr. Suleyman SARITAS

September, 1989, 142 Pages.

The subject of the present investigation was to produce metal powders by centrifugal atomization technique.

Initially, centrifugal atomization and other powder production methods were reviewed to determine the factors that affect the characteristics of the metal powders produced.

An experimental centrifugal atomization set-up was designed and constructed. Rotating speed of atomizer disc, flow rate of liquid metal and temperature of the liquid metal can be adjusted at the required values in the set-up. In this way, the factors controlling the powder characteristics were investigated.

To investigate the effect of the disc shape and size on the powder characteristics, flat and cup shaped discs, which are generally used in the centrifugal atomization, and vaned discs were designed and constructed in different sizes and shapes.

About hundred runs were made on lead, aluminum and steels. The mean powder size of each run was determined by sieve analysis. Microstructural examination of the powders were made on optical microscopy.

The experimental results showed that, the set-up produced powders in the size range suitable for powder metallurgy applications. Small powders (less than 20 μm .) were spherical in shape which showed that solidification was completed in air before reaching to the water wall. Large powders were irregular in shape which means that solidification was completed in water wall.

The production rate of the set-up is very high. Especially, in the case of new developed vaned disc and lead atomization, production rate is 1000 kg/h. Mean size of the powder is 75 μm .

Key Words: Metal Powder, Centrifugal Atomization.

ÖZET

SANTRAFUJ ATOMİZASYON YONTEMIYLE METAL TOZU İMALATINA ETKİ EDEN FAKTORLERİN İNCELENMESİ

DOĞAN, Cengiz

Doktora Tezi; Makina Muhendisliği

Tez Yöneticisi: Doç. Dr. Süleyman SARITAŞ

Eylül, 1989, 142 Sayfa.

Bu araştırmanın amacı santrifuj atomizasyon tekniğiyle metal tozu imalatıdır.

Araştırmanın başlangıcında, santrifuj atomizasyon ve diğer metal tozu üretim yöntemleri hakkında literatur taraması yapılarak toz karakterlerine etki eden faktörler tesbit edildi.

Deneysel bir santrifuj atomizasyon düzenekinin tasarımı ve imalatı gerçekleştirildi. Düzenekte; disk dönüş hızı, sıvı metal akış hızı ve sıvı metal sıcaklığı istenilen değerlerde ayarlanabilir. Böylece, Toz karakterlerine etki eden faktörler incelendi.

Atomizasyon diskinin metal tozları üzerindeki etkisini incelemek için genel olarak kullanılan düz ve çanak disklere ilaveten kanallı disk modeli tasarlanarak çeşitli şekil ve ebatlarda imal edildi.

Kurşun, alüminyum ve çelikler üzerinde toplam yüz adet deney yapıldı. Üretilen tozlar elek analizinden geçirilerek ortalama toz büyüklükleri ve toz dağılımları incelendi. Tozlar metalografik yöntemlerle optik mikroskopta incelendi.

Deney neticeleri üretilen tozların, toz metallurji uygulamalarına uygun olduğunu göstermektedir. Küçük tozlar ($20 \mu\text{m}$ 'dan küçük) küresel şekildedirler. Bu onların su duvarına kavuşmadan havada katılaştıklarını göstermektedir. Büyük tozların şekilleri suda katılaşmadan dolayı karmaşıktır.

Düzenegin üretim hızı çok yüksektir. Özellikle, yeni geliştirilen kanallı disk ile kurşun atomizasyonunda 1000 kg/saat üretim hızına kavuşulmuştur. Tozların ortalama büyüklüğü $75 \mu\text{m}$ 'dir.

Anahtar Kelimeler: Toz Metal, Santrifuj Atomizasyon.

ACKNOWLEDGEMENTS

I would like to express my deepest gratitude to Assoc. Prof. Dr. Suleyman SARITAS for his patient supervision, valuable guidance, criticism and helpfull encouragement through out this thesis.

I wish to express sincere thanks to Mr. Ali OZAVCI, Ugur KEPEKCI, Nesimi AKSOY, Okkes KURTOGLU and other workshop personnel for their kind assistance during the production of the test rig.

TABLE OF CONTENTS

	Page
ABSTRACT	ii
OZET	iv
ACKNOWLEDGEMENTS	vi
TABLE OF CONTENTS	vii
LIST OF TABLES	xi
LIST OF FIGURES	xiii
NOMENCLATURE	xvi
CHAPTER	
1. INTRODUCTION	1
2. PRODUCTION OF METAL POWDERS	9
2.1 Introduction	9
2.2 Atomization	10
2.2.1 Two-Fluid Atomization	10
a) Gas Atomization	10
b) Water Atomization	12
2.3 Centrifugal Atomization	14
2.3.1 Rotating Disc Atomization	15
2.3.2 Rotating Electrode Process	15
2.4 Vacuum Atomization	16
2.5 Ultrasonic Atomization	16
2.6 Chemical Methods of Powder Production	19
2.6.1 Oxide Reduction	19
2.6.2 Precipitation From Solution	22
2.6.3 Thermal Decomposition	22
2.7 Milling of Brittle and Ductile Materials	23
2.8 Electrodeposition of Metal Powders	24
2.9 Comparison of Principal Methods of producing Metal Powders	25

3	CHARACTERIZATION AND TESTING OF METAL POWDERS	27
	3.1 Introduction	27
	3.2 Sampling	27
	3.3 Chemical Tests	29
	3.3.1 Hydrogen Loss Test	29
	3.3.2 Insoluble Matter Test	29
	3.4 Physical Tests	30
	3.4.1 Particle Size and Size Distribution	30
	a) Sieve Analysis	31
	b) Light Scattering	32
	c) Sedimentation	32
	d) Electrozone Size Analysis	33
	e) Optical Sensing Zone	33
	f) Microscopy and Image Analysis	34
	g) Fisher Sub-sieve Sizer	34
	3.4.2 Particle Shape of Metal Powder	34
	3.4.3 Surface Area, Density, And Porosity of Metal Powders	36
	a) Gas Absorption Method	37
	b) Permeametry	37
	c) Pycnometry	37
	d) Mercury Porosimetry	37
	3.4.4 Apparent Density of Metal Powders	38
	3.4.5 Tap Density of Metal Powders	39
	3.4.6 Flow Rate of Metal Powders	40
	3.4.7 Angle of Repose	42
	3.5 Tests Simulating the Behaviour of the Powder in Fabrication	42
	3.5.1 Compressibility of Metal Powders	42
	3.5.2 Green Strength of Compacted Metal Powders	43
	3.5.3 Dimensional Change of Sintered Metal Compacts	44
	3.6 Distinguishing Characteristics of Metal Powder	45

4.	CENTRIFUGAL ATOMIZATION	47
4.1	Introduction	47
4.2	Mechanisms of Atomization	48
4.2.1	Flat Disc Atomization	49
a)	Flow Over Flat Discs	53
4.2.2	Vaned Disc Atomization	55
a)	Flow Over a Vaned Disc	57
b)	Effect of Operating Variables on Droplet Size	63
4.2.2	Particle Shape	64
a)	Gas Cooling	65
b)	Water cooling	67
5.	DESIGN AND CONSTRUCTION OF EXPERIMENTAL SET-UP	69
5.1	Introduction	69
5.2	Design of the Melting Unit and the Tundish	70
5.3	Design of the Disc Drive System	74
a)	Air Turbines	74
b)	Constant Speed Electrical Motors With Gear-Box or Belt Pulley Arrangement	74
c)	High Speed Electrical Motors With Speed Control	75
5.4	Design of the Atomization Disc	77
6.	EXPERIMENTAL RESULTS	84
6.1	Introduction	84
6.2	Flat Disc Atomization	85
6.2.1	Flat Disc Atomization of Lead	85
6.2.2	Flat Disc Atomization of 12 % Mn Steel	89
6.3	Cup Shaped Disc Atomization of Lead	90
6.4	Vaned Disc Atomization	94
6.4.1	Vaned Disc Atomization of Lead	94
a)	Atomization at 24000 rpm	94
b)	Atomization at 19000 rpm	94
6.4.2	Vaned Disc Atomization of Aluminum	100
6.4.3	Vaned Disc Atomization of Steel 8640	105
6.5	Shape and Microstructural Analysis of the Powders	107

6.5.1 Shape Analysis of the Powders	107
6.5.2 Microstructure of the powders	109
6.6 Special Features Observed	111
6.6.1 Cavity	111
6.6.2 Collisions	115
6.6.3 Microhardnesses of Powders	121
7. DISCUSSION	122
7.1 Introduction	122
7.2 Flat Disc Atomization	123
7.3 Cup Shaped Disc Atomization	125
7.4 Vaned Disc Atomization	126
7.5 Shape Analysis of the Powders	129
CONCLUSIONS	133
FEATURE WORKS	135
REFERENCES	

LIST OF TABLES

Tables	Page
1.1 Comparison of Properties of Wrought and Powder Forged Steel	5
2.1 Comparison of Principal Commercial Methods of Producing Metal Powders	26
3.1 Information on Sieves of Use in Powder Metallurgy	
3.2 Some Distinguishing Characteristics of Metal Powders Made by Various Present Commercial Methods	31
4.1 Droplet Size Prediction For Smooth Flat Discs	46
4.2 Values of $X = r(Rw^2)$	56
6.1 The Powder Size Distribution of the Flat Disc Atomized Lead(Disc Speed = 19000 rpm, Disc Diameter = 32 mm)	86
6.2 The Powder Size Distribution of the Flat Disc Atomized Lead(Disc Speed = 24000 rpm, Disc Diameter = 32 mm)	87
6.3 The Powder Size Distribution of the Flat Disc Atomized 12 % Mn Steel(Disc Speed = 24000 rpm, Liquid metal temp. = 1750 °C, Metal flow rate = 200 g/s, Disc Diameter = 32 mm)	89
6.4 The Powder Size Distribution of the Cup Shaped Disc Atomized Lead(Disc Speed = 24000 rpm, Disc Diameter = 32 mm)	91
6.5 The Powder Size Distribution of the Cup Shaped Disc Atomized Lead(Disc Speed = 19000 rpm, Disc Diameter = 32 mm)	93
6.6 The Powder Size Distribution of the Vaned Disc Atomized Lead(Disc Speed = 24000 rpm, Disc Diameter = 32 mm, Vaned Number = 4)	95
6.7 The Powder Size Distribution of the Vaned Disc	

	Atomized Lead (Disc Speed = 19000 rpm, Disc Diameter = 32 mm, Vaned Number = 4)	96
6.8	The Powder Size Distribution of the Vaned Disc Atomized Aluminum	101
6.9	The Powder Size Distribution of the Vaned Disc Atomized Steel 8640 (Disc Speed = 24000 rpm, Liquid metal temp. = 1750 °C, Metal flow rate = 200 g/s, Disc Diameter = 32 mm)	105
6.10	Microhardness Test of the Steel Powders	121



LIST OF FIGURES

Figures		Page
1.1	Influence of Porosity on Mechanical Properties of Iron	4
1.2	The Effect of Porosity on the Fatigue Curves of Sintered Iron Parts	4
1.3	Powder-Forged Connecting-rod Fatigue Test Results With Drop-Forged Curves Superimposed	6
1.4	Comparative Trend of Iron Powder Consumption in the World	7
2.1	Diagrammatic View of Vertical and Horizontal Gas Atomizers	11
2.3	Schematic Diagram of Water Atomization	13
2.4	Schematic Diagram of Rotating Disc Atomization	15
2.5	Schematic Diagram of Rotating Electrode Process	16
2.6	Schematic Diagram of the Vacuum Atomization Process	17
2.7	Schematic of Ultrasonic Gas Atomization	18
2.8	Standard Free Energy of Formation of Metal Oxides	20
3.1	Sample Splitting Devices	28
3.2	Various Shapes of Powder Particles and Their Methods of Manufacture	35
3.3	Cross Sectional View of Hall Flowmeter	39
3.4	Diagram of Tapping Apparatus	40
3.5	Four Methods Used to Measure the Angle of Repose	42
4.1	Mechanism of Atomization	50
4.2	Mechanism of Atomization (represented photographically)	51
4.3	Atomization Mechanism For Rotating Discs	54
4.4	Liquid Flow to and From Edge of the Vaned Disc Atomizer	57

4.5	Flow of the Liquid Metal Through the Vane	59
4.6	Variation of the Particle Shape With Particle Size in Gas Atomization of Cast Iron	67
4.7	Fraction of Rough Particles F_i as a Function of Mean Particle Size in Water Atomization For 4620 Steel	68
5.1	Cross Sectional view of the Steel Tundish	72
5.2	Schemating Drawing of the Graphite Tundish	73
5.3	Speed Characteristics of the Main Drive Motor	76
5.4	Schematic Drawing of the Adapter	78
5.5	Detail Drawing of the Mandrel and its Mounting	79
5.6	Crass Sectional views of the Flat and Cup Shaped Discs	80
5.7	Assembly Drawing of a Vaned Disc Made From Graphite	80
5.8	Crass Sectional views of a Graphite Vaned Disc	81
5.9	Cross Sectional Drawing of the Set-Up	82
5.10	General View of the Set-Up	83
6.1	Powder Size Distribution of the Flat Disc Atomized Lead at the Optimum Conditions ($d_m = 119 \mu\text{m}$); $N = 24000 \text{ rpm}$, $T = 700 \text{ }^\circ\text{C}$, $Q = 75 \text{ g/s}$	87
6.2	The Effect of the Temperature and Flow Rate of the liquid Metal on the Powder Size of the Flat Disc Atomized Lead at the Disc Speed of: (a) $N = 24000 \text{ rpm}$, (b) $N = 19000 \text{ rpm}$	88
6.3	Powder Size Distribution of the Flat Disc Atomized 12 % Mn Steel ($d_m = 153 \mu\text{m}$) at $N = 24000 \text{ rpm}$, $T = 1750 \text{ }^\circ\text{C}$, $Q = 200 \text{ g/s}$	90
6.4	The Effect of the Temperature and Flow Rate of the liquid Metal on the Powder Size of the Cup Shaped Disc Atomized Lead at the Disc Speed of: (a) $N = 24000 \text{ rpm}$, (b) $N = 19000 \text{ rpm}$	92
6.5	Powder Size Distribution of the Cup Shaped Disc Atomized Lead at the Optimum Conditions ($d_m = 150 \mu\text{m}$); $N = 19000 \text{ rpm}$, $T = 700 \text{ }^\circ\text{C}$, $Q = 75 \text{ g/s}$	93

6.6	The Effect of the Temperature and Flow Rate of the liquid Metal on the Powder Size of the Vaned Disc Atomized Lead at the Disc Speed of: (a) $N = 24000$ rpm, (b) $N = 19000$ rpm	97
6.7	Powder Size Distribution of the Cup Shaped Disc Atomized Lead at the Optimum Conditions ($d_m = 119 \mu\text{m}$); $N = 24000$ rpm, $T = 550 \text{ }^\circ\text{C}$, $Q = 75 \text{ g/s}$	98
6.8	Cumulative Weight Percent Distributions of the Flat, Cup Shaped and Vaned Disc Atomized Lead	99
6.9	The Effect of the Disc Speed (rpm), Liquid Metal Temperature ($^\circ\text{C}$) and on the Mean Powder Size (μm) in Vaned Disc Atomized Aluminum	102
6.10	Powder Size Distribution of the Vaned Disc Atomized Aluminum at the Optimum Conditions ($d_m = 129 \mu\text{m}$); $N = 24000$ rpm, $T = 800 \text{ }^\circ\text{C}$	103
6.11	Cumulative Weight Percent Distributions of the Vaned Disc Atomized Aluminum	103
6.12	The Effect of Disc Peripheral Speed on the Mean Powder Size of the Atomized Aluminum	104
6.13	Powder Size Distribution of the Vaned Disc Atomized Steel 8640 ($d_m = 153 \mu\text{m}$) at $N = 24000$ rpm, $T = 1750 \text{ }^\circ\text{C}$, $Q = 200 \text{ g/s}$	106
6.14	Cumulative Weight Percent Distributions of the Flat, and Vaned Disc Atomized 12 % Mn Steel and Steel 8640	106
6.15	Transverse Sections of Aluminum Powders	107
6.16	Transverse Sections of lead Powders	108
6.17	Transverse Sections of Steel Powders	108
6.18	Microstructural Views of Aluminum Powders	109
6.19	Microstructural Views of Lead Powders	110
6.20	Microstructural Views of Steel 8640 Powders	110
6.21	Microstructural Views of 12 % Mn Steel Powders	111
6.22	General Cross Sectional Views of Aluminum Powders Contain Cavities	112

6.23	General Cross Sectional Views of Aluminum Powders Contain Cavities	113
6.24	Cross Sectional Views of Aluminum Powders Contain Cavities Created by Separation of the Bonded Powders	114
6.25	Encapsulation of the Steel 8640 Powders Created by Collision of the Powders During the Atomization	116
6.26	Encapsulation of the Aluminum Powders Created by Collision of the Powders During the Atomization	117
6.27	Various Types of Collisions Observed in the Steel 8640 Powders	118
6.28	Transverse Sections of Steel 8640 Powders Holed Through Themselves Produced Due to Collisions	119
6.29	Transverse Sections of Steel 8640 Powders Cracked During The Atomization	120

CHAPTER 1

INTRODUCTION

In the last ten years powder metallurgy and powder technology have made remarkable progress. The powder processing route is now recognized and respected as a competitive technology and an alternative to casting or conventional metal forming [1]. Potential has also given way to prove capability in the production of new and unusual materials, parts, and components solely by powder fabrication.

The two distinguishing features, pressing powders to shape and sintering below the melting point, have permitted this production method to supply special metallurgical and mechanical properties unobtainable by any other production process involving one or more of the many techniques of casting, forging, stamping, screw-machine operation or the machining of cast or wrought metal.

Powder metallurgy has many technical advantages over the other manufacturing technologies which are well publicized in literature [2].

The advantage of the powder-metallurgy method arises from the diversity of its applications to a number of different products, which may be grouped in the following three main categories [3] as they appeared in industry:

i) Special Metallurgical Properties: The refractory, or high-melting metals, such as, tungsten molybdenum, tantalum, columbium, titanium, zirconium, and their alloys with each other, must of necessity be made by pressing their powders into bar form, sintering

and hammering or rolling to massive and useful shape. No refractory crucibles are known which can be used commercially for melting these metals, and indeed the resulting properties of some of them, if melted, would make them unfit for their present uses.

The cemented carbide industry is built on the use of the powder metallurgy techniques [4,5]. Part of WC-Co composition melts and causes up to 20 % linear shrinkage, although the parts retain all the details of their former pressed shape.

Metals which are immiscible in the liquid state may be intimately mixed in the powdered condition. Examples include tungsten-copper for welding electrodes and silver-graphite and silver-molybdenum for electrical contact points [6].

ii) **Special Mechanical or Structural Properties;** No other known production method can give controlled porosity in a piece of metal. Porosity up to 50 % by volume of interconnecting pores has made possible the porous-bearing industry [7,8]. Other porous parts and available materials include metallic filters made from a variety of metals, tantalum condenser elements, and porous molybdenum.

Duplex structures include thermal strips which are made by pressing on layer of powder on top of another, such as iron and nickel, and rolling to strip. The two metals are perfectly welded together so that use can then be made of their differences in thermal expansion.

Nonmetallics may be blended with metallic powders to give a friction material for brake linings [9]. The metallic part dissipates the heat while the nonmetallic constituent supplies the frictional quality.

Insulated metallic powders are used extensively for electronic applications. Particles of carbonly iron powder are so treated that

when pressed together they are insulated from each other. This special structure is advantageous in tuning coils and can not be made by any other production method.

iii) Economic Advantages Over Competing Production Methods;

Many structures of functional parts are made by powder metallurgy in preference to the machining of cast or wrought metal because of economies which may arise from any or all of the following considerations [10,11] :

- a) reduction or elimination of secondary operations,
- b) the saving of metal, which may run as high as 50 % ,
- c) a tooling time which is often more favorable, and
- d) many design features that can be used which are costly to machine by conventional methods.

Tolerances and production rates may be other deciding factors in choosing the powder metallurgy process for making the part under consideration.

Many parts exhibit elements of all three of main advantages described above. Although the first two are of prime importance in supplying special products, the third or economic advantage is the one that must be carefully analyzed. Powder metallurgy is chosen as the production method to be used in making a part that might be possible to obtain by other means.

It is well known that the mechanical properties of sintered materials are dependent on their density [12-28]. Fig.1.1 clearly shows that tensile strength is decreasing linearly, but elongation and especially the impact strength are decreasing exponentially with increasing porosity.

Fig.1.2 shows similar tendency for the fatigue properties. However, today by full density processing techniques, densities better

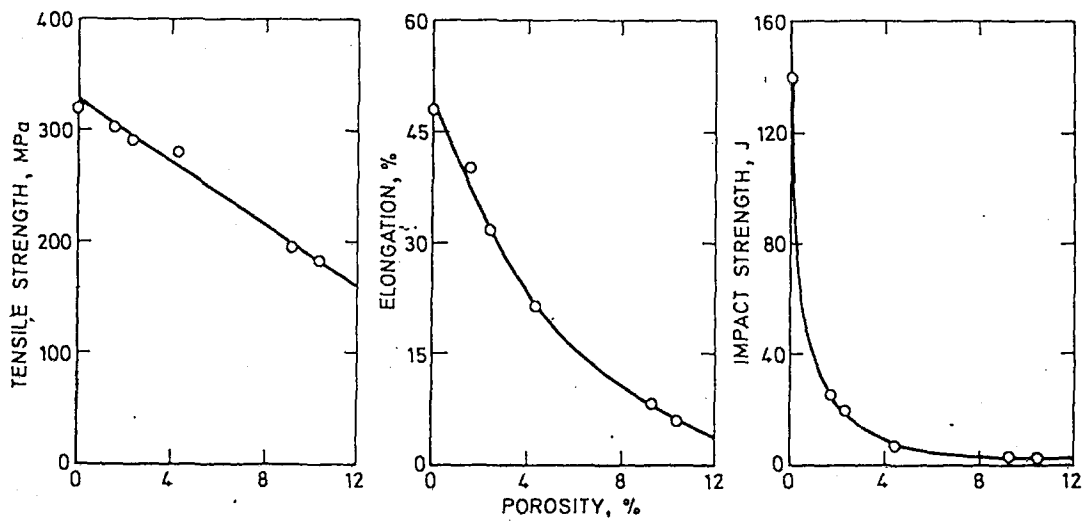


Fig.1.1 Influence of porosity on mechanical properties of iron [5,6,8].

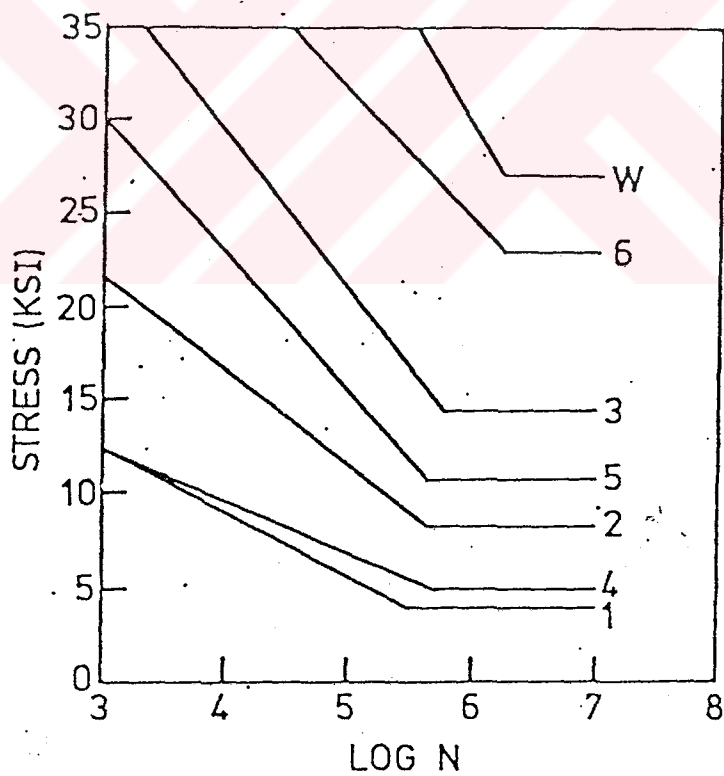


Fig.1.2 The effect of porosity on the fatigue curves of sintered iron parts [23].

than 99.99 % of theoretical density can be achieved. At full density, mechanical properties are almost equal and sometimes higher than conventional cast-wrought components [22].

Table 1.1 compares mechanical properties of equivalent cast-wrought and powder forged steels. Also, in full scale component testing, due to very high surface finish, powders forged connecting rods perform better than conventional drop forged connecting rods [21]. This is shown in Fig.1.3.

TABLE 1.1 COMPARISON OF PROPERTIES OF WROUGHT AND POWDER FORGED STEEL [22].

MATERIAL		UTS N/mm ²	Elongation %	Red. Area %	Impact Stress Joul
Steel	Longitudinal	920-980	17-19	60-62	100
	Billet				
Mn-Mo	Transverse	910-950	5-12	8-24	10
Powder Forged	Ni-Mo	900-930	13-15	40-50	27

Powder metallurgy is expanding its application unbelievable in energy decade. In early days, only sintered products were produced by P/M. But, in the last ten years, P/M processing techniques have been developed so much that, today, it is possible to produce almost any shape in any density level [29]. Hot forging, cold and hot isostatic pressing, powder injection molding and spray forming processes in addition to the original compacting and sintering processes make powder metallurgy a very versatile and competing alternative to cast-wrought processing techniques [29].

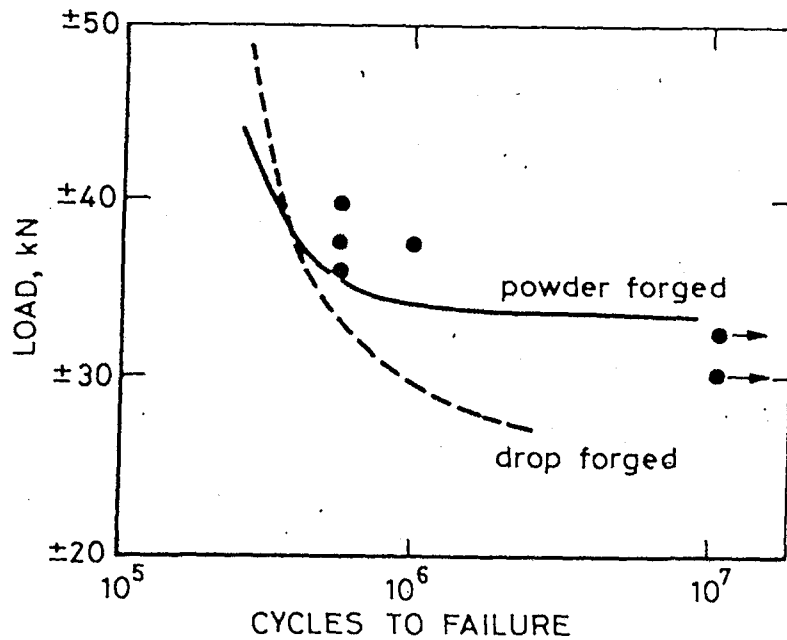


Fig.1.3 Powder-Forged connection-rod fatigue test results with drop-forged curve superimposed [21].

Application of powder metallurgy includes:

- 1) Cemented Carbides,
- 2) Self-lubricating Bearings,
- 3) Metallic Filters,
- 4) Tool Steels,
- 5) Non-machining Structural Parts,
- 6) Electrical Contact Materials,
- 7) Friction Materials,
- 8) Magnetic Materials, and
- 9) High-strength Full-density Components.

The demand for metallic powders is continuously increasing as shown in Fig.1.4. Iron powder has become the single most important powder in the P/M industry. Statistics on iron powder shipment have been used to measure the growth of the P/M industry. Iron powder consumption only in North America for 1986 is 325 thousand tons which corresponds to 650 billion US-\$ market value.

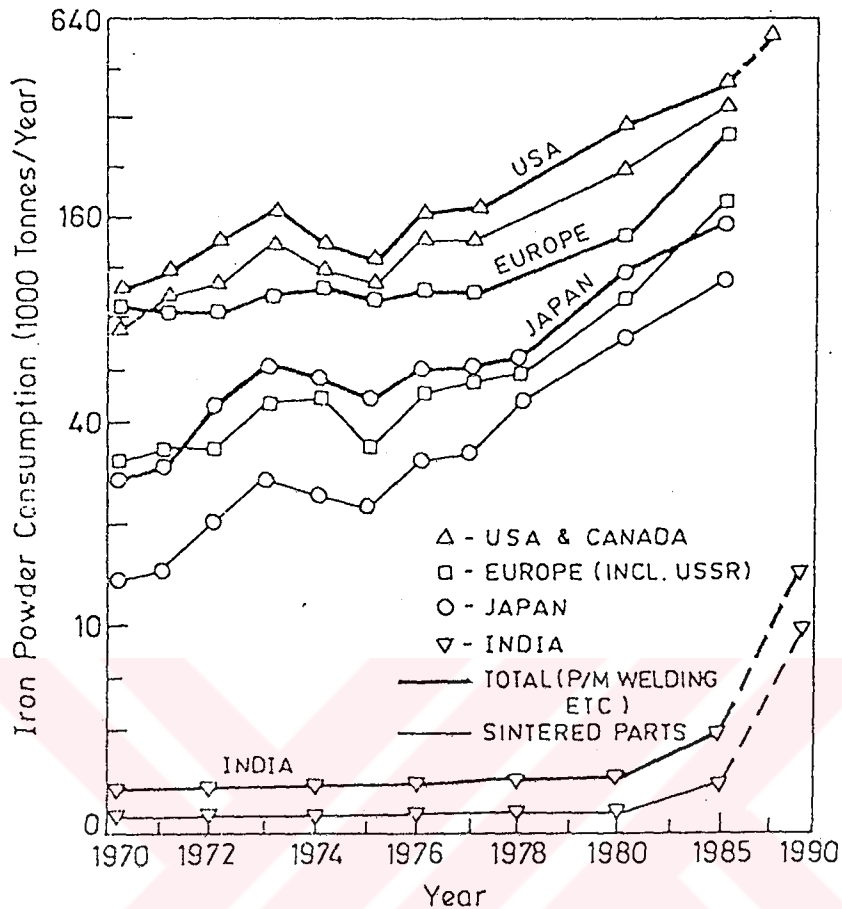


Fig.1.4 Comparative trend of iron powder consumption in the world [30].

Today, in Turkey, there are about ten companies producing powder metallurgy components. These components are generally produced to automotive industry. They are small in size and low in strength. Full density processing techniques have not been introduced yet. All of these companies are using imported metal powders. To the author knowledge, there is no metal powder producing company in Turkey.

Author believes that, metal powder production technology should be brought to Turkey. Either by licence agreements or developing it in

a suitable metal powder production technique in Turkey. Atomization is selected because more than 80 % of all metal powder consumption is atomized powders.

Initially, a water atomization set-up was aimed. But, later it is seen that high pressure and high delivery water pump is very expensive (more than 20 000 US- $\text{\$}$). The project is then, diverted towards centrifugal atomization. A centrifugal atomization set-up was designed and constructed. Characteristics of various metallic powders produced under various atomization conditions have been investigated. It is shown that, the set-up produced powders which have the characteristics of water atomized powders.

CHAPTER 2

PRODUCTION OF METAL POWDERS

2.1 INTRODUCTION

All metal powders, because of their individual physical and chemical characteristics, can not be manufactured by using the same method. The procedures vary widely, as do the sizes and structures of the particles obtained from the various processes [2,31].

Atomization or the operation of metal spraying, is an excellent means of producing powders from many metals such as stainless steel, brass, iron, aluminum, zinc, tin, and lead [2]. The particles are irregular in shape and are produced in many different sizes. The direct reduction method reduces metal oxides to metal powder form by processing them under a reducing gas at temperatures below the melting point [32]. Electrolytic deposition is a common means for producing powders of iron, silver, tantalum, and several other metals [33]. Milling process, utilizing various types of crushers, rotary mills and stamping mills, break down the metals by crushing and impact.

Various other methods involving precipitation, condensation and other chemical processes have been developed for producing metal powders.

In this chapter, principles, methods of producing powders will be briefly explained.

2. 2 ATOMIZATION

Atomization may be defined simply as the breakup of a liquid into fine droplets, typically smaller than about 150 μ m. For larger particles, this process is referred to as "shotting". Consequently, any material available as a liquid can be atomized. The breakup of a liquid stream brought about by the impingement of high-pressure jets of a water or gas is referred to as "water" or "gas atomization", respectively, or more generally, two-fluid atomization. The use of centrifugal forces to break up a liquid stream is known as "centrifugal atomization". Atomization into a vacuum is known as "vacuum" or "soluble-gas atomization". The use of ultrasonic energy to effect breakup is referred to as "ultrasonic atomization".

In this chapter, the methods of atomization will be briefly explained.

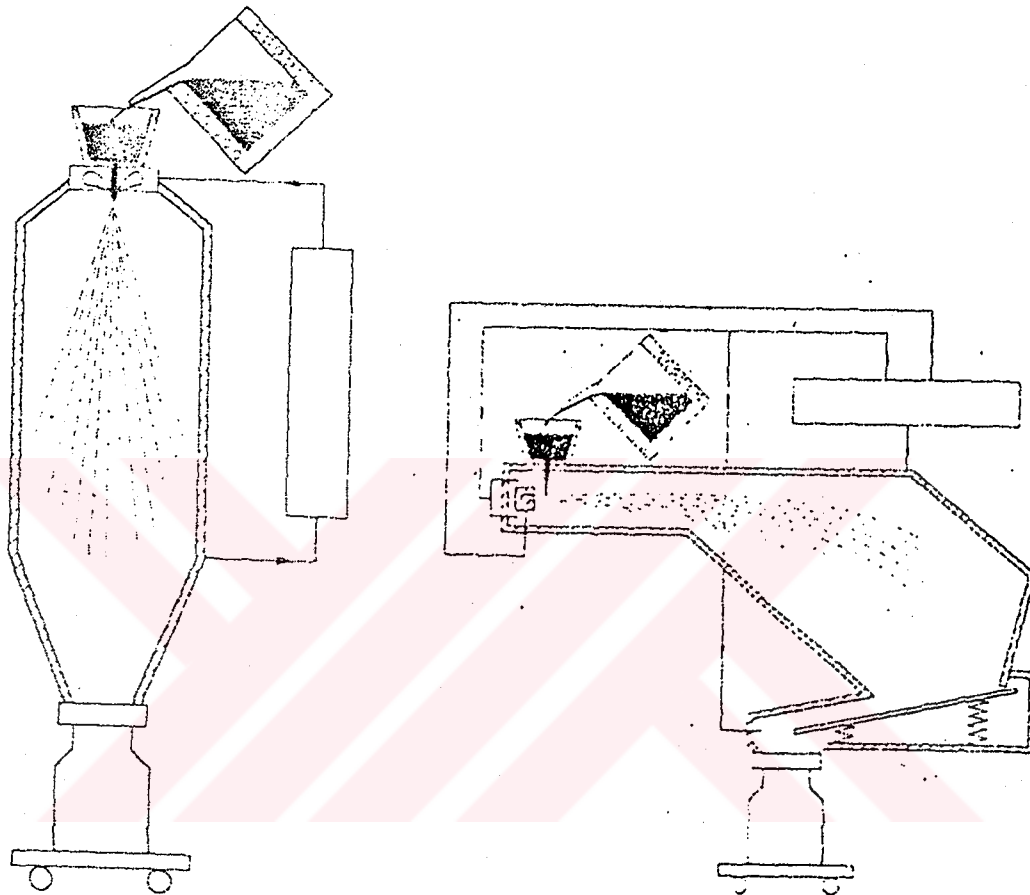
2.2.1 Two-Fluid Atomization

The atomization occurs when a stream of liquid metal falls vertically (usually) through the cross-fire of either a liquid or a gaseous stream. In general, only a small amount of energy of the stream impinging on the liquid metal is used to break up the liquid metal so that a great deal of this energy is wasted [34]. In general, gaseous atomization produces rounded or spherical particles water atomization produces irregular particles [2,31].

a) Gas Atomization

Fig.2.1(a) shows schematically the set-up of a vertical gas atomizer. The molten metal emerges from a nozzle of a tundish and is impinged by high pressure nitrogen jets. The melt is disintegrated into fine droplets which solidify before making contact with the walls of

the atomizer. The droplets contract under the influence of surface tension and form a spherical powder which is collected and cooled down to room temperature under a protective nitrogen atmosphere which avoids undue oxidation.



a) Vertical gas atomizer [35]. b) Horizontal gas atomizer [37].

Fig.2.1 Diagrammatic view of vertical and horizontal gas atomizers.

The long flight path before solidification necessitates high atomization towers. The height of the buildings for large scale production atomizer can easily amount to 25 m and more, the atomizer itself making up about half that figure. In larger units the atomization gas is recycled. To reduce the height of the atomization chamber the powder can be quenched and collected in liquid nitrogen [37].

The expenses associated with the construction of high buildings have initiated research to reduce the height by intensive cooling of the atomized melt [37]. A different development deal successfully with the introduction of horizontal atomization which does not require any special building [36]. A diagrammatic view of a horizontal gas atomizer is given in Fig.2.1(b). The melt stream is impacted and atomized by strong horizontal jets of nitrogen and solidifies under the influence of additional low pressure cooling gas.

The contour of the atomization chamber is roughly adjusted to the flight path of the particles. The powder is collected on a vibratory tray or a fluidising bed and further cooled down to near room temperature with a third stream of cooling gas.

Particle size distribution for gas atomization is given by the following equation [38]:

$$d_m = \ln(P/C)^n \quad (2.1)$$

where d_m = mean particle diameter, P = atomization pressure,
 n, C = constants.

b) Water Atomization

The water atomization process has been used for many years for the production of metal powders and probably now accounts for a large portion of world output. Water atomization is probably the cheapest method of producing free flowing irregular shaped powders in most materials, and is widely used in the production of iron, stainless steel, and other powders [39,40]. A major disadvantage of water, however, is its readiness to dissociate at high temperatures in the presences of a reducing agent, and therefore water atomized powders tend to have higher levels of surface oxides. Depending upon the

densification process and the final application of these powders, these oxides can inhibit densification in sintering, or lower the mechanical strength of the final product. Consequently, where low oxygen contents are of paramount importance; powders are produced by other techniques, such as atomization by inert gas or oil.

The water atomizing process consists of six steps; melting, atomizing, drying, screening, and annealing. Each step has an important bearing on the final product.

Fig.2.3 shows schematically a water atomization unit. The molten metal is poured into a ladle from which it is poured into a preheated tundish. The tundish contains an orifice through which the metal flows downward in a smooth stream. The stream of molten metal drops through a set of high-velocity jets of water at pressures commonly of 50-200 bar which break the metal stream into fine, irregular particles. The particles instantly solidify and drop into a water tank.

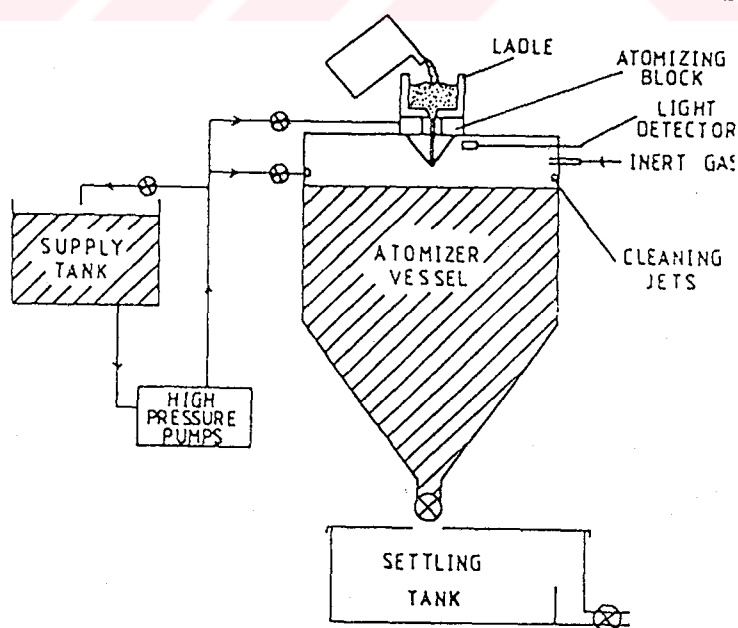


Fig.2.3 Schematic diagram of water atomization [40].

The types of atomizing jets, the angle of jet streams and the velocity of water are three of several factors which control the size and the shape of the particles [2,37-45]. The final properties of the powder are strongly influenced by atomizing procedure.

The range of alloys currently produced in large quantities by water atomization is not particularly wide. Iron powder, alloy steel powders, ferrosilicone powder, ferromanganese powder, nickel and cobalt flame spraying powders and a wide range of copper alloys are commonly produced in this way. However, in many cases commercial exploitation would be attractive. Any metal (or non metal) that does not react violently with water can be atomized providing it can conveniently be melted and poured [42].

Particle size distribution for water atomization of 4620 steel is given by the following equation [1]:

$$d_m = (8700)/(P)^{0.62} \quad \text{or} \quad d_m = (5500)/V_w \quad (2.2)$$

where d_m = mean particle diameter, micrometers;

P = water pressure, MPa;

V_w = water jet velocity, m/s.

2.3 CENTRIFUGAL ATOMIZATION

Centrifugal atomization involves molten metal that comes in contact with a rotating disc or cup. The molten metal is mechanically atomized and thrown off the edges of the rotating substrate into a cooling gas and then solidified. The process is divided into two branches:

- (a) Rotating Disc, and
- (b) Rotating Electrode.

2.3.1 Rotating Disc Atomization

Rotating disc atomization involves the impinging of a stream of molten metal onto the surface of rapidly spinning disc [47]. The liquid metal is mechanically atomized and thrown off the edges of the spinning disc. Solidification occurs in flight and can be enhanced by blasting the emerging particles with a stream of helium.

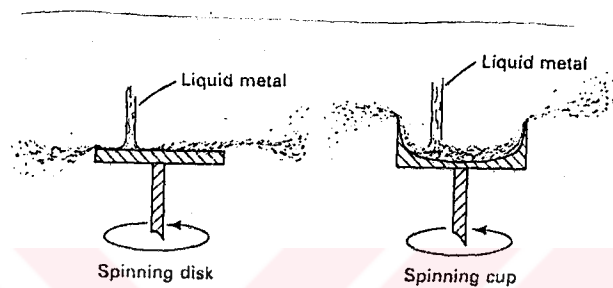


Fig.2.4 Schematic diagram of rotating disc atomization.

Particles are generally spherical, with the average particle size decreasing with increasing disc speed. Rotating disc atomization is a form of centrifugal atomization in which solidification rate on the order of 10^4 to 10^6 °C/s [47] can be achieved. This phenomenon also places rotating disc atomization under consideration as a form of rapid solidification rate (RSR) powder atomization.

Most rotating disc atomized powders are used in aerospace engine parts. As a result, the powder is handled and processed under vacuum or inert gas. Consolidation to theoretical density is accomplished by hot extrusion.

2.3.2 Rotating Electrode Process

The rotating electrode process is a method for producing metal powders where the end of a metal bar is melted while it is rotated about its longitudinal axis.

Molten metal is centrifugally ejected and forms of droplets which solidify to spherical powder particles [48]. The basic process is shown in Fig.2.5, where the melting method is by electric arc.

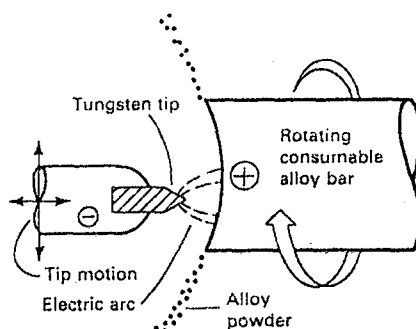


Fig.2.5 Schematic of rotating electrode process

The rotating electrode process has evolved to include equipment that consists of a tank in which powder is generated. This is mounted with its circular plane section in the vertical position. The consumable rotating electrode is introduced through a seal-and-bearing assembly; the long axis of the electrode is horizontal and centrally located in the tank and is made the anode of a direct current power circuit. The nonmelted permanent cathode may be a simple tungsten-tipped device provided with adequate cooling (REP) or a transferred arc plasma torch (PREP). This equipment projects through the other face of the tank to oppose the rotated electrode. Usually, melting is conducted under inert gas; the preferred medium is helium, which offers improved heat transfer properties and electric arc characteristics.

2.4 VACUUM ATOMIZATION

Vacuum or soluble gas atomization is a commercial batch process based on the principle that, when a molten metal supersaturated with gas under pressure is suddenly exposed to vacuum, the gas expands,

comes out of solution, and causes the liquid metal to be atomized. Alloy powders based on nickel, copper, cobalt, iron, and aluminum can be vacuum atomized with hydrogen. Powders are spherical, clean, and of a high purity compared to powders to produced by other powder processing methods [49].

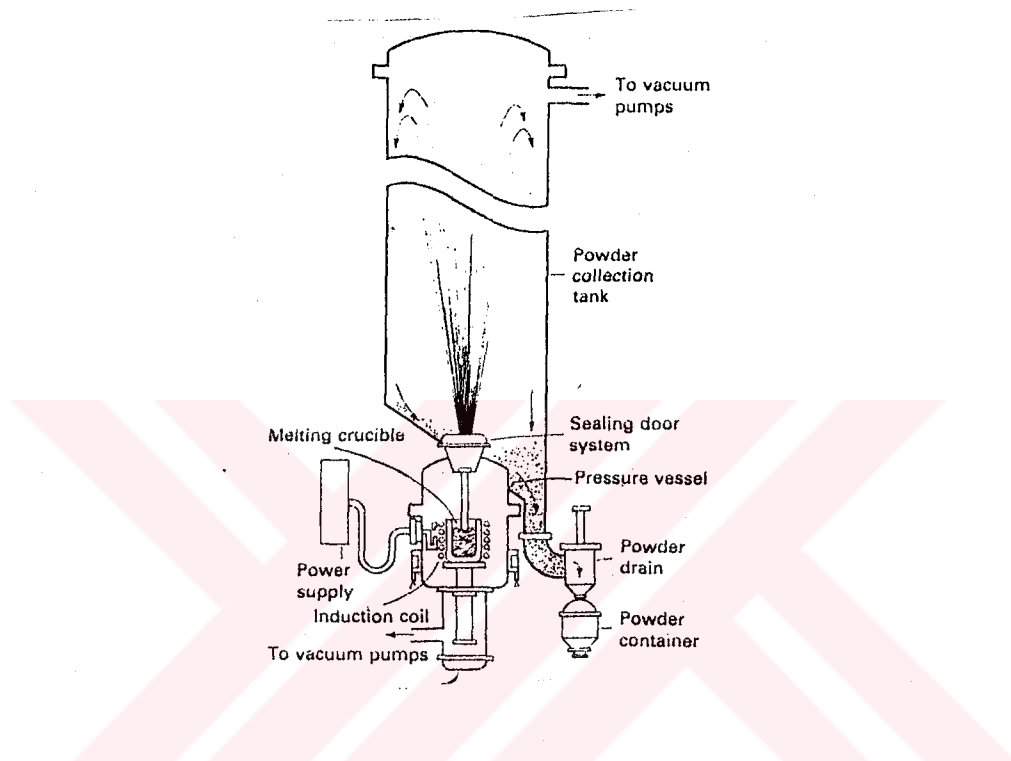


Fig.2.6 Schematic of the vacuum atomization process [50].

A schematic of equipment used in the vacuum atomization is shown in Fig.2.6. Typically, there are two vertical chambers—a lower vacuum induction melting section and upper powder collection tank. Powder is produced by saturating a molten metal bath with a soluble and/or nonreactive gas. The molten metal stream is atomized by introducing the gas-saturated stream through a ceramic transfer tube into the reduced-pressure collection chamber. The concentration of gases in molten metals increases with the pressure of a gas over the liquid. This phenomenon provides the energy to disperse the molten metal stream into droplets. The intimate mixture of gas and metal under pressure in the stream has significant impact on powder yields and is more effective than conventional gas atomization.

2.5 ULTRASONIC ATOMIZATION

Ultrasonic atomization of liquids has been known for a long time and more recently has been used [51,52] for the production of high-quality powders for, inter alia, solders and soldering pastes of metals with melting points of up to 1000 °C. However, adoption of ultrasonic atomization on a wide scale industry has up to now been hindered by lack of sufficient information concerning the key parameters of the process determining its efficiency.

Ultrasonic atomization involves production of ultra fine atomized molten droplets that are rapidly cooled by convection in a gaseous medium. A liquid stream is disintegrated, or atomized, by impact with the multiple high-velocity gas pulses. The gas is accelerated by a shock wave tube at the speeds up to Mach 2 at frequencies ranging from 60 to 120 kHz. The particles of gas travelling at extremely high velocities in pulsed waves strike the metallic stream (Fig.2.7). On impact, the gas pulses shear the liquid metal stream into fine droplets, usually less than 30 μm . Fine liquid droplets solidify convectively at high cooling rates.

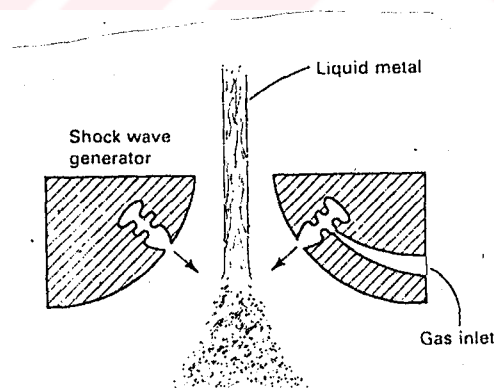


Fig.2.7 Schematic of ultrasonic gas atomization.

Ultrasonic atomization has been used for commercially for production of low-melting alloys such as aluminum alloys. However, only laboratory and pilot-scale operations have been reported for high

melting-temperature alloys (stainless steels and nickel- and cobalt-based alloys). Quench rates experienced by 30- to 70- μm aluminum particles produced by ultrasonic atomization are about 10^5 $^{\circ}\text{C}/\text{s}$, yielding highly refined structures. Three advantages of this process are:

- (1) high relative velocities between gas and metal droplets,
- (2) small powder size, and
- (3) a gas chilling factor due to expansion of the high-pressure gas.

2.6 CHEMICAL METHODS OF POWDER PRODUCTION

Chemical and physiochemical methods of metal powder production allow great variations in powder properties. The wide variety of processing variables and production parameters currently available permit close control of particle size and shape. The most widely used processes within this category include oxide reduction, precipitation from solution and thermal decomposition [32].

2.6.1 Oxide Reduction

The production of iron, copper, tungsten, and molybdenum powders from their respective oxides are well established commercial processes.

Oxide-reduced powder grades of iron and copper compete with powder grades made by other processes. Oxide-reduced powders characteristically exhibit the presence of pores within each powder particle and thus are called sponge powders. This sponginess is controlled by the amount and size of the pores and accounts for the good compactibility (high green strength) and sinterability of such powders.

Processing conditions for oxide reduction are based on the generally known equilibria for the reduction reactions using hydrogen, carbon monoxide, and carbon as the reducing media, as shown in Fig.2.8.

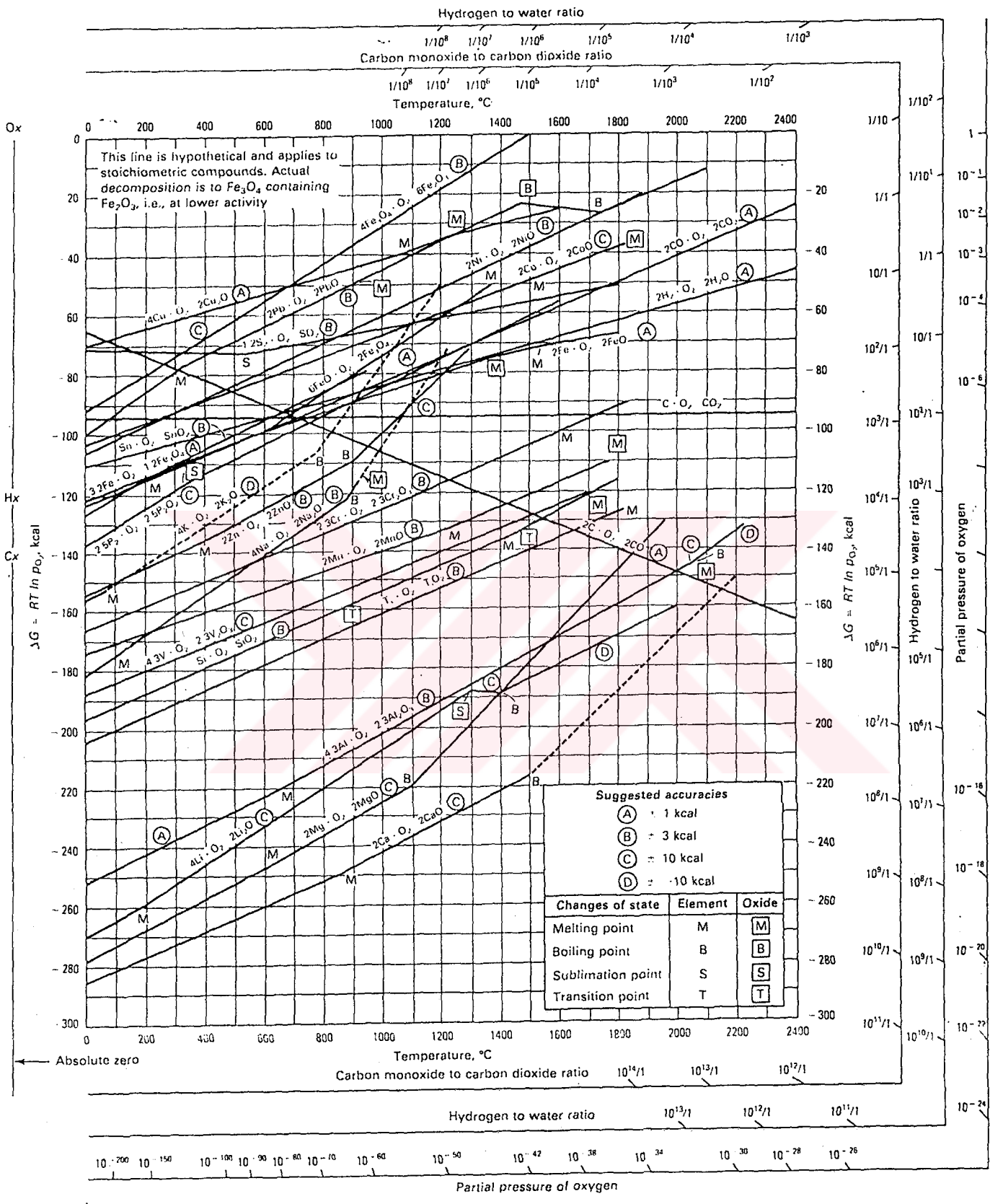


Fig.2.8 Standard free energy of formation of metal oxides [32]

The ratios of carbon monoxide to carbon dioxide, hydrogen to water, and the partial pressure of oxygen and phosphorus permit determination of the minimum ratios necessary to maintain reducing conditions at a given temperature and at a total gas pressure of 1 atm.

In practice, however, reduction temperatures are usually much higher than indicated by thermodynamic data. Final powder properties such as particle size, particle porosity, and hydrogen loss that critically determine performance properties (apparent density, powder flow, and compacting and sintering properties) primarily depend on purity and size of the starting material and the kinetic of the reduction process. The kinetics of the reduction process depend on composition and flow rate of the reducing gas, reduction temperature, temperature profile in the furnace, and bed depth of the oxide if reduction is performed in a stationary system.

Process Variables. The various combination of processing parameters used by powder manufacturers to produce numerous grades of powder are proprietary. The most important process variable is the reduction temperature. Typically, low reduction temperatures result in powders possessing fine pores, large specific surface areas, and high green strength. High reduction temperatures ($>0.6T_m$) produce large intraparticle pores and small specific surface area powders that exhibit high compressibility. Extremely low reduction temperatures ($<0.3 T_m$) can readily produce pyrophoric powder. High temperatures can cause excessive sintering and agglomeration, which lead to difficulties with the breakup of the sinter cake.

With the tungsten and molybdenum, oxide reduction is used partly for economic reasons, because of the melting points of these metals are very high. Reduction processes, which use hydrogen as the reducing medium, are similar for both tungsten and molybdenum oxides.

In contrast to atomized powders where oxides often are enriched on the surface of a particle, oxide-reduced powders, at least when the freshly reduced or stabilized against tarnishing, contain most of their residual oxides within the particles.

2.6.2 Precipitation From Solution

Production of metal powders by hydro-metallurgical processing is based on leaching an ore or ore concentrate, followed by precipitating the metal from the leach solution. Metal precipitation from solution can be accomplished directly by electrolysis, cementation or chemical reduction. Indirect precipitation may be achieved by first precipitating a compound of the metal (hydroxide, such as carbonate, or oxalate, for example), followed by heating, such as decomposition and reduction.

The most widely used commercial processes based on hydrometallurgy are copper cementation and the separation and precipitation of copper, nickel and cobalt from salt solutions by reduction with hydrogen.

2.6.3 Thermal Decomposition

Both iron and nickel are produced by decomposition of the respective carbonyls. Carbonyls are obtained by passing carbon monoxide over spongy metal at specific temperatures and pressure.

Powder is produced by boiling the carbonyls in heated vessels at atmospheric pressure under conditions that allow the vapors to decompose within the heated space and not on the sides of the container. The powder is collected and sieved and may be milled followed by an anneal in hydrogen. The chemical purity of the powders can be very high (over 99.5%), with the principal impurities being

carbon, nitrogen, and oxygen. Particle size can be controlled closely. Iron carbonyl powder is usually spherical in shape and very fine (less than 10 μm), while the nickel powder is usually quite irregular in shape, porous, and fine.

2.7 MILLING OF BRITTLE AND DUCTILE MATERIALS

Milling of materials, whether hard and brittle or soft and ductile, is of prime interest and economic importance to the P/M industry [31]. Mechanical comminution is the most widely used method of powder production for hard metals and oxide powders. Secondary milling of spongy cakes of oxide-reduced, atomized, or electrolytic powders is the most common milling process; hammer and rod mills are used for this type of milling. Depending on the degree to which the material is sintered, either primary particle size distribution is reestablished during milling or larger agglomerates are produced.

Mechanical comminution is restricted to relative hard, brittle metals (electrolytic iron or bismuth, for example), some reactive metals such as beryllium and metal hydrides, ductile metals used for producing metal flakes, and chemically embrittled materials such as sensitized stainless steel.

Increasing interest in metal powder with particle sizes that are finer than the particle size of powders produced by atomization has reactivated interest in milling, particularly in solid-state alloying or high-energy milling. However, milling of metal powders has received minimal attention to date. Research conducted on ball milling of metals is primarily proprietary and empirical, and thus restricted to specialized P/M applications. Objectives of milling include:

- a) Particle size reduction (comminution or grinding)
- b) Particle size growth
- c) Shape change (flaking)

- d) Agglomeration
- e) Solid-state alloying (mechanical alloying)
- f) Solid-state blending (incomplete alloying)
- h) Modifying, changing, or altering properties of a material (density, flowability, or work hardening)
- e) Mixing or blending of two or more materials or mixed phases.

In most cases, the objective of milling is particle size reduction.

2.8 ELECTRODEPOSITION OF METAL POWDERS

Electrodeposition of metals from aqueous solutions produces a variety of metal powders [33].

There are two practical methods of obtaining powder by electrodeposition: (1) direct deposition of a loosely adhering powder or spongy deposit that can easily be disintegrated mechanically into fine particles, and (2) deposition of a dense, smooth, brittle layer of refined metal that can be ground into powder. Choice of production method depends mainly on the metal used. For example, copper and silver produce powdery or spongy cathode deposits. Conversely, iron and manganese produce coherent cathode deposits; because of these deposits will be crushed and ground into powder, it is highly desirable that they are brittle. Brittleness of the cathode deposit can be achieved by proper control of the electrolytic cell conditions.

Although electrodeposition produces a high-purity powder with excellent properties for conventional P/M processing, current usage of electrolytically produced powder is limited, because the production involves the control and manipulation of many variables and sometimes is significantly more expensive than other techniques. Consequently, only iron, copper, and silver powders are produced commercially to any extent by electrodeposition.

2.9 COMPARISON OF PRINCIPAL METHODS OF PRODUCING METAL POWDERS

Table 2.1 summarized the methods currently used to produce metal powders and their typical applications.

Atomization and reduction processes are most widely used in high tonnage production, while mechanical crushing and electrolysis are used primarily for production of specialty materials in small quantities. The most flexible process is atomization since it provides the capability to produce alloy powders and affords greatest control over powder properties.



TABLE 2.1 COMPARISON OF PRINCIPAL COMMERCIAL METHODS OF PRODUCING METAL POWDERS [2]

Production method	Powders Produced	Typical application of the same powder	Advantages	Disadvantages	Relative cost
Atomization	Stainless steel, brass, bronze, other alloy powders, aluminum, tin lead, iron, zinc	Stainless steel elements Mechanical parts, iron Mechanical parts (medium to high density), welding rods, cutting and scarfing, general flaking stock for pigement, solid fuels, mechanical parts	Best method for alloy powders. Applicable to any metal or alloy melting below 3000°F	Wide range of particle sizes, not all saleable. Particles too spherical for some applications	Low to medium
Gaseous reduction of oxides	Iron, copper, nickel, cobalt, tungsten, molybdenum	Mechanical parts, welding rods, friction materials, general Bearings, motor brushes contacts, iron copper parts, friction materials, brazing, catalysts	Easy to control particle size of powder. Good compacting powder	Requires high grade oxides. Restricted to reducible oxides	Low
Gaseous reduction of solutions	Nickel, cobalt, copper	Iron nickel sinterings, fuel cells, catalysts, Ni strips for coinage Friction materials, bearings, iron copper parts, catalysts	One can be used. Purification during leaching, fine particles	Applicable to few metals such as nickel, cobalt, and copper	Medium
Reduction with carbon	Iron	Mechanical parts, welding rods, cutting and scarfing, chemical, general	Low cost. Control of variation in properties possible	Requires high grade ore on mill scale	Low
Electrolytic	Iron, copper, nickel, silver	Mechanical parts high density, food enrichment, electronic core powders Bearings, motor brushes, iron copper parts, friction materials, contacts, flaking stock	High purity of product. Easy to control	Limited to few metals, cost	Medium
Carbonyl decomposition	Iron, nickel, cobalt	Electronic core powders, additive to other metal powders for sintering Storage batteries, additive to other metal powders for sintering	Produces fine pure powders	Limited to few powders, high cost	High
Grinding	Iron, beryllium, manganese, nickel, antimony, bismuth	Waterproofing concrete, iron from electrolytic cathodes Welding rod coatings, pyrotechnics Filters, welding rods, sintered nickel parts	Controlled size of powder	Limited to brittle or embrittled materials Quality of powder limits use. Slow	Medium

CHAPTER 3

CHARACTERIZATION AND TESTING OF METAL POWDERS

3.1 INTRODUCTION

The success of a P/M processing technique depends to a great extent on understanding and evaluating the physical and chemical properties of metal powders, both as individual particles and in bulk form. Relationships between these powder properties and their behaviour during processing (for example, compressibility, sinterability, dimensional change during sintering) in most cases are qualitative in nature. Nevertheless, a good description of powder properties is important for several reasons:

- * To improve understanding of powder behaviour
- * To determine tolerances in property specifications
- * To ensure reproducibility of powder behaviour during processing

The processing of a powder into a compact and the resultant properties of P/M parts are affected by such physical characteristics as particle size, particle size distribution, particle shape and structure, and surface condition. Other characteristics, such as apparent density and flowability, depend on these basic physical properties.

3.2 SAMPLING

The properties of a given lot of powder are determined from a sample taken from that lot. The properties of the sample must be

representative of the properties of the lot. Standard methods of sampling finished lots of powders may be found in ASTM Standard B215 and MPIF1-61.

For sampling from mechanically blended lots the sample should be taken from the entire cross-section of the moving stream as the powder is removed from the blender. A 5000 g sample should be taken halfway through the filling of the first container, when the blender is half full, and halfway through the filling of the last container. The three samples should be blended and split into a correct sample size with a sample splitter.

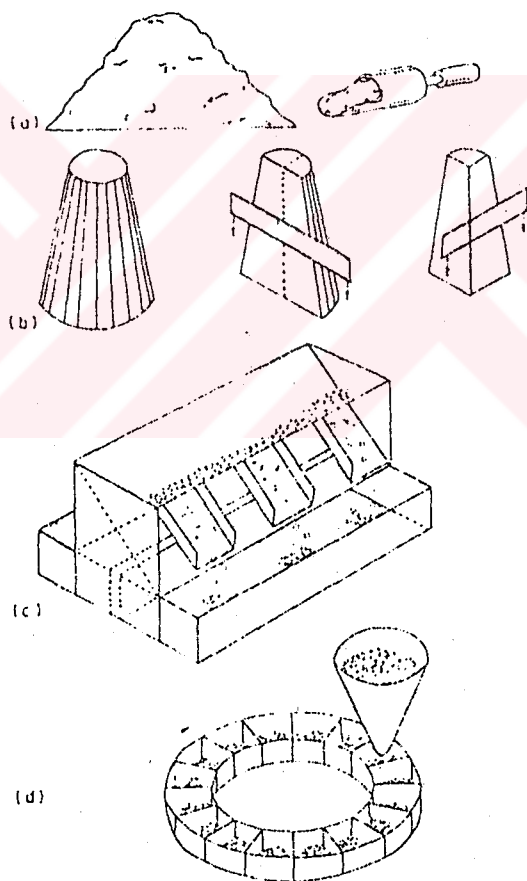


Fig.3.1 Sample splitting devices [54].

When sampling from containers, a scoop should be taken from each container and passed through a scalping screen into a sample.

container. The sample should be taken at a point halfway between the center and the wall of the container. It is preferable to use a sample thief in order to obtain samples beneath the surface. The resulting samples should be blended and split to the desired size.

There are several techniques and devices available to reduce a quantity of powder to a desired sample size. Some of the most commonly used are the scoop and the cone and quartering techniques, chute splitter and spinning rifler (see Fig.3.1).

Test for metal powders may be divided into [2,31,55-57].

Chemical tests

Physical tests

Tests simulating the behaviour of the powder in fabrication.

3.3 CHEMICAL TESTS

The usual methods of chemical analysis for metals may also be applied to powders. In addition, two types of tests are specific for metal powders: the hydrogen loss test and the insoluble matter test.

3.3.1 Hydrogen Loss Test

The hydrogen loss test is an empirical test, in which sample of powders is heated in hydrogen for a given length of time at a given temperature and the loss in weight during this treatment determined. MPIF specification 2-64.

3.3.2 Insoluble Matter Test

The objective of the insoluble matter is to determine the amount of impurities insoluble in acid which have been introduced

into the powder during its production. Like the hydrogen loss test it is an empirical test. The details are given in MPlF specification 6-64.

3.4 PHYSICAL TESTS

These are tests for :

- 1) Particle size and particle size distribution.
- 2) Particle shape
- 3) Surface area, density and porosity
- 4) Apparent density
- 5) Tap density
- 6) Flow rate
- 7) Angle of repose

3.4.1 Particle Size And Size Distribution

In the P/M industry, the traditional and most widely used method of particle size measurement is by sieving. Sieves or screen are used not only for particle size measurement, but also for separation of powders into different sieve fractions. This twofold use of sieves, in addition to the fact that most P/M powders are -80 mesh (smaller than about 177 μm in diameter, with only minor amounts smaller than 10 μm) has been well suited to industrial application. For powders with larger percentages of -400 mesh (37 μm) particles, sieve distribution data are often complemented with Fisher sub-sieve size analysis, microsieve data, or specific surface area data.

Several electronic methods of particle size analysis have been developed during the past two decades. These generally provide higher measurement speed, resolution, and small-size sensitivity than sieves, saving time and labor while yielding more precise data.

Common methods of determining particle size and size distribution and their limits of applicability are briefly explained below.

a) Sieve Analysis

Sieve analysis is the most widely used method of determining particle size distribution of metal powders.

Particle size distribution is controlled and certified by the powder producer and is frequently checked by the end user. Typically, a series of sieves is selected that spans the full range of particle sizes present in a powder. Sieves are stacked in order, with the largest mesh size at the top and a pan at the bottom. An appropriate sample weight of metal powder is spread on the top sieve and covered. The stack of sieves is agitated in a prescribed manner (shaking, rotating, or tapping) for a specified period of time. The powder fractions remaining on each sieve and contained in the bottom pan are weighed separately and reported as percentages retained or passed by each sieve. The details are given in MPIF specification 5-62.

TABLE 3.1 INFORMATION ON SIEVES OF USE IN POWDER METALLURGY

Sieve Designation		US Standard Sieve Opening		Tyler Standard Mesh No
		inches	mm	
μm	Mesh No			
117	80	0.0070	0.177	80
149	100	0.0059	0.149	100
124	120	0.0049	0.125	115
105	140	0.0041	0.105	150
88	170	0.0035	0.088	170
74	200	0.0029	0.074	200
63	230	0.0024	0.063	250

b) Light Scattering

Light scattering provides a rapid, reproducible, and convenient method of determining particle size and size distribution. Powder particles used in P/M applications vary in size from 0.1 to 300 μm . This range of sizes conveniently corresponds to the capabilities of light scattering techniques.

Previous optical instruments based on light scattering enjoyed only limited use for particulate measurements. Transmissometer-type instruments have been calibrated to measure particulate mass, but such instruments can maintain calibration only as long as the particle size distribution remains unchanged from the calibration distribution. Other instruments are available that rely on scattering theory to provide mass measurement over a wider particle size range. These instruments historically have required extensive computational capability and thus have not been suitable for continuous measurements. However, an instrument is now available that employs an optical transform and masking technique that performs the necessary computation directly and continuously.

c) Sedimentation

Sedimentation is a mechanism for classifying metal powders according to their rate of settling in a fluid. This measurement technique is based on Stoke's law of fluid dynamics, which states that, at low velocities, the frictional force on a spherical body moving through a fluid at constant velocity is proportional to the product of the velocity, the fluid viscosity, and the radius of the sphere. Sedimentation is routinely used to determine particle size and size distribution.

Among the number of sedimentation methods available, only a few are commonly used for metal powders—the micromerograph and light

and x-ray turbidimetry. Another analyzer using the sedimentation method is the Roller Air Analyzer; however, it is no longer manufactured, and its standards are being withdrawn.

d) Electrozone Size Analysis

Electrozone (electric sensing zone) measurement of particles detects the volumes of individual particles in a liquid suspension, at rates ranging from tens to thousands of particles per second. Electrical pulse amplitudes, representing individual particle volumes, are processed via microcomputer to yield particle size distribution data in whatever form may be required. Overall, the electrozone method is capable of measuring particle diameters ranging from 0.1 to 2000 μm , depending on particle density. For wide distributions, the computer program can blend data sets, which is facilitated by logarithmic scales.

Collection of size distribution data normally requires several minutes and consists of transfer of the digitized values for many thousands of particle-pulses to their proper locations in computer memory.

e) Optical Sensing Zone

The light blockage principle (obscuration) was used by Carver in 1958 to develop a method for counting and sizing particulate contamination in hydraulic fluids. To date, this principle has found application in other particle-fluid systems and has been used for the measurement of metal powder particles.

In apparatus using the light-obscuration principle, particles are suspended in a fluid with a refractive index that differs from the reactive index of the particles. The suspension is then passed through a restricting orifice—the sensing zone—across which a collimated light beam passes. The beam of the light falls on a photodetector

which measures the intensity of the light passing through the zone.

f) Microscopy and Image Analysis

Microscopy is the most definitive method of particle size analysis, because individual particles are observed and measured. Some of the techniques used are more art than science, and some measurement techniques are subjective. However, if the basic principles of sampling, preparation, and counting are followed, a precise count can be made with a thorough understanding of the nature of the particles being studied. ASTM standard E 20 details the use of microscopy for particle sizing.

g) Fisher Sub-sieve Sizer

The fisher sub-sieve sizer is a simple, inexpensive permeameter, which measures the flow of air through a packed powder bed. From this measurement, average particle size and porosity can be calculated from a chart that is an integral part of the instrument. The Fisher sub-sieve sizer is used extensively through-out industry, especially for process control purposes where only relative values are required [11]. The details are given in specification MPIF 32-60.

3.4.2 Particle Shape of Metal Powder

Shape and size are probably the two most fundamental characteristics of a particle. Both are interrelated: without knowing the shape of a particle it makes little sense to speak of particle size. Schematic diagrams of typical powder particle shapes are given in Fig.3.2.

One-dimensional

Acicular:
Chemical decomposition



Irregular rod-like:
Chemical decomposition, mechanical comminution



Two-dimensional

Dendritic:
Electrolytic



Flake:
Mechanical comminution



Three-dimensional

Spherical:
Atomization, carbonyl precipitation from a liquid



Nodular:
Atomization, chemical decomposition



Irregular:
Atomization, chemical decomposition



Porous:
Reduction of oxides



Fig.3.2 Various shapes of powder particles and their methods of manufacture.

The shape of the particles affects several properties of a powder [2].

Flow. Spherical powders have good flow, flake powders have poor flow and some types of irregularly shaped powders have essentially no flow.

Apparent Density. Spherical powders have the highest apparent density. Angular powders have high apparent density while some sponge powders have low apparent density due to internal porosity.

Surface Oxidation. The more irregular the particle the higher will be the proportion of surface oxidation.

Compressibility. Some irregular shapes also tend to absorb the powder lubricant, thereby reducing its effectiveness.

Green Strength. Rectangular shapes, such as spheres, have lower green strength. Mechanical interlocking is usually required for green strength.

Sinterability. As the irregularity of a particle increases, there are more points of contact after pressing, thereby, giving more areas for bonding. An irregular particle has more surface energy which promotes sintering by surface diffusion. Alloy additions are better dispersed if the base powder particles are irregular and total diffusion of the additions is increased.

Permeability. Irregular particles show lower permeability for the same porosity. This aids in oil retention and in filtering.

Despite the basic significance of particle shape on powder properties, there is as yet no accepted test(s) other than the use of fairly simple and qualitative comparisons. However, this problem is currently receiving some attention.

3.4.3 Surface Area, Density, And Porosity Of Metal Powders

In determining the behaviour of a metal powder during processing and the mechanical properties of the resulting P/M material, the surface area (m^2/kg , or cm^2/g), density (g/cm^3), and porosity (% porosity = 100% of theoretical density) can be useful indicators. For example, surface area is helpful in understanding sintering behavior; density permits the distinction between different materials and/ or the determination of inaccessible porosity of a powder of P/M part; and porosity can greatly influence the hardness of P/M materials as measured by microscopic methods.

The values for these three characteristics can be determined by a variety of methods; in reporting data, the method should also be

indicated, because the values will often differ depending on the test method used.

The method used to determine surface area, density, and porosity are not specific to metal powders; many have been developed for testing other materials in powder form. The major techniques used to determine these powder characteristics are summarized below:

a) *Gas absorption method*. Determines the surface area of a powder sample by measuring the amount of gas absorbed by a monomolecular coverage of the powder. Nitrogen is the most common gas used; krypton has also been used for very small surface areas. This method can also be used to determine pore volume and size distribution for pore diameters ranging from 600 to 14 \AA .

b) *Permeametry*. Measures the resistance to fluid flow through a compacted powder bed. This information is used to determine related properties of a powder, such as specific surface area and average particle size. This method does not give information on a surface area of internal pores. Gas permeametry is the most commonly used testing procedure.

c) *Pycnometry*. Determines density by measuring the difference between the specific and bulk volumes of a sample. This method is based on the displacement principle, using the powder as the solid body and helium or mercury as the displaced medium. Pycnometry can be used to determine total pore volume. However, it does not provide quantification of pore size or distribution.

d) *Mercury porosimetry*. Measures the volume of mercury intruded into the pores of a powder sample as a function of the pressure applied to the mercury. This method gives pore size and distribution over a wide range $5 \times 10^6 \text{ \AA}$ to 30 \AA - depending on the capability of the apparatus used.

3.4.4 Apparent Density Of Metal Powders

Apparent density of a metal powder, or the weight of a unit volume of loose powder expressed in grams per cubic centimere, is one of the fundamental properties of a powder. This characteristic defines the actual volume occupied by a mass of loose powder, which directly affects processing parameters such as the design of compaction tooling and the magnitude of the press motion required to compact and densify loose powder.

In most compacting operations, dies are filled by volume measure, and presses operate either to a fixed position or a fixed pressure. If the press operates to a fixed position, pressure can be maintained at a constant level only if the apparent density of the powder does not change. If, however, the press operates to a fixed pressure, consistency in apparent density is necessary to ensure compacts of equal height. Small fluctuations in apparent density can be compensated by adjustments of pressure or stroke of the presses, but large scale compacting requires that the apparent density of the powder be controlled within close limits.

Apparent density of a metal powder depends on the density of the solid material, particle size, particle size distribution, particle shape, surface area and roughness of individual particles, and particle arrangement. Apparent density is strongly affected by particle size. It generally (1) decreases with decreasing particle size, (2) decreases as the particle shape becomes less spherical and more irregular, (3) decreases with increasing surface roughness, and (4) is frequently controlled by mixing various size of particles.

Standard testing procedures are outlined ASTM Standard B212 and MPIF Standard 4-45. An oven-dried 30-35 cm³ sample is poured through a standard funnel (Hall flowmeter) and overflows into a 25 cm³ cup. The powder is leveled with a spatula and the tare weight is

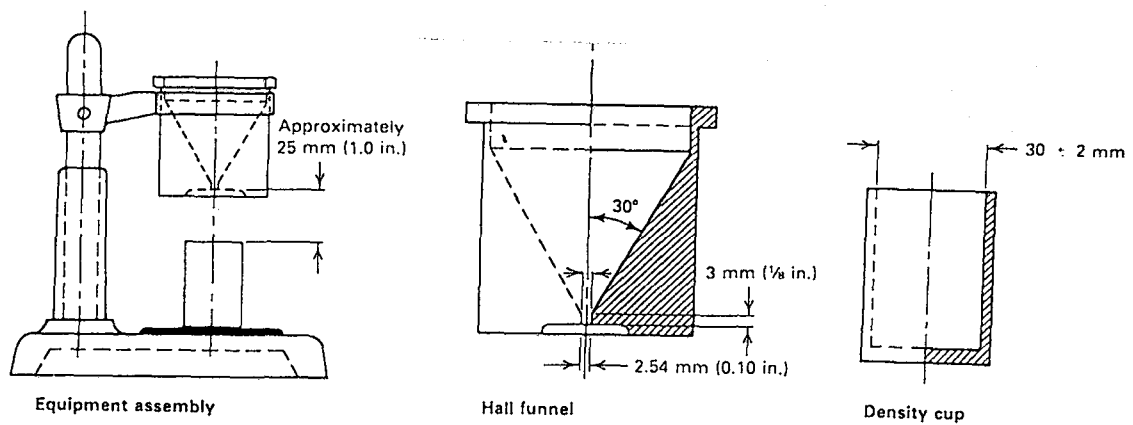


Fig.3.3 Cross-sectional view of Hall flowmeter.

determined. The tare weight divided by 25 percent is the apparent density in g/cm^3 . A Hall flowmeter is shown in Fig.3.3.

3.4.5 Tap Density Of Metal Powders

Tap density is defined as the density of a powder when the volume receptacle is tapped or vibrated under specified conditions. Tapping or vibrating a loose powder induces movement and separation and lowers the friction between the powder particles. This short-term lowering in friction results in powder packing and in a higher calculated density of the powder mass. Tap density is always higher than the free-flow apparent density.

Tap density is a function of particle shape, particle porosity, and particle size distribution. It is commonly included as a control specification for metal powder, but is used in other industrial applications as a practical measure of the degree of powder packing that occurs in containers.

The amount of increase from apparent to tap density depends to a great extent on particle shape. Usually the lower the apparent density, the higher the percentage increase in density on tapping.

To determine tap density, a standard weight (usually 50 g) of powder is weighed to ± 0.01 g. The powder is poured into a clean, dry graduated cylinder, taking care that a level surface of powder is obtained.

The powder is settled in the cylinder by mechanical or hand tapping. If mechanical tapping (Fig.3.4) is used, the filled cylinder is placed in the mechanical apparatus, which is operated until no further decrease in the volume of the powder is observed.

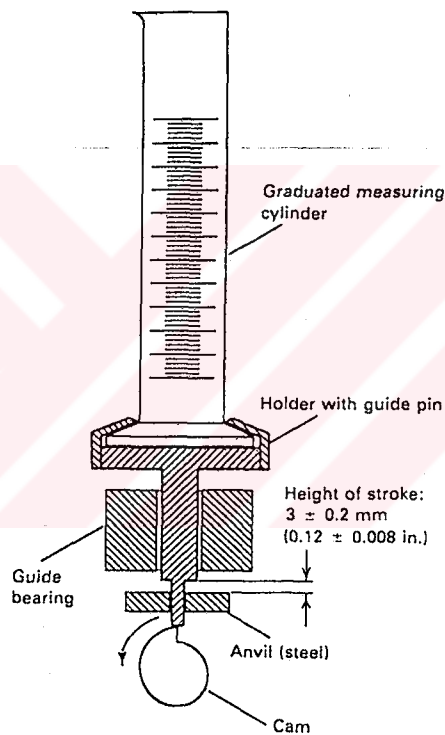


Fig.3.4 Diagram of tapping apparatus.

3.4.6 Flow Rate Of Metal Powder

Flow rate is the time required for a powder sample of a standard weight (50 g) to flow under atmospheric conditions through a funnel into the cavity of a container or mould. A determination of the flow rate of a powder is important in high-volume manufacturing, which depends on rapid, uniform, consistent filling of the die cavity.

Poor flow characteristics cause slow and nonuniform press feeding and difficulty in ensuring even fills of the die cavity.

Before a powder is used in production, its flow characteristics must be known, because some compacting tools require a free-flowing powder, while others can be used with a relatively poor-flowing powder. The term free-flowing refers to those physical properties of a powder, such as composition, particle fineness, and particle shape, that permit the powder to flow readily into the die cavity.

Flow of metal powders is determined by standard methods developed by the American Society for Testing and Materials (ASTM) and the Metal Powder Industries Federation (MPIF).

The device most commonly used for measuring flow rate is the Hall flowmeter (Fig.3.3), taken from ASTM B 213 and MPIF 3. The test equipment consists of a funnel with a calibrated hole 2.5 mm (0.1 in.) in diameter. The funnel, which is made of aluminum alloy 6061-T6, is supplied with a smooth finish to minimize wall friction.

With the help of a stopwatch and weighing balance, the flow rate of metal powders can be easily determined. A dry 50-g weight sample is transferred to the funnel, the orifice of which is covered with the operator's fingertip. The stopwatch is started when the fingertip is removed and is stopped when the last quantity of the powder leaves the funnel. The flow rate (s/50 g) of the sample is reported as the elapsed time in seconds for 50 g of powder to flow through the orifice. A powder that does not flow through a 2.5-mm (0.1 in.) orifice Hall funnel, with or without an external impulse, is said to be a nonfree-flowing powder (as per ASTM B 213 and MPIF 3 method).

3.4.7 Angle Of Repose

The angle of repose of an aggregate, or the angle the surface of an unconstrained pile of solids with the horizontal, is of practical interest rather than of theoretical concern. Of the various physical properties of bulk powders, the angle of repose is the easiest to obtain. It is closely related to interparticle friction and the flowability of cohesionless materials. This property is frequently used to characterize powdered materials.

The angle of repose of a powdered material does not always give satisfactory reproducibility and is often masked by other factors that are not inherent to the material (most frequently, the presence of a liquid). Thus, before a standard measuring method that provides reasonable reproducibility is developed, its usability as a measure of powdered material property must be established.

Several methods have been used to measure the angle of repose of materials. Train, studied the angle of repose of a number of grades of glass spheres, lead shot, and silver and using four different methods, as illustrated in Fig.3.5. These methods are:

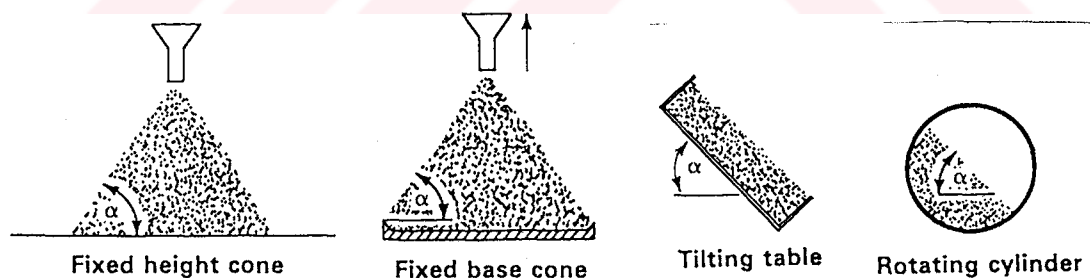


Fig.3.5 Four methods used to measure the angle of repose [19]

3. 5 TESTS SIMULATING THE BEHAVIOUR OF THE POWDER IN FABRICATION

3.5.1 Compressibility of Metal Powders

Compressibility and compactibility are terms used to describe the extent to which a mass of powder can be densified by the application

of pressure. Compressibility of a powder is a major factor in the design of pressing tools, the part density attainable, and the size of press needed to press to that density. A related term, compression ratio, is the ratio of the final pressed density to the apparent density of the powder. This ratio determines how deep the part die must be in order to hold all the powder needed to meet the specified part density. Powders of high apparent density are preferred, because tooling can be made shorter and thus stronger.

Typically, a cylindrical or rectangular test piece is made by pressing powder in a die, with pressure applied simultaneously from top and bottom. The pressure required to achieve a specified density is a measure of compressibility. Compressibility can also be specified as the density achievable at a given pressure. By plotting the density obtained by a series of increasing levels of pressure against these pressures, a compressibility curve is developed.

3.5.2 Green Strength of Compacted Metal Powders

Green strength is the mechanical strength of a green—that is, unsintered—powder compact. This property is very important, as it determines the ability of a green compact to maintain size and shape during handling prior to sintering. Strength of green compacts results mainly from mechanical interlocking of irregularities on the particle surfaces, which is promoted by plastic deformation during pressing. Much information on green strength is available, especially regarding iron and copper, which are the most commonly used powders in the P/M industry. The details are given in specifications MPlF 15-62.

Although metal powder compacts are seldom used in the green condition, green compacts must be strong enough to resist abrasion and breakage while being transferred from a compacting press to a sintering furnace. This is particularly important for thin parts, thin sections of large parts low-density parts, and part edges.

The Rattler test, adapted from a method used to test paving bricks, was used in the early P/M industry to determine green strength. Five compacts of predetermined weight and size were placed in a bronze-screened cylinder and rotated for a certain number of revolution for a specified time. The compacts were then removed from the cylinder, weighed, and the weight loss determined. The Rattler test provided information on the abrasion resistance of a compact and its ability to retain its shape (edge stability).

3.5.3 Dimensional Change of Sintered Metal Compacts

Changes in dimensions of metal powder compacts can occur during the production process. The ability to control or forecast the changes is an important facet of the fabrication process, because the attractive economics achieved through near-net shape manufacturing is the principal drive for the process. The metal powder blend employed, as well as various processing parameters, determines whether shrinkage, growth, or virtually no change in dimension will be exhibited by the finished metal powder compact. Generally, the size change is defined as the linear difference between die size and the size of the sintered part after cooling to room temperature, expressed as a percentage. However, the size change is occasionally specified as the difference between the green part and the size of sintered, cooled P/M part.

Specifications that describe the standard test methodology for determination of dimensional change of metal powder specimens as a result of sintering include ASTM B 610, MPIF44, and ISO 4492. These standard methods employ a rectangular test bar that is pressed to a uniform specified density from the powder being tested. The test specimen is sintered simultaneously with bars from an approved standard powder lot of the same composition, preferably under the actual production conditions. Dimensional changes in the bar made from the powder being tested are compared with those of the standard powder test bars to determine whether the test powder is satisfactory.

3.6 DISTINGUISHING CHARACTERISTICS OF METAL POWDER

As explained in chapter 2 and 3, powder production methods control the characteristics of the powders produced, and these characteristics control the mechanical properties of the parts produced from these powders.

Some distinguishing characteristics of metal powder produced by various present commercial methods are given in Table 3.2.



TABLE 3.2 SOME DISTINGUISHING CHARACTERISTICS OF METAL POWDERS MADE BY VARIOUS PRESENT COMMERCIAL METHODS [2]

<i>Method of production</i>	<i>Typical purity^a</i>	<i>Shape</i>	<i>Particle characteristics</i> <i>Mesher available</i>	<i>Compressibility (softness)</i>	<i>Apparent density</i>	<i>Green strength</i>	<i>Growth-with-copper of iron^b</i>
Atomization	High 99.5+	Irregular to smooth, rounded dense particles	Coarse shot to 325 mesh	Low to high	Generally high	Generally low	High
Gaseous reduction of oxides	Medium 98.5 to 99.0+	Irregular, spongy	Usually 100 mesh and finer	Medium	Low to medium	High to medium	Low
Gaseous reduction of solutions	High 99.2 to 99.8	Irregular, spongy	Usually 100 mesh and finer	Medium	Low to medium	High	Iron not produced by this method
Reduction with carbon	Medium 98.5 to 99.0+	Irregular, spongy	Most meshes from 8 down	Medium	Medium	Medium to high	Medium
Electrolytic	High+ 99.5+	Irregular, flaky to dense	All mesh sizes	High	Medium to high	Medium	High
Carbonyl decomposition	High 99.5+	Spherical	Usually in low micron ranges	Medium	Medium to high	Low	?
Grinding	Medium 99.0+	Flaky and dense	All mesh sizes	Medium	Medium to high	Low	High

^a Purity varies with metal powder involved. Above are estimates of typical purity.

^b Growth-with-copper of iron is increase in radial dimension of compacted iron plus copper powders during sintering.

CHAPTER 4

CENTRIFUGAL ATOMIZATION

4.1 INTRODUCTION

The atomizing of molten metals into small particles can be carried out in many ways, but the major methods are gas, water and centrifugal atomization. The three processes are essentially different in character, in the powder they produce and in the amount of energy they consume. The gas atomization process is accepted as having very low energy efficiency (approx. 3 % efficient) and is expensive when an inert gas other than nitrogen has to be used. The metal powder produced are mostly spherical and are therefore not generally acceptable for making cold compacts.

Water atomizing uses large quantities of energy to supply the water at high pressures (approx. 4 % efficient). The metal powders, although suitable for cold compacting, are produced in a wet condition and also have a perceptible oxygen content [34].

Centrifugal atomizing is not so widely used as the above, but has the distinct advantages that the energy used in atomizing is very low. The metal powders produced, are of a large size ($>200\mu\text{m}$) and large size distribution. The efficiency of the centrifugal atomization is approx. 10 to 30 % depending upon the type of the rotating disc. Since the solidification of the particles occur in flight by blasting the stream of helium, particles are generally spherical as produced in gas atomization.

In the present work, general set-up of centrifugal atomization unit was modified to improve the size distribution and shape of produced powders. First different disc geometries were used to vary the droplet formation conditions. Flat discs, cup shaped discs and vaned spray drying type discs were designed and constructed for this purpose. Later, further modification was carried out in the cooling conditions of the metal droplets. Instead of an inert gas medium a forced water vortex wall was created in a steel cylinder as the cooling media. Flight of the droplets in air was for a very short while and the solidification was generally taking place in water. Powders produced showed the characteristics of conventional water atomized powders.

4.2 MECHANISMS OF ATOMIZATION

In centrifugal atomization, the liquid metal is centrifugally accelerated to high velocity before being discharged into a gas atmosphere. The liquid metal is distributed centrally on the rotating disc. The liquid extends over the rotating surface as a thin film.

The degree of centrifugal atomization depends upon peripheral speeds, feed rate, liquid properties and atomizer design. The maximum centrifugal energy is imparted to the liquid metal when the liquid acquires the disc peripheral speed prior to discharge. If a flat smooth disc is rotating at high speed and liquid metal is fed on to its top surface, severe slippage occurs between the liquid metal and disc. The velocity of liquid from the disc edge is much lower than the disc peripheral speed. Conditions of no slippage occur at very low speeds, but available centrifugal energy permits only the smallest of feed rates to be satisfactorily atomized. Slippage can be reduced by increasing friction between liquid and rotating surface. This is often done by feeding to liquid metal on to the lower surface of a disc shaped as an inverted plate, bowl or cup. As the liquid is flung outwards due to

centrifugal force, the liquid film is pressed against the disc surface[58].

Radial vaned type disc which is used in spray drying processes prevent the slippage. In this case the liquid is confined to the vane surface, and at the periphery the maximum liquid release velocity possible is attained. The maximum release velocity is the resultant of radial and tangential components acquired by the liquid.

The mechanism of atomization on the flat disc and vaned disc will be discussed seperately in this chapter.

4.2.1 Flat Disc Atomization

For a flat smooth disc, the degree of atomization obtainable will depend upon the magnitude of feed acceleration toward the edge over the smooth surface. The final liquid release velocity depends upon the slippage between liquid and rotating surface. The extent of slippage depends upon feed rate and physical properties of the liquid, namely the viscous drag and the ability of the liquid to wet the surface.

The disintegration of liquid into droplets from a rotating disc is governed by[58]:

- a) the viscosity and surface tension of the liquid metal,
- b) inertia of the liquid metal at the disc periphery,
- c) frictional effects between the liquid metal droplets and surrounding air at the point of droplet release from the disc,
- d) readjustment of shear stresses within the liquid metal droplet once the droplet is airborne.

At low disc peripheral speeds, the liquid metal viscosity and surface tension are the predominating factors. The higher the disc speed, the more inertia and air friction contribute to the mechanism of droplet

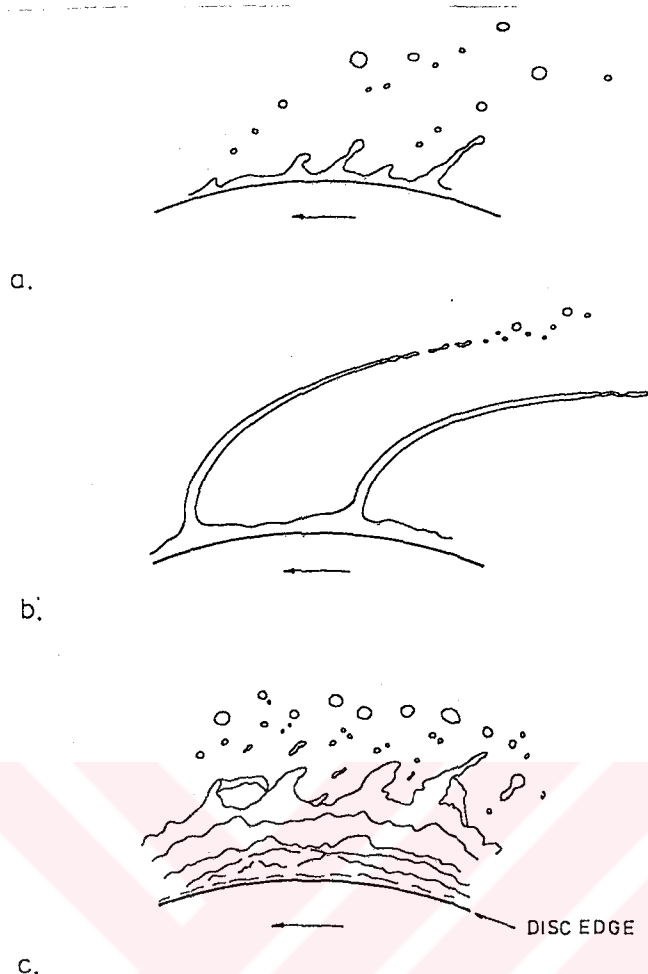
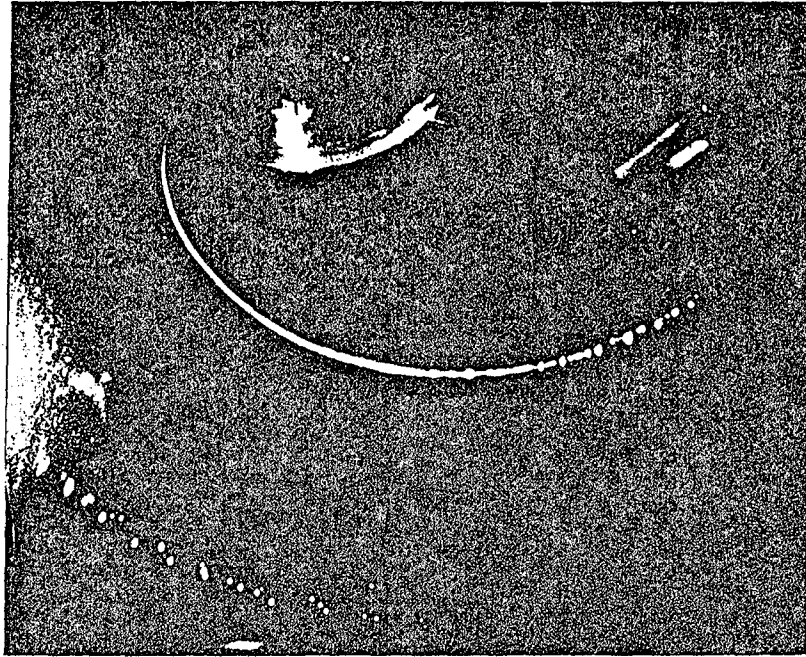


Fig.4.1 Mechanisms of atomization. (a) Direct droplet formation. (b) Ligament formation. (c) Sheet Formation [58].

formation. Due to liquid metal slippage over the disc surface, liquid metal inertia never becomes high and as release velocities are low, air frictional effects are minimized too. Only in the commercial atomizer designs of vaneless discs do inertia and air friction play a dominant role at high feed rates and high liquid metal release velocities

For smooth flat discs, when viscosity and surface tension predominate the mechanism of atomization, sprays are formed by individual formation and release of droplets from the disc edge. This is shown diagrammatically in Fig.4.1a. Feed rates and disc speeds are very low. Sprays consist of two or three prominent droplet size, i.e. parent droplet and two satellites.



(a)



(b)

Fig.4.2 Mechanisms of atomization (represented photographically)
a) Ligament formation. (b) Transition between ligament and sheet formation [59,60].

With continued disc speed increase and higher feed rates, the direct droplet mechanism changes to one of ligament break-up. The point concentrations of liquid that gave rise to direct droplet formation contain more liquid, and ligaments being to extend out from

disc edge. The ligaments again disintegrate into sprays of parent and satellite droplets as illustrated in Fig.4.1(b). Larger parent droplets are formed from higher feed viscosities and surface tensions. Increases in feed viscosity increase the proportion of satellite droplets in the spray. Spherical droplets are formed irrespective of the surface tension value.

The mechanisms illustrated in Fig.4.1(a and b) are controlled by the physical properties of the feed liquid metal. The transition between the predominance of liquid metal properties and of inertial forces occurs when the liquid metal ligaments join to form a liquid metal sheet extending from beyond the disc edge (Fig.4.1(c)). The mechanism of liquid metal atomization at the transition between liquid metal ligament and sheet formation is shown photographically in Fig.4.2. Atomization by liquid metal sheet formation is often referred to as the velocity spraying mechanism [61]. The mechanism is accentuated by highly viscous liquids. The sheet disintegrates giving a spray of broad droplet size distribution. With further increase of disc speed at constant feed rate the liquid metal sheet retracts towards the disc edge. If feed rate is increased with disc speed, velocity spraying continues. If slippage over the disc is minimized or prevented, liquid metal release velocity from disc edge becomes high enough to enable air frictional effects at the liquid metal-air interface to become the controlling atomization mechanism. The mode of disintegration of the retracting sheet makes the formation of completely homogeneous sprays appear a remote possibility. Use of high viscosity and surface tension reduces the broad distribution as does increase of disc peripheral speed at constant feed rate. To produce narrow distribution, high speeds are required at low disc loadings.

Bauer and Kruger [62] and Mehrhardt [63] discuss current knowledge of atomization mechanisms from vaneless discs and theory pertaining to flow over the disc and release of liquid metal from the

disc edge is discussed. Photographic evidence of the mechanisms involved have assisted visual appreciation of the atomization process.

Once the droplets have left contact with the disc edge and are airborne further disintegration can take place due to readjustment of shear stresses set up within the liquid during liquid flow over the disc surface. Droplet disintegration by this mechanism is difficult to distinguish from disintegration by air friction effects, which also causes droplet distortion when droplets are airborne. In centrifugal atomization the air friction effects are considered the major mechanism, but atomization in low vacuum has shown the mechanism of shear stress readjustment to occur liquid when flow is turbulent.

a) Flow Over Flat Discs

The mechanism of liquid atomization has been reported widely on flat vaneless discs. With the degree of atomization dependent upon the velocity of liquid release, which in turn depends upon the slippage between liquid and surface, Frazer [64] defines the occurrence of severe slip by the relation (4.1), where M = mass feed rate (lb/hr), μ = feed viscosity (cp) and d = disc diameter (ft)

$$\frac{M}{\pi \mu d} \geq 1440 \quad (4.1)$$

Quite high feed rates that can be handled on a disc. Atomization by flat discs would be poor, illustrating the additional factors like air-liquid frictional effects that make for effective liquid disintegration.

Frazer [64] proposed functions to express flow conditions over an ideal disc surface, where liquid break-up at the disc edge is due to ligament or sheet disintegration. The transition between the two disintegration mechanism is stated as a function of two dimensionless parameters A^1 and B^1 where

$$A^I = N d \left\{ \frac{\rho d}{\sigma} \right\}^{1/2} \quad (4.2)$$

$$B^I = \frac{Q}{d} \left\{ \frac{\rho}{\sigma d} \right\}^{1/2} \left\{ \frac{\mu}{(\rho \sigma d)^{0.5}} \right\}^{1/6} \quad (4.3)$$

The parameters show the roles played by viscosity and surface tension on resulting liquid break-up conditions. The transition is represented on Fig.4.3 by a line of separation.

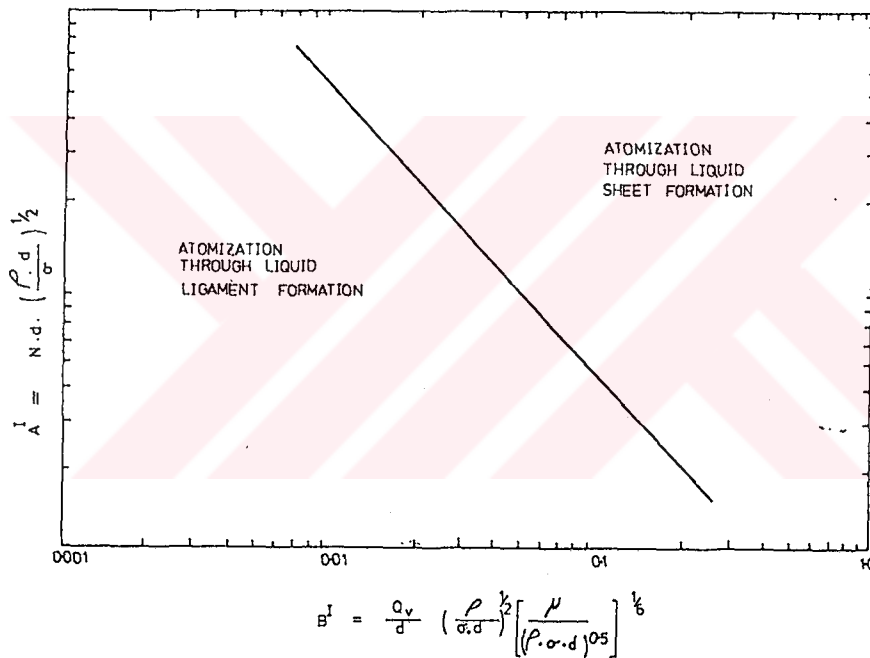


Fig.4.3 Atomization mechanism for rotating discs [64].

(Relationship between operating variables and atomization mechanism)

Six equations to predict droplet size from smooth flat vaneless discs are given in Table 4.1. Other equations in this field are given by Lapple [65] and Dombrowski [66]. All are applicable to the simplest of systems involving low feed rates of low viscous liquids. Surface tension and liquid density appear as the only liquid properties of influence, which is misleading as viscosity is of prime importance. This is

illustrated in equation (4.5), where the author claimed close agreement between experimental and predicted results for low viscous liquids but not for high viscous liquids. Droplet size appears inversely poroportional to the first power of disc speed for these simple systems. Sprays are homogeneous to a high degree [67].

The conditions of experimentation produced uniform sprays, although the presence of satellite droplets was evident. The D_{\max} value in the Bar[68] equation refers to the parent droplet. Frazer [64], Walton and Prewett[69] and Hege [70]give the average diameter of the spray. Oyama and Endou[71] use the Sauter mean diameter. In Table 4.1; D is microns, N is rev/min, d is cm, σ is dynes/cm, ρ is g/cm³, Q is cm³/sec.

The equations of Table 4.1 are of limited interest to spray drying conditions. However, the equations indicate the relationships between droplet size and the operation variables; relationships that do hold into commercial atomization conditions.

$$D \propto N^{-p}; \quad D \propto \sigma^q; \quad D \propto d^{-r}; \quad D \propto Q^s$$

where p,q,r,s are respective integers, the values of which depend upon atomizer operating conditions.

4.2.2 Vaned Disc Atomization

The mechanism of atomization applicable for vaned discs is similar to that discussed for flat vaneless discs in section 4.2.1. Mechanism are shown photographically by Marshall [59] and Kurabayasi [60]. At low speeds and feed rates, viscous and surface tension forces predominate to give direct droplet formation. For intermediate speeds,

TABLE 4.1 DROPLET SIZE PREDICTION FOR SMOOTH FLAT DISCS

<i>Atomization mechanism</i>	<i>Equation</i>	<i>Investigator</i>	
Direct droplet formation	$D_{av} = 7.6 \left\{ \frac{\sigma g^{1/2}}{F_R P} \right\} * 10^4$	Hege	(4.4)
	$D_{max} = \frac{64}{N} \left\{ \frac{\sigma}{dp} \right\}^{1/2} * 10^4$	Bar	(4.5)
Ligament break-up	$D_{av} = 3 \left\{ \frac{\sigma g^{1/2}}{F P} \right\} \left\{ \frac{C_k^{1/12}}{V} \right\} * 10^4$	Hege	(4.6)
	$D_{max} = \frac{52.2}{N} \left\{ \frac{\sigma}{dp} \right\}^{1/2} * 10^4$	Walton, Prewett	(4.7)
	$D_{vs} = \frac{2.67Q^{0.2}}{Nd^{0.3}}$	Oyama, Endou	(4.8)
Sheet disintegration	$D_{av} = \frac{45.5}{N} \left\{ \frac{\sigma}{dp} \right\}^{1/2} * 10^4$	Frazer	(4.9)

$C_k = 0.5-1$

the disintegration of liquid ligaments extending out from vane edge is by centrifugal and to a lesser extent by gravitational forces. In the commercial range of conditions (high liquid flows at high wheel peripheral speeds), liquid disintegration occurs right at the wheel edge by frictional effects between air and the liquid surface as liquid emerges as a thin film from the vane. The mechanism does not lend itself to the formation of homogeneous spray formation, although sprays of small droplet sizes can be produced. Increasing the viscosity and surface tension of the liquid will act to increase the spray uniformity, but at the expense of a low mean droplet size. To obtain optimum droplet size uniformity for a given feed rate the maintenance of the following six conditions is essential:

- 1) Vibrationless disc rotation.
- 2) Large centrifugal forces compared with gravitational forces (i.e. high peripheral speeds).
- 3) Smooth vane surfaces.
- 4) Uniform liquid feed rates.
- 5) Complete wetting of the vane surface.
- 6) Uniform distribution of feed to the vaned disc.

a) Flow Over a Vaned Disc

Liquid fed on to a disc moves across the surface until contained by the rotating vane. Liquid flows outwards under the influence of centrifugal force and spreads over the vane wetting the vane surface as a thin film. At very low liquid vane loadings, the thin film can split into streams.

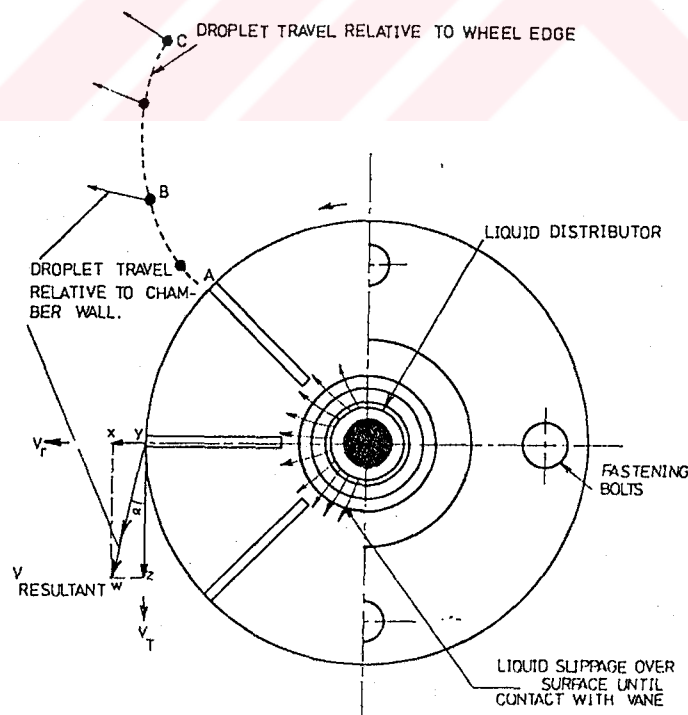


Fig.4.4 Liquid flow to and from edge of the vaned disc atomizer [59].

Unlike the flat smooth vaneless disc, no liquid slippage occurs on a wheel once liquid has contacted the vane. The vanes, whether radial or curved, prevent transverse flow of liquid over the surface. The basic equations developed in the previous section, is not valid. For vaned discs, only viscous resistance is acting.

Droplet travel from a wheel is shown in Fig.4.4. The liquid film on leaving the vane edge has radial (XY) and tangential (YZ) velocities giving a resultant component (WY). The angle of release is less than 45° to the disc edge. For commercial vaned discs, the radial velocity component is much smaller than the tangential, and release velocity approximates to the peripheral disc velocity, and at an angle of release approaching the tangent to the wheel edge [58].

D) Radial Velocity (V_r)

Radial velocity of the liquid film at the wheel edge is calculated from differential equations derived from consideration of forces acting upon the liquid film [59].

Considering the forces on the element (dr) (Fig.4.5)

$$P = mf \quad (4.10)$$

where the force for acceleration is provided by the centrifugal force-frictional force.

Thus

(a) Mass of the element (m) = $bh \, dr \rho_1$

(b) Centrifugal force ($m\omega^2 r$) = $bh \, dr \rho_1 \omega^2 r$

(c) Frictional force (F) (at the vane surface) ($y = \theta$)

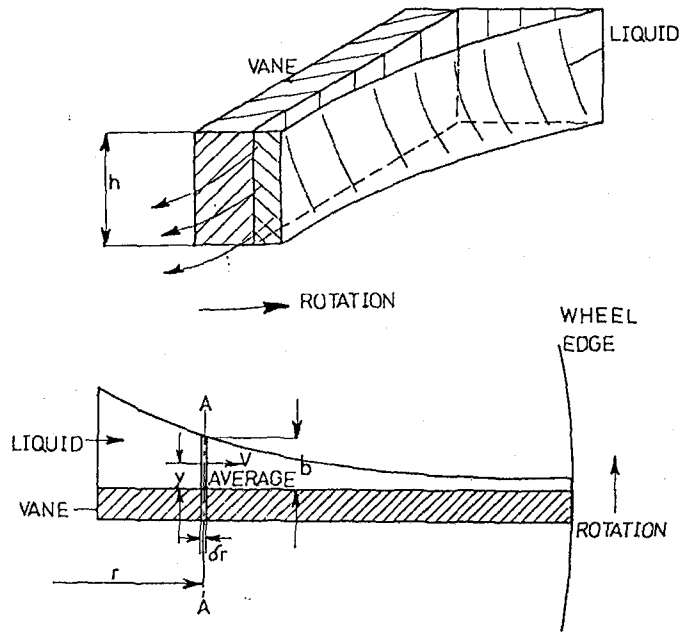


Fig.4.5 Flow of the liquid metal through the vane

Where

$$\mu = \frac{\text{shear force}}{\text{shear rate}} = \frac{F/A}{dV/dr} = \frac{F/h*(dr)}{(dV/dr)_{y=0}}$$

$$F = \mu h dr \left\{ \frac{dV_r}{dr} \right\}_{y=0}$$

$$(d) \text{ Acceleration} = \left\{ \frac{dV_{AV}}{dt} \right\}$$

Substituting in Eqn.4.10

$$hh dr p_1 \omega^2 r - \mu h dr \left\{ \frac{dV_r}{dr} \right\}_{y=0} = hh dr p_1 \left\{ \frac{d(V_r)_{AV}}{dt} \right\} \quad (4.12)$$

With the assumption of laminar flow (no slippage and only viscous resistance) a parabolic velocity gradient through the film exists, where

$$\left\{ \frac{dV}{dy} \right\}_{y=0} = \frac{3V_r}{b} \quad (4.13)$$

As there is no hold-up of liquid on the vane, the continuity equation applies, where

$$b = \frac{Q_v}{h V_r} \quad (4.14)$$

where Q_v = volumetric flow rate per vane.
Substituting Eq.4.13 and Eq.4.14 in Eq.4.12

$$\frac{Q_v}{hV_r} h dr p_1 \omega^2 r - \mu h dr \frac{3V_r^2}{Q_v} = \frac{Q_v}{hV_r} h dr p_1 \frac{dV}{dt}$$

and dividing through by $\left\{ \frac{Q_v dr p_1}{V_r} \right\}$

$$\omega^2 r - \frac{\mu h dr}{Q_v} \frac{3V_r^2 h V_r}{Q_v dr p_1} = \frac{Q_v h dr p_1}{hV_r} \frac{dV}{dt} \frac{V_r}{Q_v dr p_1} \quad (4.15)$$

$$\omega^2 r - \frac{3\mu h^2 V_r^3}{p_1 Q_v^2} = \frac{dV}{dt}$$

However

$$\frac{dV}{dt} = \frac{dr}{dt} \frac{dV}{dr} = V_r \frac{dV}{dr}$$

The general form of the non-linear differential equation, representing flow over vane

$$V_r \frac{dV}{dr} + R^* V_r^3 - S^* r = 0 \quad (4.16)$$

where

$$R^* = \frac{3\rho h^3}{\rho_1 Q_v^2}; \quad S^* = \omega^2$$

Dimensions of R^* and S^* are (time, length⁻²) and (time⁻²).

Marshall [59] suggests that for vaned disc sizes and peripheral speeds used in industrial spray drying liquid acceleration along the vane has ceased upon reaching the disc edge. The radial velocity is given by

$$V_r = \left\{ \frac{\rho_1 Q_v^2 \omega^2 r}{3 \rho h^3} \right\}^{1/3} \quad (4.17)$$

The error in this simplification is minimal, but Marshall [59] has stated the error can be reduced further if Eqn.(4.16) is used where X has values greater than 1.

$$Z = X^{1/3} - \frac{1}{9X} - \frac{1}{27X^{1/3}} - \frac{1}{218X^{2/3}} \quad (4.18)$$

where

$$X = r(R^* \omega^2)^{1/2} \quad \text{and} \quad R^* = \left\{ \frac{3\mu h^2}{P_1 Q_V^2} \right\}$$

$$Z = V_r \left\{ \frac{R^*}{\omega} \right\}^{1/2}$$

A 5 in (125 mm) 24-vaned disc atomizing water gives values of X as shown in Table 4.2. Eqn.(4.18) is valid for calculating radial velocities in this case.

TABLE 4.2 VALUES OF $X = r(R^* \omega^2)^{1/2}$

Feed rate(lb/min)	wheel speed (rev/min)		
	15750	20600	24000
4.0	28	32	35
7.0	16	18	20
10.0	11	13	14

Frazer [64] has forwarded an estimation of radial velocity (ft/sec) from a vaned atomizer disc.

$$V_r = 0.043 \left\{ \frac{P_1 \pi^2 N^2 d Q^2}{\mu h^2 \pi^2} \right\}^{1/3} \quad (4.19)$$

Where d is ft, μ is cP, h is ft, N is rev/min, Q is ft³/min, P_1 is lb/ft³.

The graph of flow rate plotted against radial velocity is a straight line on log-log plot.

ii) *Tangential Velocity* (V_T). The vanes prevent slippage and the liquid acquires the peripheral velocity of the wheel on release.

$$V_T = \pi d N \quad (4.20)$$

iii) *Resultant Release Velocity* (V_{res}). The resultant release velocity is the square root of the sum of the radial and tangential components.

$$V_{res} = (V_r^2 + V_T^2)^{1/2} \quad (4.21)$$

iv) *Angle of Liquid Release* (α). The angle of liquid release follows from Eqn.(4.21) by basic geometry

$$\alpha = \tan^{-1} \left\{ \frac{V_r}{V_T} \right\} \quad (4.22)$$

In practice α is very small, and V_{res} approximates to the peripheral speed of the vaned disc.

b) Effect of Operating Variables on Droplet Size

Operational variables that influence droplet size produced from discs are speed of rotation, disc diameter, disc design (number and geometry of vanes or bushings), feed rate, viscosity of feed and air, density of liquid metal and air, surface tension of liquid metal.

The effect of these variables on mean droplet size of a spray is best studied through dimensionless analysis, where variables are grouped to represent basic atomization mechanisms. Forms of Reynolds number

(defining the inertial and viscous force ratio on the liquid) and Weber number (defining the inertial to surface energy ratio) are commonly used. Friedman, Gluckert and Marshall [72] used the following groupings where the atomizer wheel speed conveniently appears in one group only (M_p = mass feed rate per unit wetted periphery).

$$\frac{D_{vs}}{r} = K \left\{ \frac{M_p}{\mu} \right\}^a \left\{ \frac{M_p}{\rho N r^2} \right\}^b \left\{ \frac{M_p}{\sigma \rho L} \right\}^c \left\{ \frac{L}{r} \right\}^d$$

Groups having exponents a,b are related to Reynolds number, the remainder to Weber number.

Effect of liquid properties and liquid release velocity on droplet size has already been introduced under the section 4.2.1. Several investigators have studied the effect of these variables and others, and reported that the variables of most influence on droplet size in commercial atomization conditions are peripheral disc speed, and liquid loading on the vanes (volumetric basis).

4.2.3 Particle Shape

The set-up developed during the investigation produces droplets by centrifugal atomization mechanisms. Initial cooling of the droplet leaving the disc, is through gas cooling in air. Later, it enters the surrounding water wall. Powder particle shape is largely dependent to cooling media. Droplets forming directly, from ligament or from sheet try to become spherical due to surface tension and air friction forces. Surface tension forces try to reduce, surface area to mass ratio. Cooling in air is rather slow, and therefore droplets have time to become spherical. If they are still not solidified, they enter water wall in viscous liquid state and change shape due to sudden impact

with water. Cooling rate in water is very high, so droplets can not change their shapes further.

So, cooling of droplets in the developed atomization set-up is composed of gas cooling followed by water cooling. Previous works regarding to powder particle shape in gas cooling and water cooling will be given in this section.

a) Gas Cooling

Rao [73] has developed the only known model for predicting particle shape. Two submodels were developed for solidification time (as a function of particle velocity, size, superheat, and fluid properties) and for shape change with the time (as a function of initial shape, drag, and fluid properties).

The solidification model was based on heat transfer during convection cooling of a sphere in flight; radiation and other flow effects were shown previously by Rao [74] to be negligible. Combining the convection rate with the transient energy balance for a particle leads to the expression for solidification time

$$t_s = (\rho C_p D_o / H) \ln [(T_m - T_g) / (T_s - T_g)] \quad (4.23)$$

where ρ is the metal density, C_p the specific heat of the liquid metal, D_o the particle diameter, H the convection coefficient, T_m , T_g , and T_s the temperatures of liquid metal, atomizing gas, and solidification, respectively.

The shape change model was based on control-volume force balance for an elongated, ligament-shaped particle. Four forces were considered:

- (a) surface tension,
- (b) viscous damping,
- (c) inertia, and
- (d) surface drag.

Drag was shown to have a small effect and for simplicity, was neglected.

The resulting differential equation [Rao, 73] predicted oscillations with an exponential decay function and characteristic time t_c . Characteristic time is a function of particle properties, including size and liquid metal viscosity. The result is prediction of the shape parameter as a function of time

$$L/D = 1 + (L_0/D_0 - 1) \exp [- t/t_c(Y/m)]^{1/2} \quad (4.24)$$

where m is the particle mass and L_0/D_0 is the initial length-to-diameter ratio of the ligament. Setting time t in Eqn. (4.24) equal to the solidification time t_s , in Eqn.(4.23), now the solidified particle shape parameter L/D can be calculated.

Using the experimental parameters for nitrogen atomization of cast iron and assumed initial L_0/D_0 values of 2.2, 2.7 and 3.2, predicted particle shapes were calculated as a function of particle size. For one particular set of conditions, these relationships are shown in Fig.4.6. This is the first known theoretical prediction of particle shape. Additional breakup models predicting initial shape L_0/D_0 would allow calculation of shape from primary atomization variables. Considerable further study is required, however, before such models can be developed.

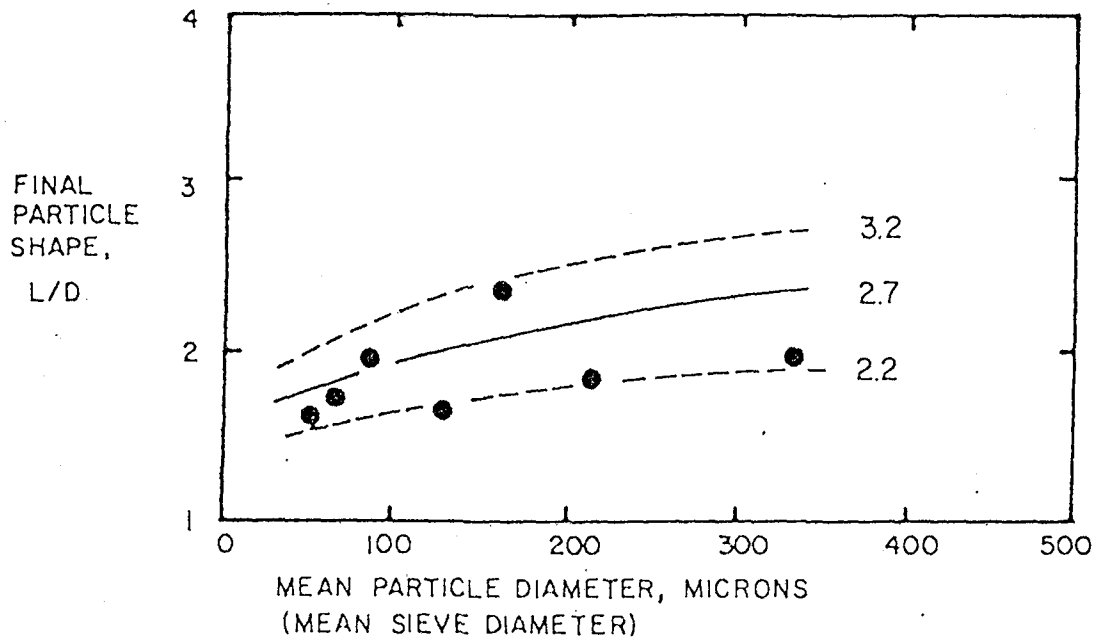


Fig.4.6 Variation of the particle shape with particle size in gas atomization of cast iron: comparison of theoretical prediction, Eqns. (4.23) and (4.24) (---, —) with experimental data (●). Jet distance 73 mm, jet pressure 4.14 MPa, jet velocity 62 m/s; initial shapes (L_0/D_0) for predicted curves are 3.2, 2.1, 2.2 [73].

b) Water Cooling

Very few systematic and quantitative studies of the effect of water jet parameters on powder shape have been published. One of the few is that of Grandzol [75], who did exploratory work on factors involving shape. It was noted that two different types of shape (smooth and spherical, rough and irregular) appeared in these and other samples, so that these shapes did not lend themselves to shape characterization parameter used previously, such as sphericity or length-to-diameter ratio. Grandzol defined shape by the fraction (F_i) of particles which were rough and irregular, as opposed to those which were smooth and spherical. The rough surface is indicative of a rapid quench, with some irregularity due perhaps to coalescence of particles.

A plot of rough fraction F_i versus size for 4620 steel powders, Fig.4.7, indicated a significant decrease in irregular shape with larger sizes. Specifically, the irregular fraction decreased from about 80 % at 40 μm to about 30 % at 120 μm .

When rough fraction F_i is plotted versus water jet pressure (or jet velocity) the scatter was greater than with Fig.4.7, but increasing pressure did result in a higher rough fraction, as expected. Changes in water jet flow rate at constant pressure, on the other hand, did not appear to change the rough fraction.

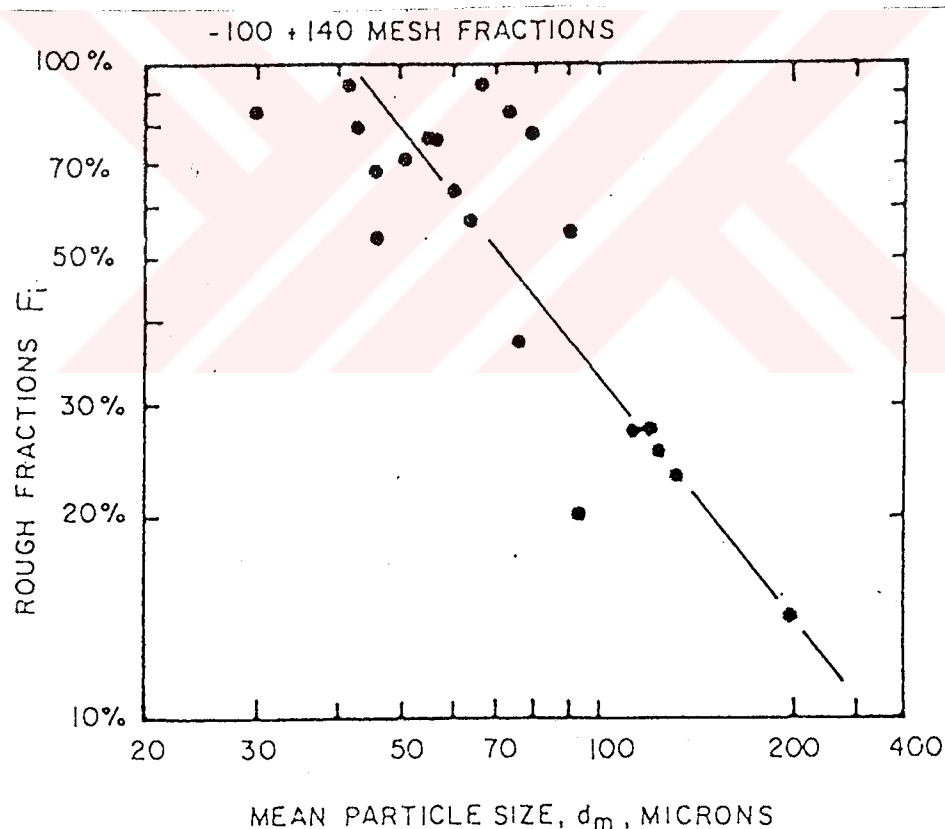


Fig.4.7 Fraction of rough particles F_i as a function of mean particle size in water atomization for 4620 steel [75].

CHAPTER 5

DESIGN AND CONSTRUCTION OF EXPERIMENTAL SET-UP

5.1 INTRODUCTION

The parameters that affected on the characteristics of the metal powders produced by the centrifugal atomization are discussed in the previous chapters . These parameters can be divided into six main groups as follow;

- a) The temperature of liquid metal,
- b) Flow rate of liquid metal,
- c) Rotating speed of atomizer disc,
- d) Shape of atomizer disc,
- e) Cooling rate of the particles,
- f) Type of liquid metal.

The aim of this work is to investigate the effect of these parameters on the characteristics of metal powders and improving the method of centrifugal atomization. Therefore the designed set-up must control these parameters at various ranges. A lot of runs should be performed to analyse their effects on the powder characteristics.

The set-up designed and constructed during this work consists of following units:

- a) Melting unit,
- b) Tundish,
- c) Atomizer disc and the drive system,
- d) Cooling media.

5.2 DESIGN OF THE MELTING UNIT AND THE TUNDISH

In the production of metal powders by the method of centrifugal atomization, the molten metal is carried from a furnace by means of a crucible. The liquid metal is poured into tundish which is used to control the flow rate of the molten metal.

The behaviour of the liquid metal is similar to the flow of a viscous fluid when the temperature is increased about 100-200 °C above melting point of the metal. The viscosity of the liquid metal is related to the temperature, i.e. when the temperature is increased, the viscosity decreases. Therefore the flow resistance of the liquid metal decreases with the increasing of the overheat temperature. Overheat temperature also controls the surface tension of the liquid metal. The effects of the temperature and the flow rate of the liquid metal on the characteristics of the metal powders will be examined by running the set-up at the various temperatures and flow rates.

The temperature drop due to heat loss during the transfer of the liquid metal from furnace to the preheated tundish is compensated by increasing the degree of overheat temperature.

This heat loss is dependent upon the physical properties of liquid metal, the environmental temperature, type of transferring method and the size of liquid metal. If the amount of the liquid metal is decreased since the surface area versus weight ratio of the liquid metal decreases, the heat lost is increased. Therefore the control of the temperature of the liquid metal becomes unstable due to the heat lost during the transferring of the small amount of liquid metals.

The set-up is considered as laboratory equipment, 250 g melting capacity is enough to take a sample of powders which shows characteristics of the particles. The temperature drop during the transferring and the pouring of the 250 g liquid metal is very high.

Small variation in the liquid metal temperature can make large variation on the viscosity and the surface tension of the liquid metal which are important parameters affecting the powder characteristics. Due to this reason the low melting point materials ($T_m < 800^\circ\text{C}$) was melted in the tundish. In a way, melting unit and the tundish was the same for these materials. The tundish is mounted directly on the top of the atomizer disc. In this unit, the material is melted and the temperature is kept at the desired point and then it is poured into the rotating disc at the desired metal flow rate. The tundish is heated by a tube furnace. The power of the furnace is 380 Watt and about 30 minutes are required to increase the temperature up to 900°C which is the maximum operating temperature of it. A temperature controller is used to regulate and monitor the temperature of the furnace. The thermocouple of the controller is directly located into the tundish to measure the temperature of the liquid metal. Another digital electronic thermometer is used to check the temperature of the liquid metal to $\pm 0.1^\circ\text{C}$ sensitivity.

For low melting materials steel tundish is used. A nozzle is placed at the bottom of crucible to control the flow of the liquid metal. The hole of the orifice is closed by a stopper. When the metal is melted the orifice is opened by pulling the stopper. Fig.5.1 shows the cross section view of the steel tundish.

Flow rate of the liquid metal at any instant is:

$$Q = C_d \frac{\pi d^2}{4} \sqrt{2gh} \quad (5.1)$$

where C_d is the coefficient of the nozzle, d is diameter of the nozzle, and h is the total head of the liquid metal.

The flow rate must be kept constant during atomization. Flow rate can be adjusted by changing the diameter of the nozzle and decreasing the effect of the variation of the total head of the liquid

metal. For this reasons the nozzle was made as a separate part. It is easy to take off the nozzle and replace with the new one which has different nozzle diameter.

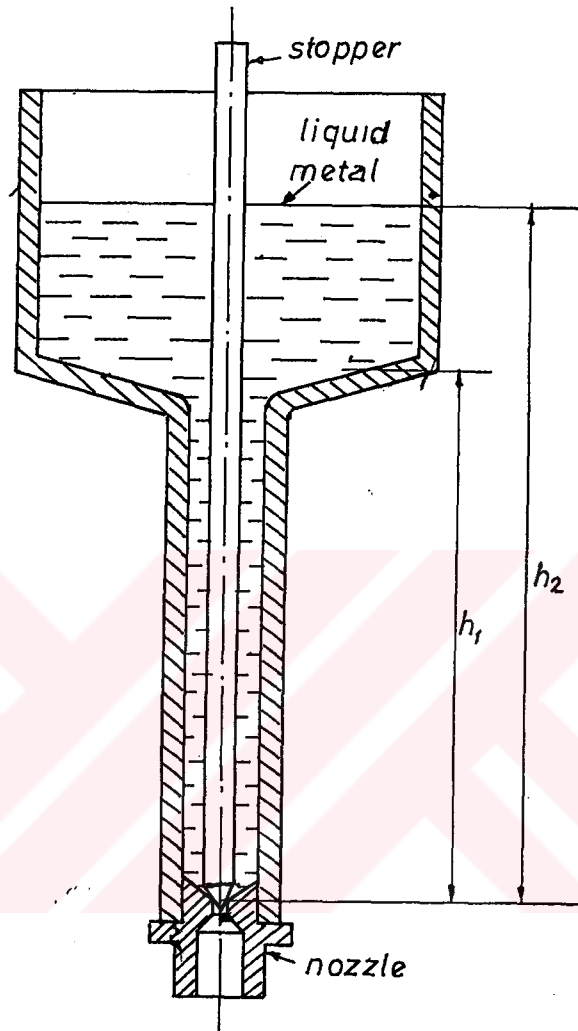


Fig.5.1 Cross section view of the steel tundish.

The effect of the head on the metal flow rate is reduced by making a reduction on the diameter of the tundish as shown in Fig.5.1. According to the tundish dimension, the variation of the pressure at the nozzle is about 10 % when the head reduces from h_2 to h_1 values. The values of C_d is related with the geometry and the fluid exit velocity of the nozzle. The values of C_d increases with decreasing the fluid velocity. Therefore the head effect and C_d effect should balance each other and the flow of the liquid metal can be considered as constant.

Induction furnace at the Gaziantep Celik Dokum Sanayii was used to melt the various alloy steels. The liquid steel was carried in a crucible from the furnace to the preheated tundish which was mounted above the atomizer disc. Tundish was heated to 800 °C. Since the inner diameter of the tube furnace was very small a new tundish heater was designed and constructed in the workshop. The tundish was made from the graphite to withstand the high temperatures. Fig.5.2 shows the schematic drawing of the tundish. At the bottom of the tundish, concentric resistance heating elements; and at the cylindrical surface of the tundish, 12 rectangular resistance heating elements are used. Total power is 2500 Watts.

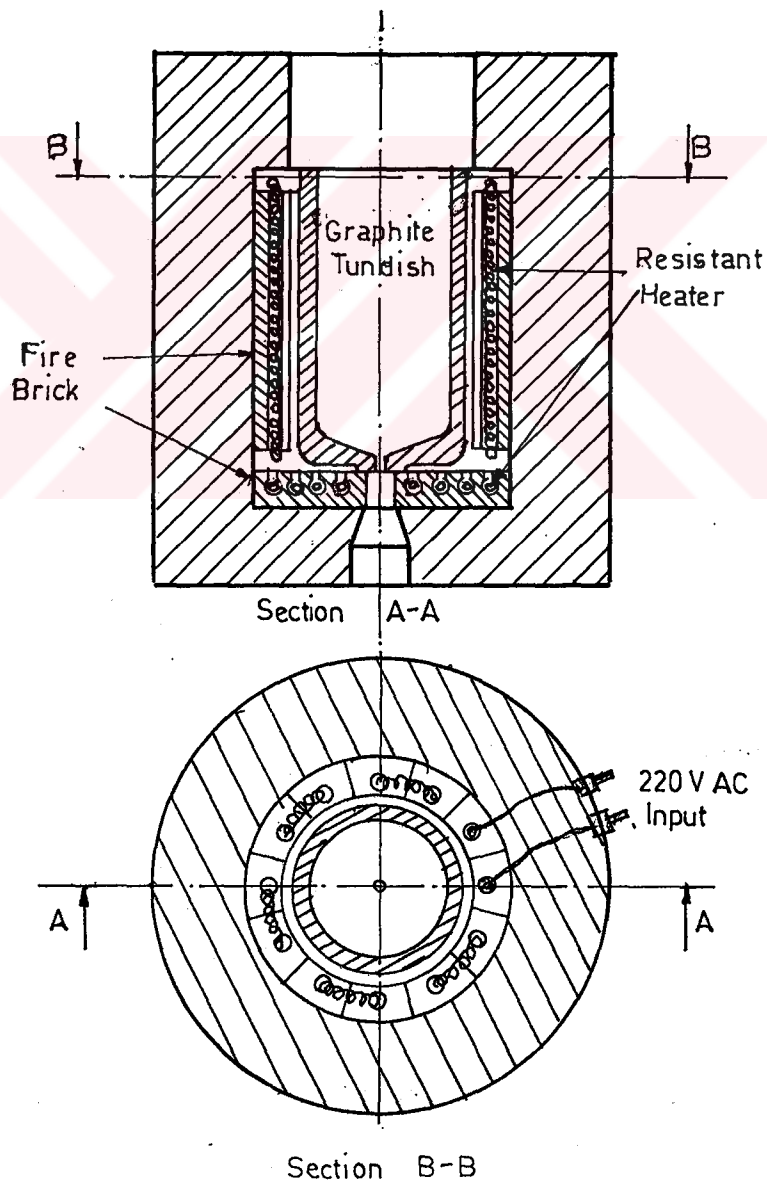


Fig.5.2 Schematic drawing of the graphite tundish.

5.3 DESIGN OF THE DISC DRIVE SYSTEM

In centrifugal atomization, the disc speed is the most important parameter that affects to the characteristics of the metal powder. The rotating speed of the disc used in the set-up must be very high and it must be adjustable for examining the variation of the powder characteristics with the disc speed.

In practice, there are three possible ways to obtain adjustable high speeds:

- a) air turbine,
- b) constant speed electrical motors with gear-box or belt-pulley arrangement,
- c) high speed electrical motors with speed control.

a) Air Turbines

Air turbines can work at various speeds and powers by adjusting the air pressure and air flow rate. At first, the supplied air is compressed into large storage tank at high pressure by compressors. The pressure and flow rate of the compressed air adjusted according to the desired speed and the power of the turbine by using air regulator.

The maximum working speed of the air turbine can be increased up to 150000 rpm. In general, air turbine is suitable for high speed and low torque applications. Compressing the air at high pressure is possible by using two or more stage air compressors. Due to high energy loss, the mechanical advantages of the system is low and also installation and operating cost of the system is very high.

b) Constant Speed Electrical Motors With Gear-Box or Belt-Pulley Arrangement

Commercially, constant speed AC electrical motors are produced in three different groups according to their working speeds as 850 rpm,

1450 rpm, and 2850 rpm for various powers. It is possible to increase these speeds upto 30000 to 40000 rpm by gear-box. The production of gears is dependent on their working speeds. For high speed applications precision machining and housing is required. Balancing is the most important problem; mounting of the gear on its shaft and also mounting the shaft into gear-box must be in balance. Vibration and the noise are also important problems of the high speed gear-boxes.

In belt and pulley system there is a speed limit. At high speed due to slippage, the system becomes unstable. The maximum permissible working speed of the V belt is 40 m/s and flat belt is 60 m/s. It is clear that belts are not suitable for high speed applications.

c) High Speed Electrical Motors With Speed Control

Commercially, there are two different types of high speed electrical motors.

i) *Series Motors* : These motors can work by AC and DC electrical current. Maximum operating speed is 24000 rpm. The operating speed of the motors can be varied by changing the supply voltage. This is generally obtained by a variac.

ii) *Asynchronous Motors* : These motors operate with AC. The operating speed of this type of motors can be changed by changing the frequency of the electrical current. This is done by a motor-generator arrangement and electronics circuits.

Mounting of a high speed shaft is very difficult due to unbalance problem and the selection of the bearings. The maximum permissible speed of journal bearings and roller bearings are about 10000 rpm. For high speeds air bearings and precision ball bearing with smallest inner diameter (<10mm) can be used.

A serial type electrical motor is selected as the main drive. Only rotor and stator of the motor is used. Another housing is designed and constructed in the work shop. The power of the motor is 2800 Watt and the maximum speed is 24000 rpm. The motor operates with mono phase AC . The speed of the motor is adjusted by using a variac. Fig.5.3 shows supply voltage versus rotating speed of the motor.

To eliminate housing problems, atomizer disc is mounted directly on the shaft of the motor. Motor is mounted vertically, so that liquid metal can flow directly to the atomizer disc with minimum unbalance.

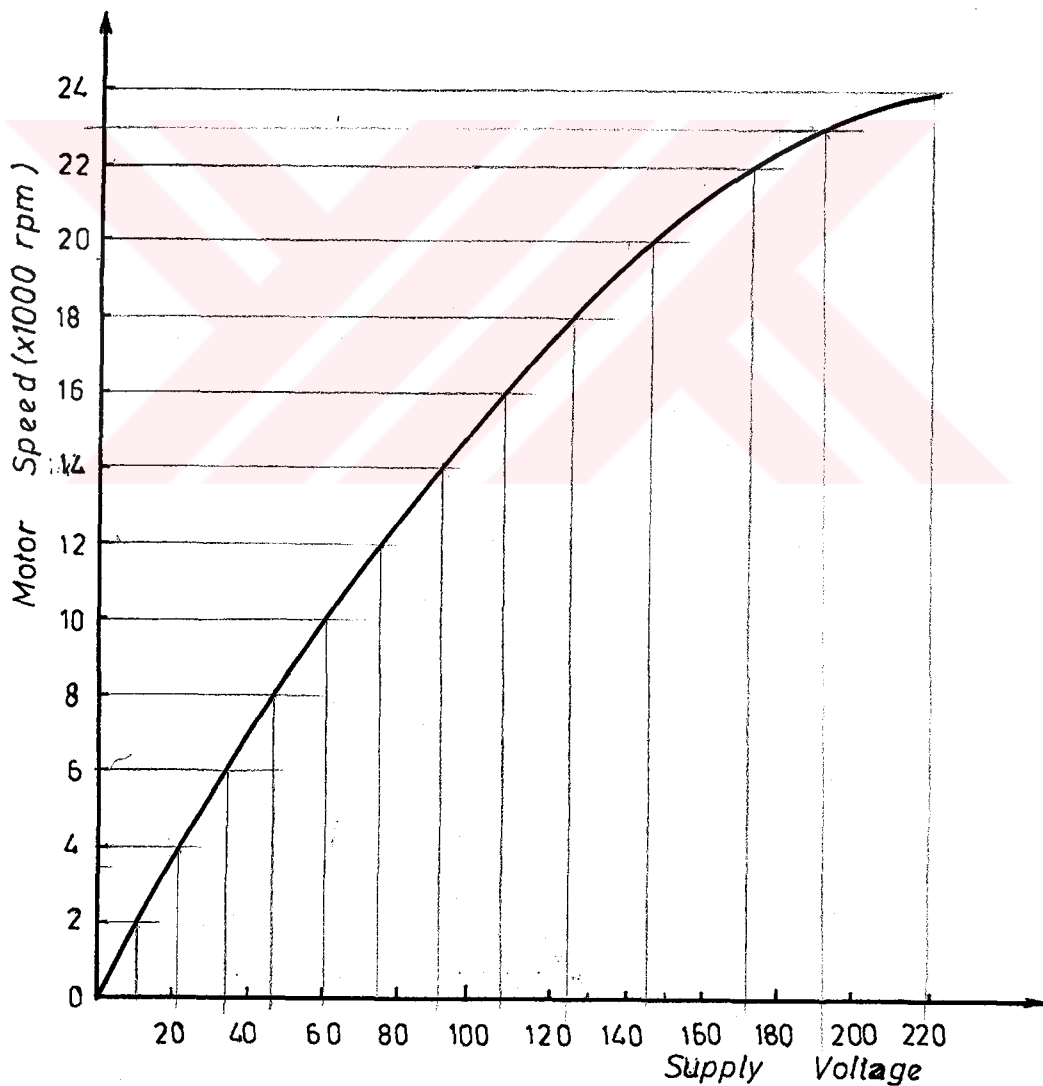


Fig.5.3 Speed characteristics of the main drive motor.

5.4 DESIGN OF THE ATOMIZATION DISC

Shape, size, surface roughness, and material are the important parameters of the rotating disc which are affecting the characteristics of metal powders produced. Flat disc, cup shaped disc, and vaned disc, which is used in spray drying, are the three different types of the discs used in this work.

Since the working speed of the rotating disc is very high (24000 rpm) balancing of the disc is an important design problem. At this speed, small unbalance can destroy the set-up suddenly. Creep and loosing the strength of the material are the another design problems, because the working temperature of the disc is very high. The balancing of the system must be taken care of on every mounting of the disc.

At the beginning of the atomization, the rotating disc must be heated about the melting point of the atomized material to prevent the sudden solidification of the liquid material on the surface of the disc. During the running, the temperature of the disc will increase up to the temperature of the liquid material.

This high temperature produces dangers for the driving electric motor and its precision bearings. The heat is transfered from the disc to the shaft of the motor by conduction. The maximum permissible operating temperature of the precision ball bearing is about 50°C. For continuous operation this heat transfer must be prevented. For this purpose an adaptor was designed and constructed in the workshop. Fig.5.4 shows detail drawing of the part. It is seen that the part is a radial air fan such that a shaft was welded on both side of it. During the operation, air enters from the inlet parts and then pass through the channel between two vanes, and cools the shafts. Therefore, the heat transfer from the hot atomizer disc to the shaft of the motor is

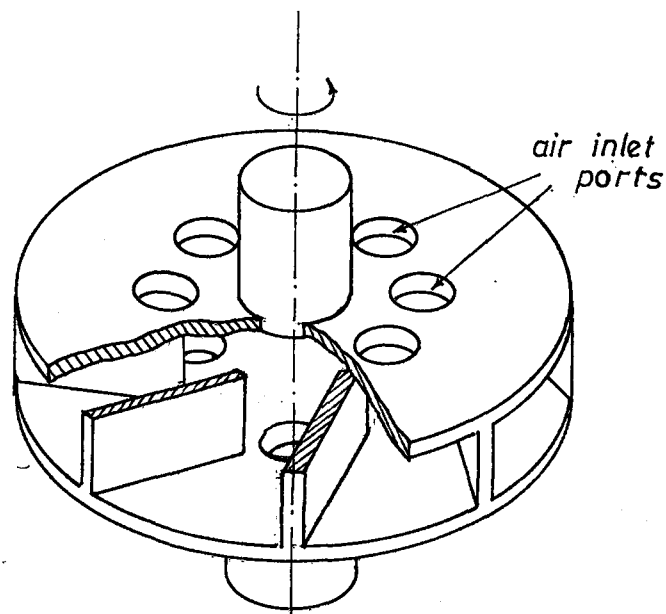


Fig.5.4 Schematic drawing of the adapter

prevented. This part was mounted between the atomizer disc and motor shaft. It was tested by heating the disc to the temperatures about 800°C . The temperature at the bottom shaft was recorded about 30°C during the test run at 24000 rpm for 5 minutes.

The atomization of the 250 g of liquid metal takes about only 2-5 seconds. For these operations there is no time to heat the motors above 50°C . Therefore, this part was omitted for short running of the set-up since it reduces the stability of the system.

The motor shaft which is used for mounting the disc is 12 mm in diameter and 10 mm in length. An interference fit is required to prevent eccentricity between the rotating axis of the disc and motor shaft. Since several discs with various types will be tested, mounting and dismounting the discs may deform the shaft. Therefore a mandrel was designed and constructed. Fig.5.5 shows detail drawing of the mandrel and its mounting. The interference fit was made between the hole of the mandrel and the shaft of the motor. All surfaces of the mandrel were machined taking the hole as reference. There was clearance fit between mandrel and atomizer disc.

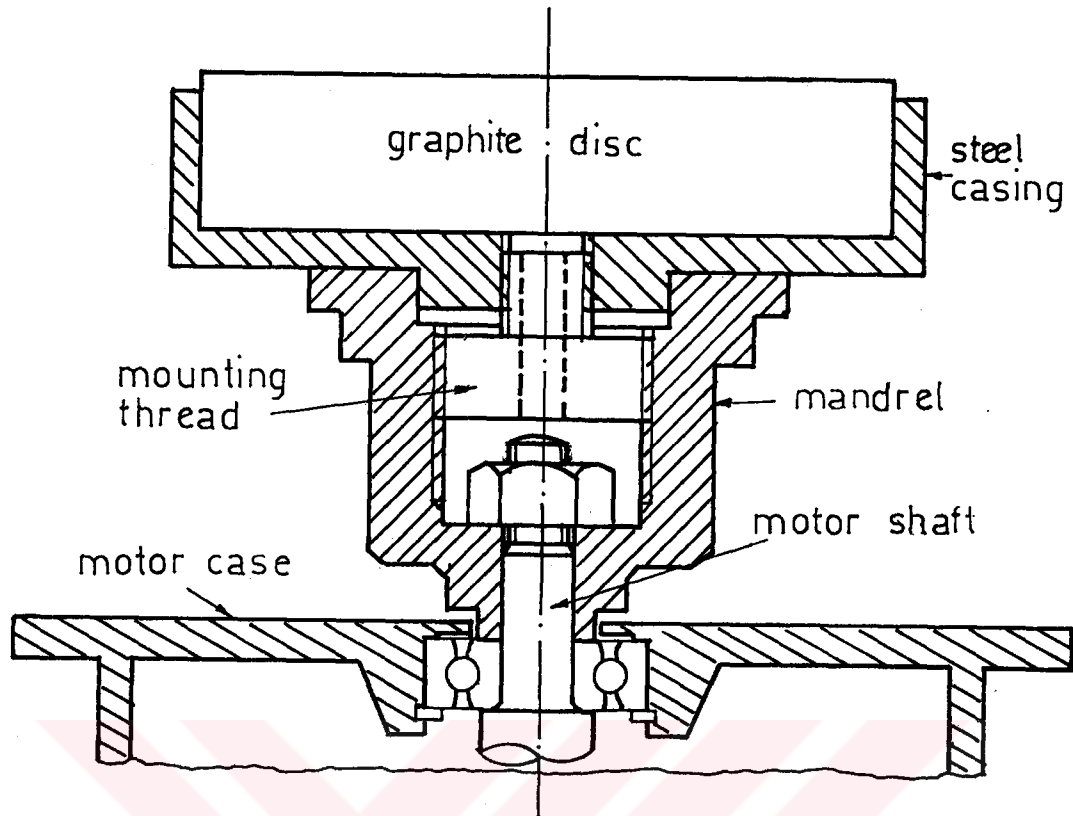
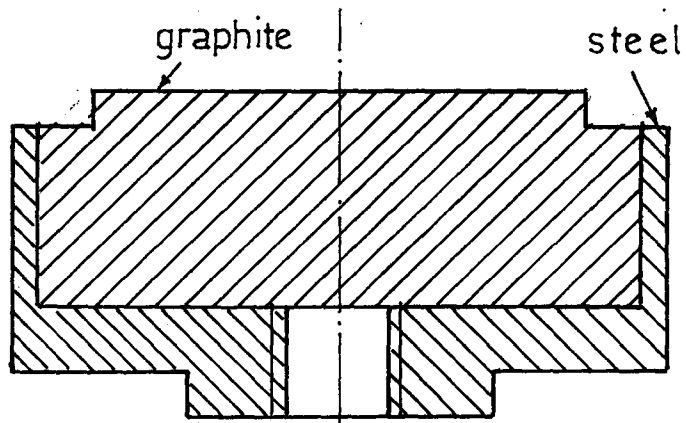


Fig.5.5 Detail drawing of the mandrel and its mounting.

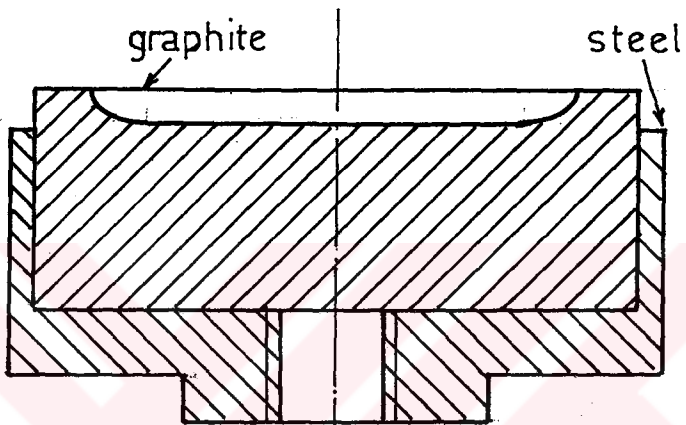
At the beginning of the experiments, steel was used as a disc material. Since, steel has high heat conductivity so, it causes sudden solidification of the liquid metal during the atomization due to heat loss of metal. Steel can be used by heating the disc above the melting point of the liquid metal. But heating the disc to high temperatures creates some problems. Therefore, the disc material should have low thermal conductivity and resists high temperature applications. Graphite is a suitable material for these requirements.

The discs were made by pressing graphite block into a steel casing and then machined to the required shape. Fig.5.6 shows cross section views of flat and cup shaped discs.

Fig.5.7 shows the assembly drawing of a vaned disc made from steel. The cross section views of a graphite disc is shown in Fig.5.8.



Flat Disc



Cup Shaped Disc

Fig.5.6 Crass sectional views of the flat and cup shaped discs

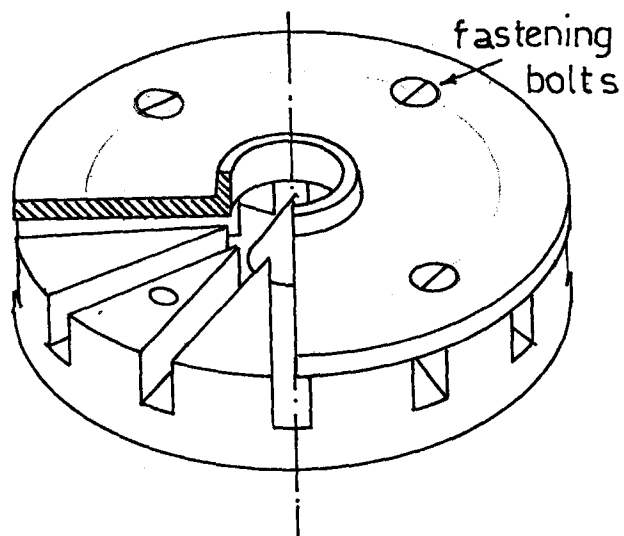


Fig.5.7 Assembly drawing of a vaned disc made from steel.

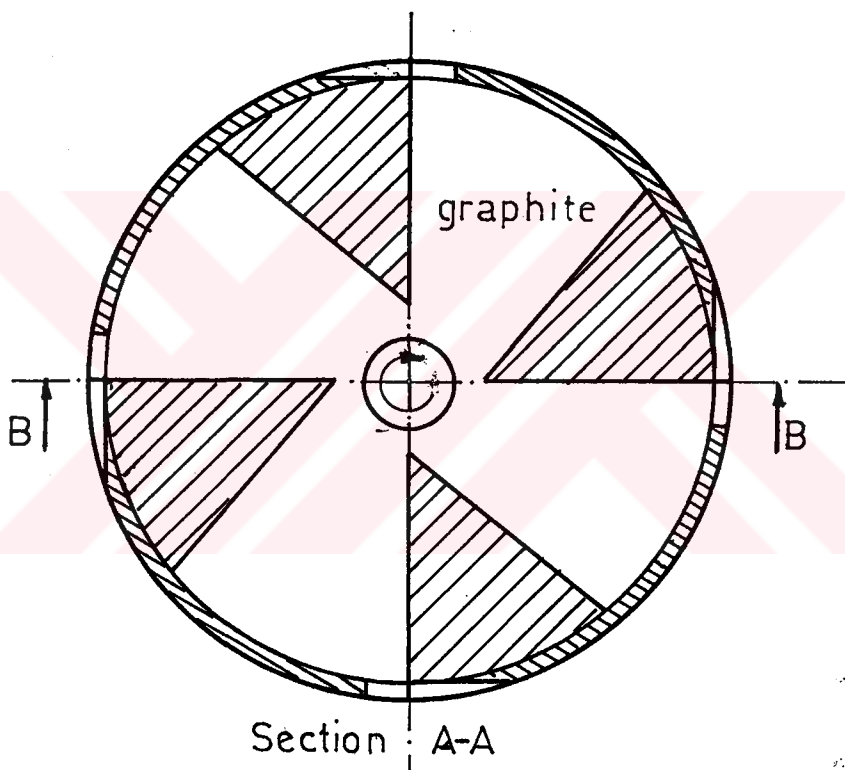
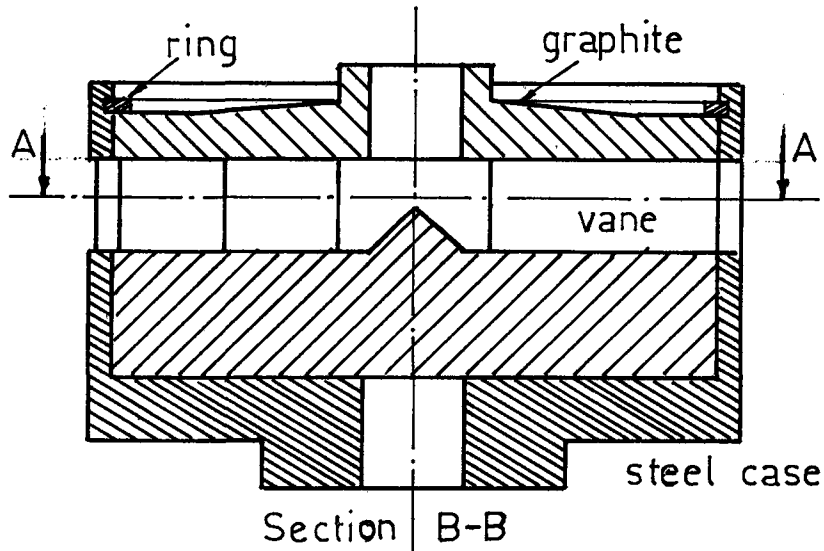


Fig.5.8 The cross section views of a graphite vane disc.

It is seen that the disc was made from two separate graphite parts by pressing into a steel casing. The vanes are made as a diverging form and then it suddenly closed at the outlet (Fig.5.8) to reduce air pumping effect.

The cross sectional drawing and a photograph of the setup are shown in Fig.5.9 and Fig.5.10 respectively.

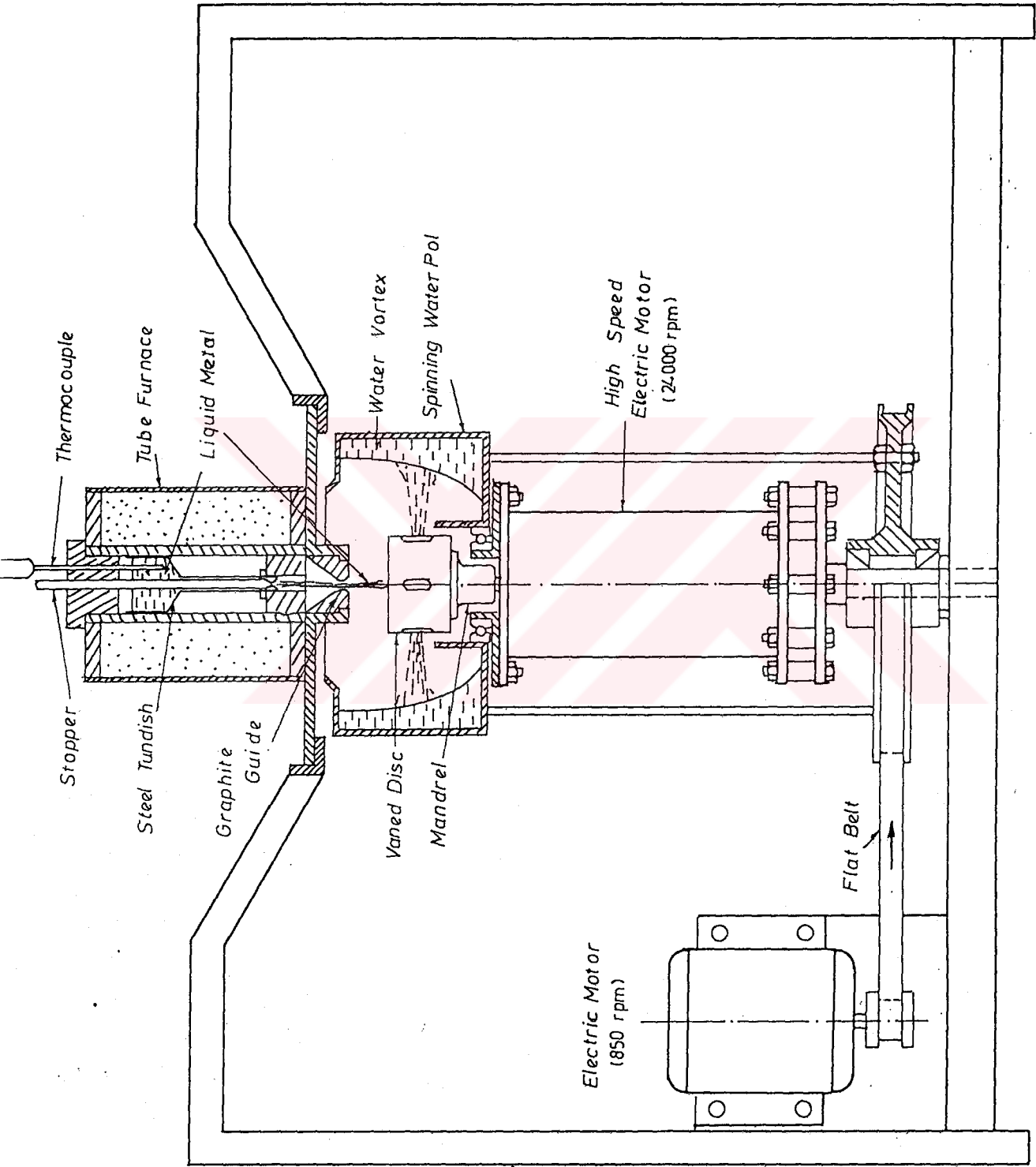


Fig.5.9 Cross sectional drawing of the set-up

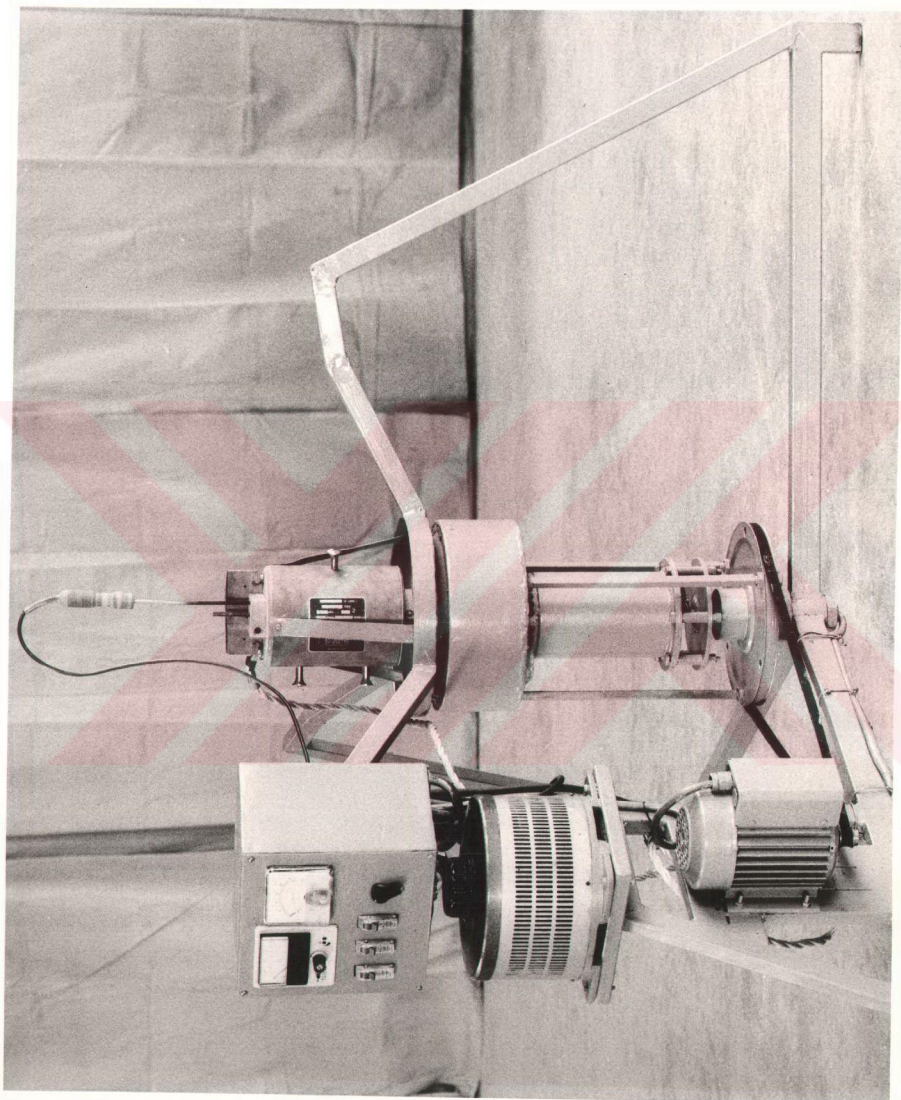


Fig.5.10 General view of the set-up

CHAPTER 6

EXPERIMENTAL RESULTS

6.1 INTRODUCTION

The parameters that affect the characteristics of the metal powders produced by centrifugal atomization were discussed in previous chapters. These parameters can be ordered as follows:

- a) The viscosity and the surface tension of the liquid material, which depend upon the temperature of the liquid materials,
- b) The rotating speed of atomizer disc,
- c) Flow rate of the liquid metal,
- d) Design of the atomizer disc,
- e) Cooling of the atomized powders.

The experiments were divided into three main groups according to the types of atomizer discs. Flat and cup shaped discs are commonly used in centrifugal atomization. A new vaned type disc was designed and constructed with varying sizes and was tried. To determine the characteristics of the metal powders by using these three types of discs, a series of experiments were conducted at various conditions. The types of material, the temperature and flow rate of the liquid material and speed of atomizer disc were chosen as the major variables.

6.2 FLAT DISC ATOMIZATION

Different types of flat discs were designed and constructed with various disc material (Fig.). Graphite proved itself to be better than steel as a disc material.

6.2.1 Flat Disc Atomization of Lead

In this group of experiments, lead was atomized by using flat disc atomizer. Eighteen experiments were carried out in various metal flow rates and temperatures at 19000 rpm and 24000 rpm disc speeds. The disc was made by pressing the graphite block into steel casing as shown in Fig. The diameter of the disc was chosen as 32mm. The metal was tested at three different temperatures (400, 550, and 700°C) and three different flow rates (50, 75, and 100 g/s) to determine the effect of the temperature and the flow rate on the powder characteristics. About 250 g lead was melted for each experiment.

The cumulative size distribution by weight of the powders produced was determined by sieving them in a George Fisher Sieving Set. The sieves used are: 1000, 710, 500, 355, 250, 180, 125, 90, and 63 μm mesh size. 50 grams of metal powder is sieved. Then the amount of powder in each sieve is weighted to miligram accuracy. Percent of powder in each sieve, and mean powder size was calculated. The mean powder size was determined from the Grain Finess number. To obtain the Grain Finess number, each percentage is multiplied by its factors, adding all the resulting products and dividing the total by the pertange of powder retained. Then, this mesh number is converted into milimetric value.

The percentage of powder in each sieve and calculated mean powder size of each run were tabulated in Table 6.1 and 6.2 for 19000 rpm and 24000 rpm disc speeds, respectively.

TABLE 6.1 THE POWDER SIZE DISTRIBUTION OF THE FLAT DISC
 ATOMIZED LEAD (Disc Speed = 19000 rpm, Disc diameter = 32 mm)

Test No	Metal Flow Rate g/s	Liquid Metal Temp. °C	M E S H				S I Z E μm				Grain Finess Number	Mean Powder Size μm	
			710	500	355	250	180	125	90	63			pan
1	50	400											
2		550	6.4	11.0	12.6	13.0	9.8	12.0	6.6	8.4	20.2	107	139
3		700	9.2	12.0	15.8	15.0	10.0	13.2	6.6	6.8	11.4	90	161
4	75	400	6.2	6.2	7.8	9.2	8.8	15.4	9.0	11.0	26.4	126	119
5		550	3.8	7.2	9.3	10.7	9.9	14.5	8.9	11.0	24.0	123	122
6		700	4.4	11.0	12.1	14.2	10.6	13.8	7.6	8.6	17.8	102	147
7	100	400	4.6	6.0	7.4	13.8	10.6	19.2	9.8	10.8	17.6	113	131
8		550	4.4	8.2	10.4	12.0	10.8	16.8	9.6	11.8	16.0	106	141
9		700	5.6	12.0	14.2	14.8	12.0	13.4	6.6	7.6	13.4	92	159

Since the powders are very fine, (119 μm < d_m < 168) and the smallest sieve used is 63 μm , about % 20 of the powders were collected in the pan. Minimum powder size was obtained as $d_m = 119 \mu\text{m}$ at the conditions of: disc speed, $N = 19000 \text{ rpm}$, metal flow rate, $Q = 75 \text{ g/s}$, and liquid metal temp. $T = 400 \text{ }^\circ\text{C}$. For these conditions; the particle size distribution is shown in Fig.6.1.

The variations of the mean powder size with respect to the temperature and the metal flow rate were plotted in three dimensional graphs as shown in Fig.6.2(a) and (b). It is seen that the powder size increases when the temperature of the molten metal increases. Also, the powder size decreases, when the metal flow rate increases.

TABLE 6.2 THE POWDER SIZE DISTRIBUTION OF THE FLAT DISC ATOMIZED LEAD (Disc Speed = 24000 rpm, Disc diameter = 32 mm)

Test No	Metal Flow Rate g/s	Liquid Metal Temp. °C	M E S H S I Z E μm										Grain Finness Number	Mean Powder Size μm
			710	500	355	250	180	125	90	63	pan			
1		400	2.2	4.8	7.4	9.6	11.4	20.8	13.0	13.6	17.2	118	126	
2	50	550	3.4	7.8	10.6	12.6	11.1	15.5	9.2	11.0	19.0	114	130	
3		700	5.2	8.1	10.8	13.6	10.6	16.8	9.6	10.1	15.2	100	140	
4		400	4.2	6.3	9.4	12.0	10.2	15.6	9.1	10.8	22.4	119	125	
5	75	550	8.0	11.0	13.4	13.6	9.4	12.4	7.2	8.4	16.6	97	152	
6		700	8.6	13.8	15.2	15.1	10.3	11.7	5.9	6.9	12.4	90	161	
7		400	7.7	3.1	3.3	6.2	6.7	10.5	17.7	29.2	15.6	122	123	
8	100	550	5.8	12.0	12.3	12.4	8.8	10.8	6.2	8.1	23.6	116	128	
9		700	7.8	13.8	15.6	15.0	10.8	11.6	6.0	7.2	12.2	86	168	

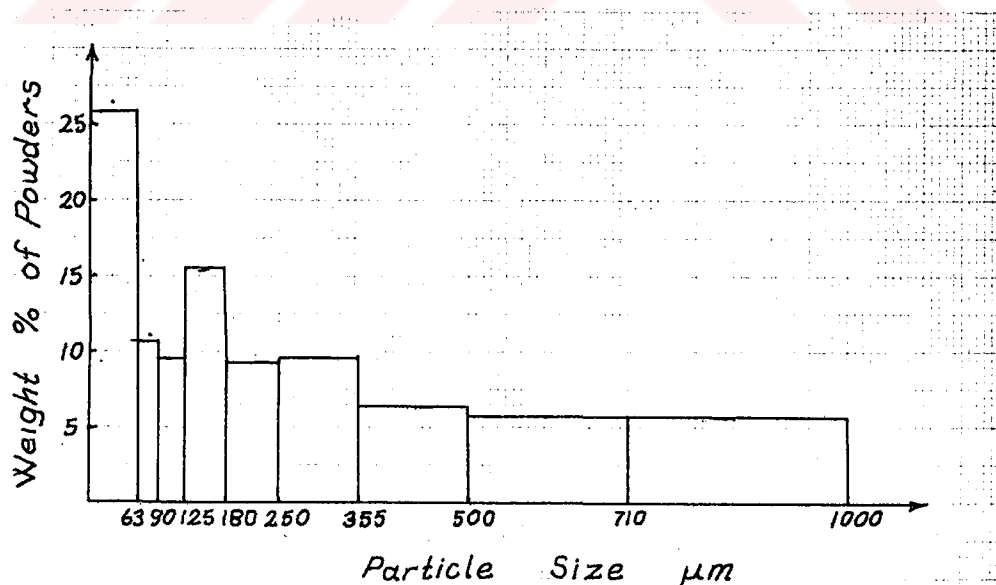
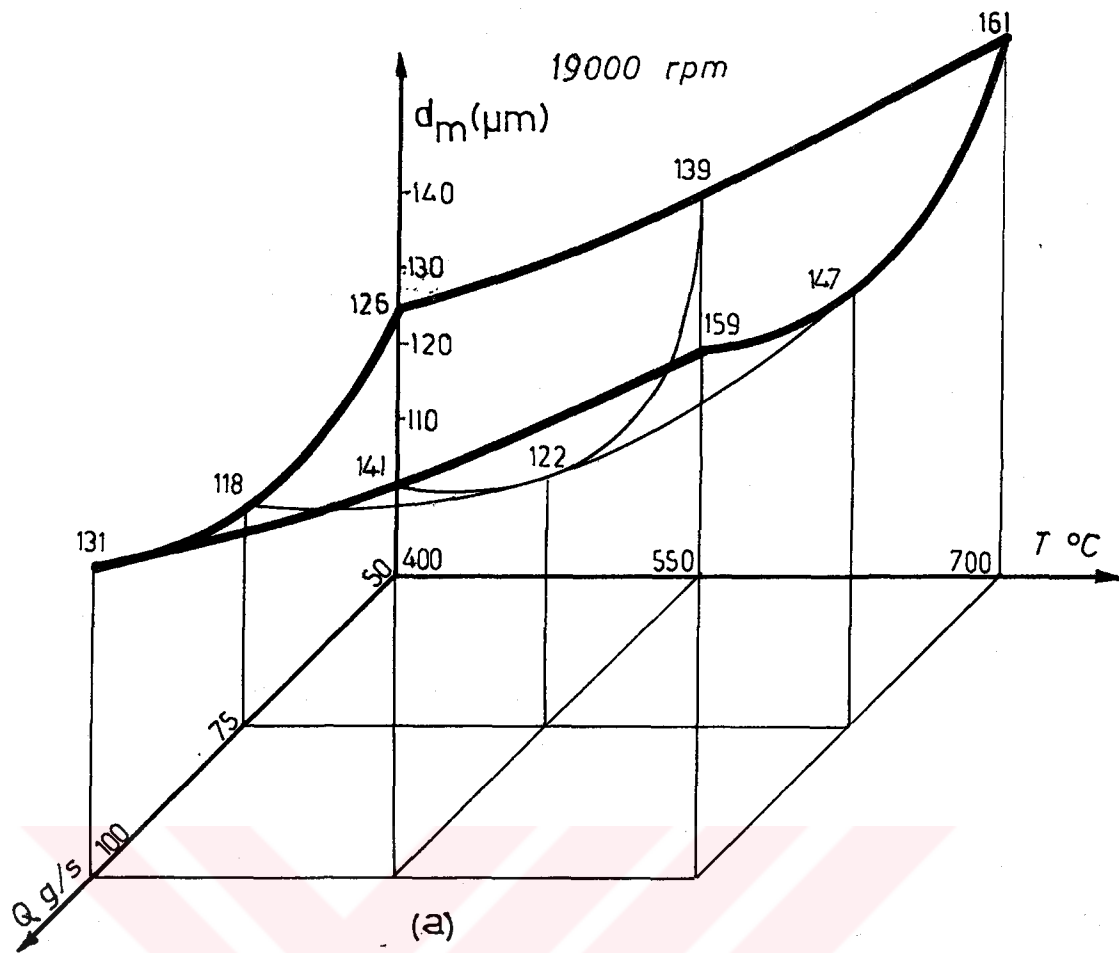
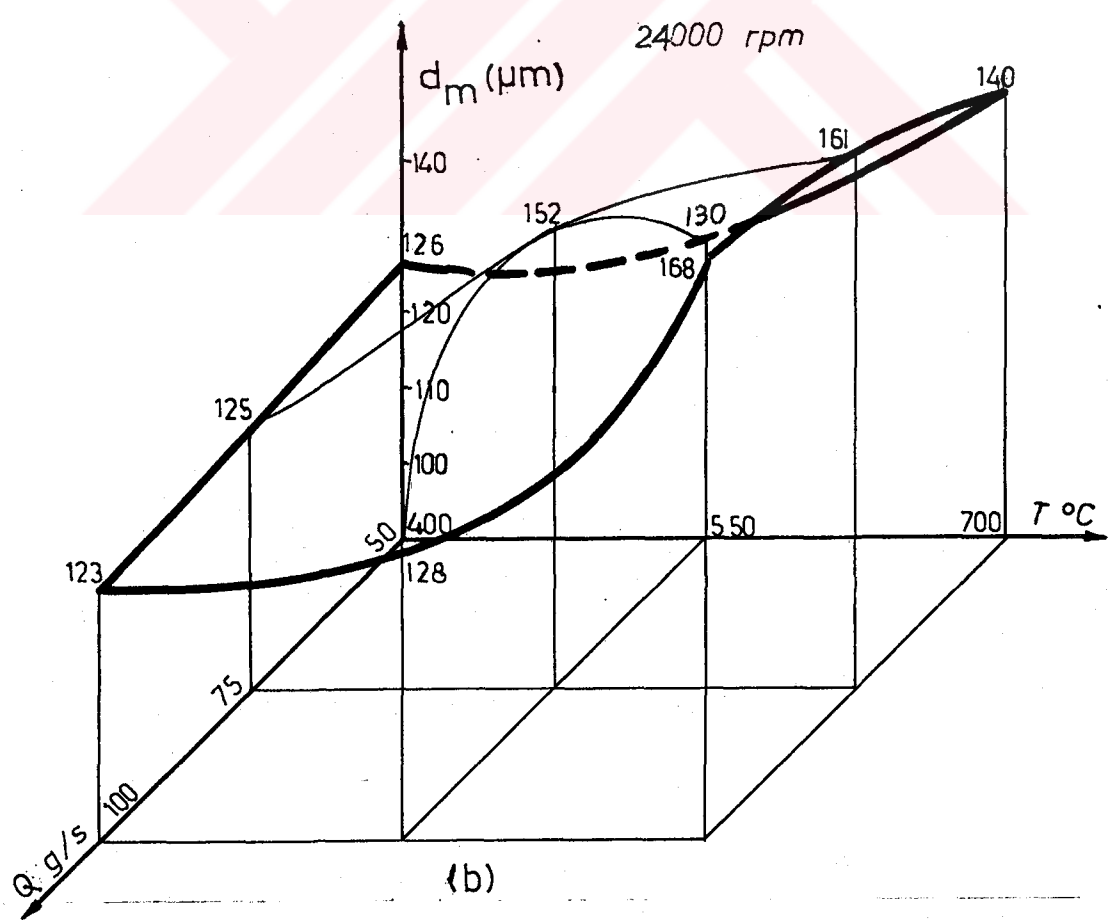


Fig.6.1 Powder size distribution of the flat disc atomized lead at the optimum conditions $d_m = 119 \mu\text{m}$, $N = 19000 \text{ rpm}$, $T = 400 \text{ }^\circ\text{C}$, $Q = 75 \text{ g/s}$.



(a)



(b)

Fig.6.2 The effect of the temperature and flow rate of the liquid metal on the powder size of the flat disc atomized lead.

The shapes of the two graphs are similar but the powder sizes of the high speed (24000 rpm) atomization a little higher than the low speed (19000 rpm) ones.

6.2.2 Flat Disc Atomization Of 12 % Mn Steel

The same graphite flat disc was chosen for atomization of the steel since the graphite can resist high temperature applications. At the beginning, the disc was heated with an oxyacetylene torch to about 300 °C. The steel was melted in an induction furnace and heated upto 1750 °C. The liquid steel was poured into the preheated tundish (800 °C) which was made from graphite. The flow rate of the liquid steel was about 200 g/s. The steel was atomized at 24000 rpm only.

The percent of powders in each sieve and calculated mean powder size are given in Table 6.3.

TABLE 6.3 POWDER SIZE DISTRIBUTIONS OF FLAT DISC ATOMIZED 12 % Mn STEEL. (Disc speed = 24000 rpm, Liquid metal temp. = 1750 °C, Metal flow rate (approx.) = 200 g/s).

M E S H										S I Z E	µm	Grain Finness Number	Mean Powder Size µm
1000	710	500	355	250	180	125	90	63	pan				
2.6	6.6	8.4	10.0	12.4	12.0	15.2	9.4	10.4	13.0	96.5	153		

It is seen that 13 % of the powders are less than 63 µm . The mean powder size according to the sieve analysis was calculated as 153 µm. The powder size distribution of the test is shown in Fig.6.3.

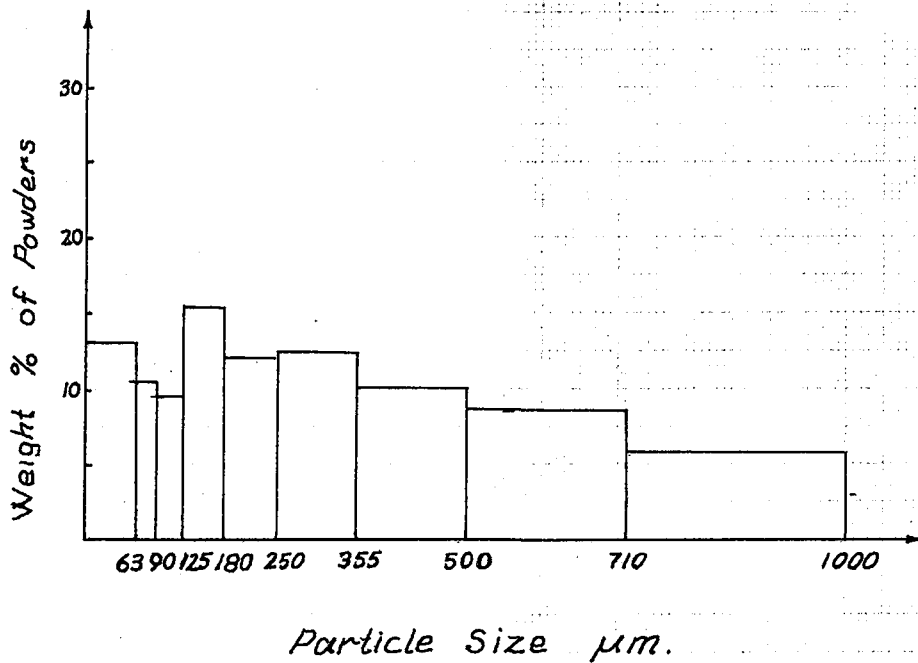


Fig.6.3 Particle size distribution of flat disc atomized 12 % Mn Steel ($d_m = 153 \mu m$) at $N = 24000$ rpm, $Q = 200$ g, $T = 1750$ °C.

6.3 CUP SHAPED DISC ATOMIZATION OF LEAD

The experiments in 6.2 were repeated by using cup shaped disc. The disc was made from graphite. The size distribution by weight and calculated mean powder size are tabulated in Table 6.4 and 6.5.

The variation of the mean powder sizes with respect to temperature and flow rate of the liquid metal plotted as three dimensional graph for 19000 rpm and 24000 rpm disc speeds (Fig.6.4).

The shape of graph changes when the speed decreases to 19000 rpm. It is seen that the powder size decreases when the temperature is decreased. They increase with the increasing of the flow rate.

TABLE 6.4 POWDER SIZE DISTRIBUTION OF THE CUP SHAPED DISC
ATOMIZED LEAD (Disc speed = 24000 rpm, Disc diameter = 32 mm)

Test No:	Metal Flow Rate g/s	Liquid Metal Temp. °C	M E S H S I Z E μm										Grain Finess Number	Mean Powder Size μm
			1000	710	500	355	250	180	125	90	63	pan		
1		400	10.8	14.1	13.8	12.4	12.5	8.7	10.4	5.8	4.7	6.8	62	239
2	50	550		6.4	10.6	9.4	12.6	11.8	16.3	10.2	12.0	10.4	93	157
3		700		7.8	16.6	14.0	12.2	9.8	13.0	6.6	7.6	12.4	86	168
4		400	5.1	9.1	10.5	11.0	11.6	11.2	13.4	8.0	8.3	11.8	86	168
5	75	550		3.4	11.0	12.8	14.8	12.8	14.8	7.2	8.8	14.0	95	155
6		700		3.8	6.8	9.6	16.6	14.3	19.0	9.0	9.0	11.6	94	156
7		400	5.5	8.5	8.5	10.7	12.1	11.2	13.9	8.6	8.8	13.2	92	160
8	100	550		4.0	9.5	11.8	13.1	15.8	15.2	10.2	9.5	10.0	85	170
9		700		2.6	10.1	13.2	15.6	15.2	17.6	8.2	7.9	9.6	87	166

It is seen that at 24000 rpm disc speed, the mean powder size varies between 155 μm to 168 μm (Fig.6.4). The variations are very small and they are not proportional with respect to temperature and flow rate of the liquid metal. This means that the effect of the temperature and flow rate can be neglected at the speed of 24000 rpm.

The minimum powder size was obtained as 150 μm at $N = 19000$ rpm, $T = 700$ °C and $Q = 75$ g/s. The powder size distribution is shown in Fig.6.5.

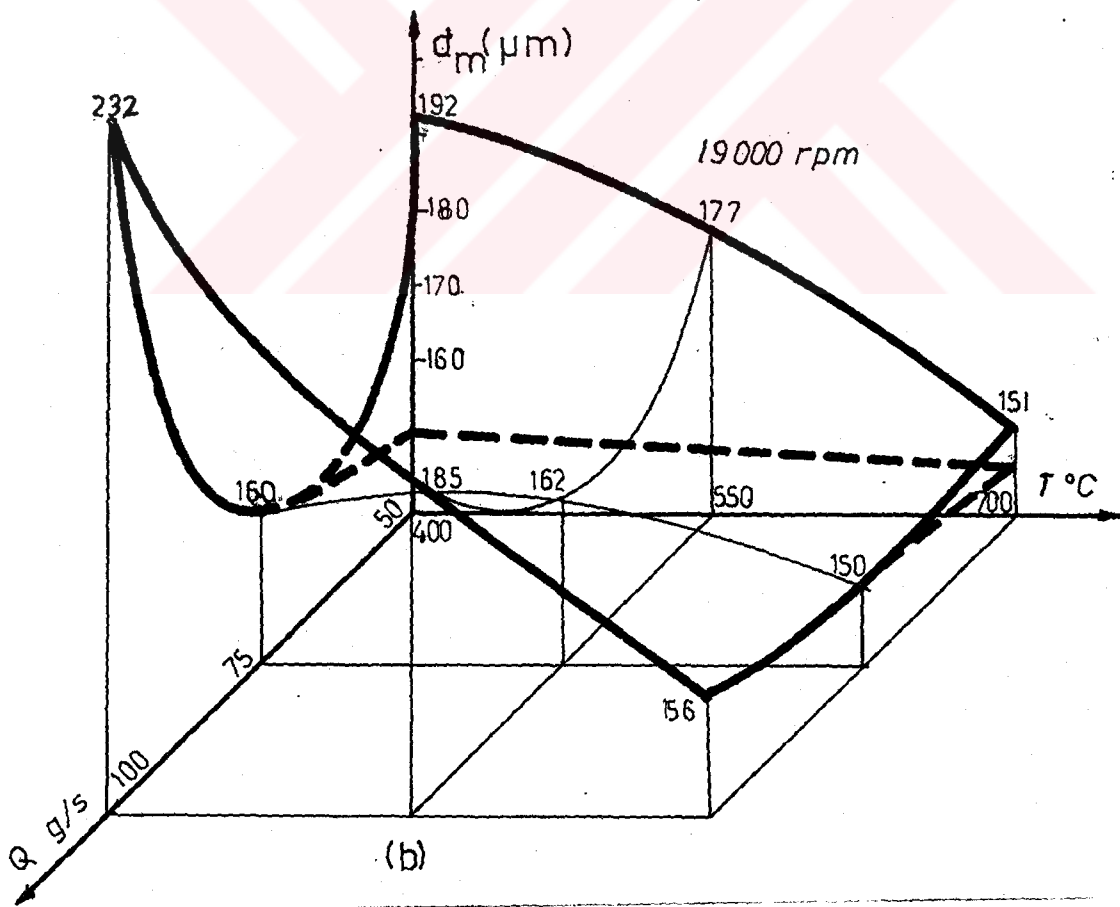
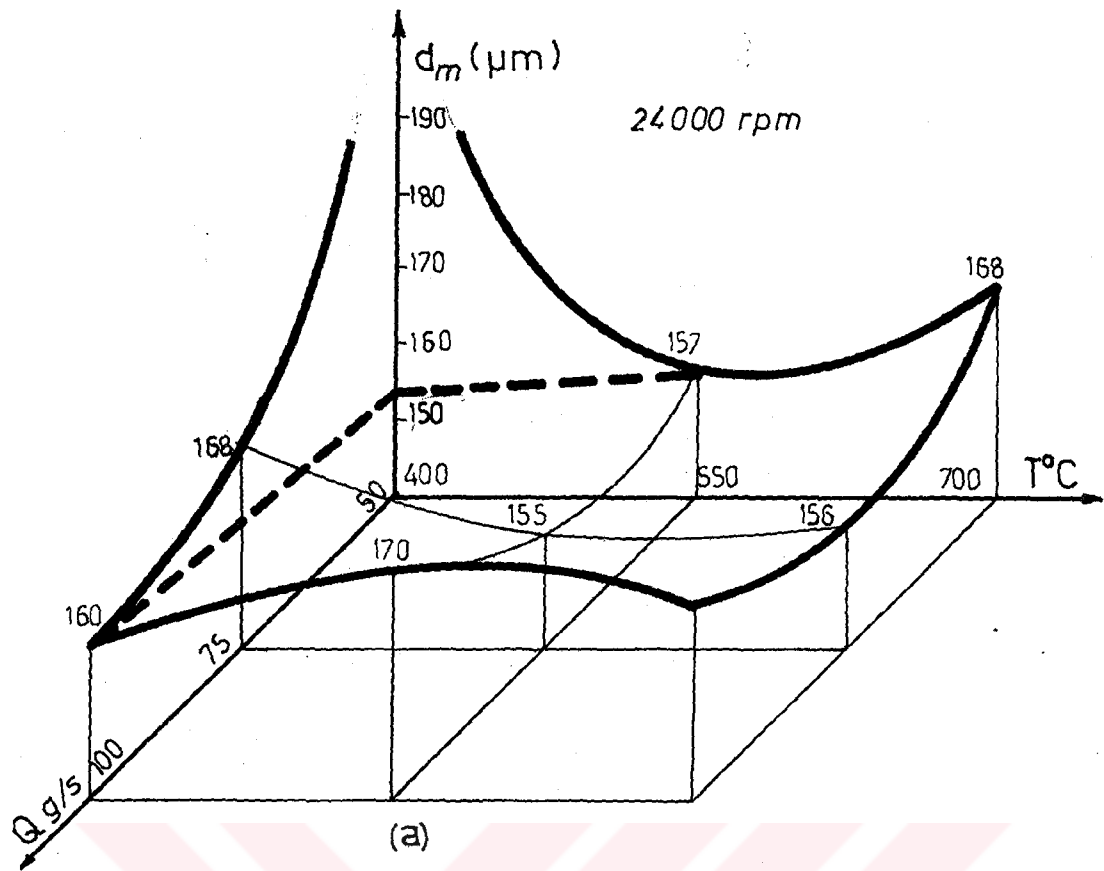


Fig.6.4 The effect of the temperature and flow rate of the liquid metal on the powder size of the cup shaped disc atomized lead at the disc speed of: (a) $N = 24000$ rpm, (b) $N = 19000$ rpm

TABLE 6.5 POWDER SIZE DISTRIBUTION OF THE CUP SHAPED DISC
 ATOMIZED LEAD (Disc speed = 19000 rpm, Disc diameter = 32 mm)

Test No:	Metal Flow Rate g/s	Liquid Metal Temp °C	M E S H S I Z E μm										Grain Finess Number	Mean Powder Size μm
			1000	710	500	355	250	180	125	90	63	pan		
1		400	8.5	11.8	12.6	10.0	10.2	10.0	13.0	7.3	7.3	9.3	76	192
2	50	550		9.6	12.4	13.4	14.0	11.2	14.0	7.8	8.6	9.0	82	177
3		700		3.2	5.8	10.2	14.8	14.0	19.1	9.8	11.5	11.6	98	151
4		400	4.5	7.6	9.2	9.2	11.8	12.6	16.2	6.6	10.5	11.8	90	160
5	75	550		3.0	11.3	14.5	14.9	12.5	15.7	8.9	8.9	10.3	89	162
6		700		2.6	8.2	11.8	14.0	13.6	16.6	9.4	10.6	13.2	99	150
7		400	5.5	11.6	15.7	15.2	14.4	10.4	10.7	5.2	4.6	6.6	65	232
8	100	550		3.0	11.2	16.2	17.8	14.2	16.0	7.4	6.6	7.6	79	185
9		700		4.9	10.4	11.7	12.7	12.8	16.1	9.8	9.5	12.1	94	156

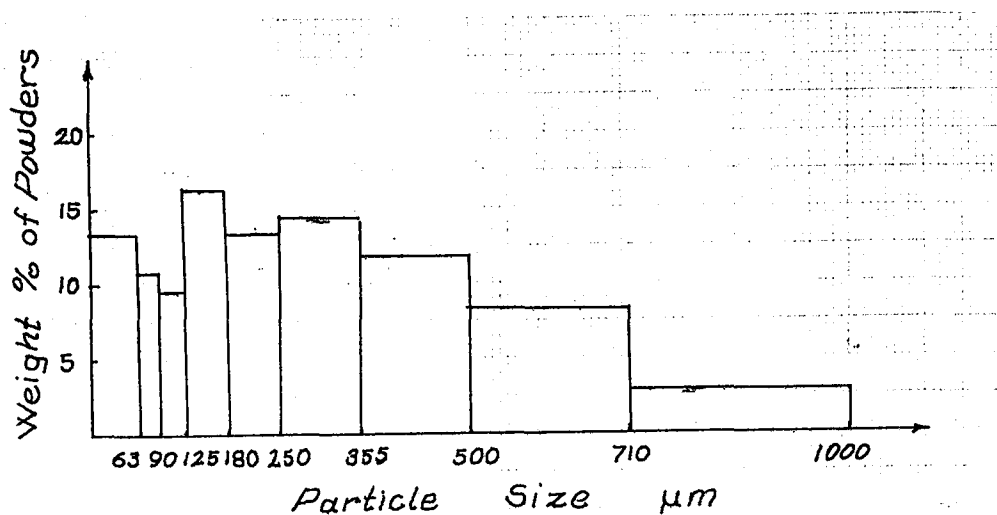


Fig.6.5 Powder size distribution of the cup shaped disc atomized lead at the optimum conditions ($d_m = 150 \mu\text{m}$); $N = 19000 \text{ rpm}$, $T = 700 \text{ }^\circ\text{C}$, $Q = 75 \text{ g/s}$.

6.4 VANED DISC ATOMIZATION

6.4.1 Vaned Disc Atomization of Lead

The smaller vaned disc which has 32 mm diameter was used. The metal was tested at four different metal flow rates (50, 75, 100, and 150 g/s) and three different temperatures (400, 550, and 700 °C) for determination of the effect of the temperature and flow rate on the powder characteristics. About 250 g lead was melted for each experiment. Two different disc speeds (19000 and 24000 rpm) were used.

a) Atomization at 24000 rpm

Twelve experiments were done with the conditions explained above. The weight percent of powders by the sieve analysis and the calculated mean powder sizes were tabulated in Table 6.6.

Since the powders are very fine ($75 < d_m < 109 \mu\text{m}$) about 30 % of powders were collected in the pan. The variation of the mean powder size with respect to the temperature and metal flow rate was plotted in three dimensional graph as shown in Fig.6.6. It is seen that the minimum powder size was obtained at high disc speed and high molten metal temperature. This curve must be as shown by dashed line in the Fig.6.6, when the flow rate is less than 75 g/s.

b) Atomization at 19000 rpm

In this group of experiments, the tests were repeated at 19000 rpm disc speed. The sieve analysis and calculated mean powder size of each run was tabulated in Table 6.7.

At low temperatures and low metal flow rates due to sudden blocking of the vane, powder could not be produced.

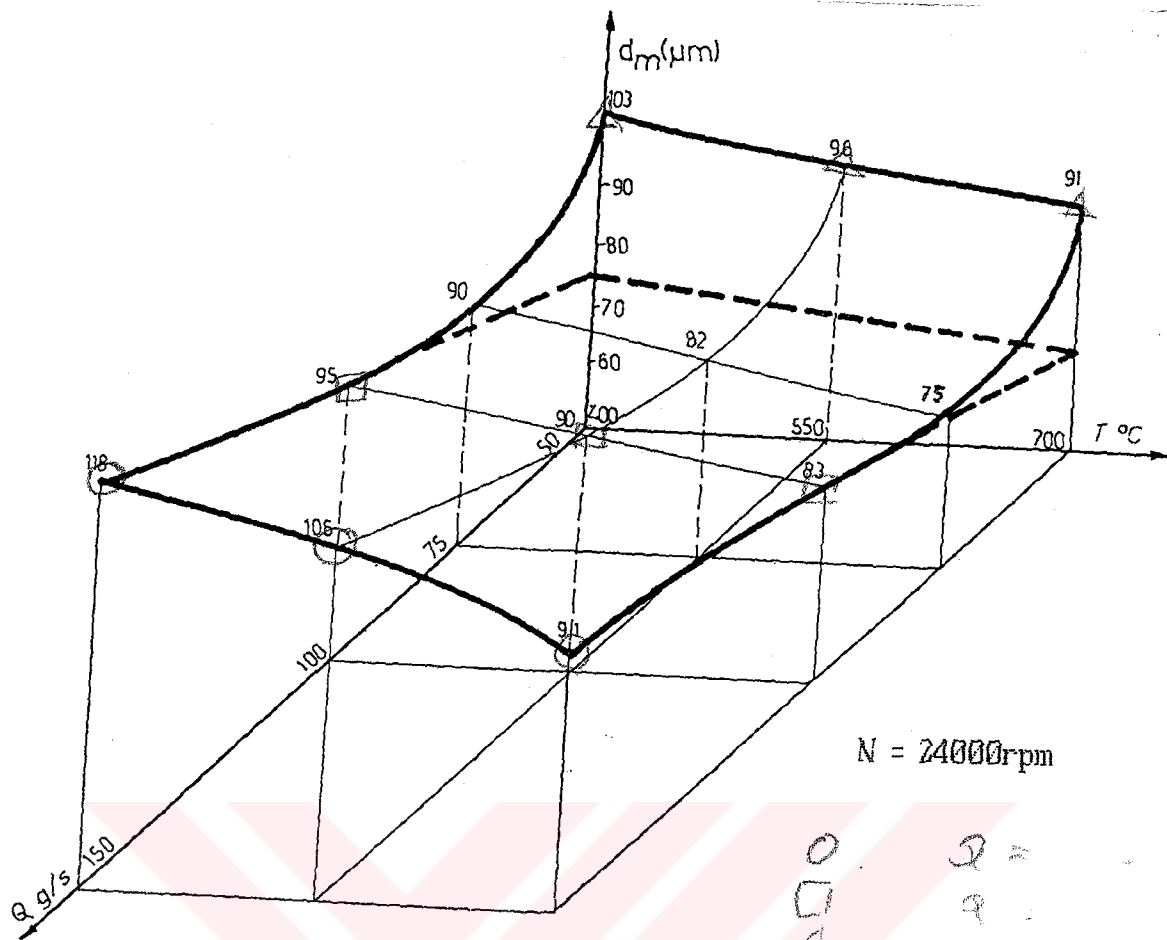
TABLE 6.6 POWDER SIZE DISTRIBUTION OF THE VANED DISC ATOMIZED LEAD

(Disc Speed = 24000 rpm, Disc Diameter = 32 mm, Vaned Number = 4)

Test No	Metal Flow Rate g/s	Liquid Metal Temp. °C	M E S H S I Z E μm									Grain Finess Number	Mean Powder Size μm
			710	500	355	250	180	125	90	63	pan		
1		400	0.8	1.2	3.0	9.4	11.2	18.0	11.2	19.8	25.5	142	103
2	50	550	0.6	1.0	1.6	6.4	11.0	19.0	13.0	16.4	31.0	153	96
3		700		1.0	2.0	5.2	8.4	18.0	12.4	16.6	36.6	162	91
4		400			0.6	3.8	7.2	20.2	13.8	18.2	34.8	167	90
5	75	550		0.6	0.8	2.2	12.2	3.4	14.0	23.0	43.8	186	82
6		700		0.8	1.0	2.0	3.4	11.4	11.0	17.4	53.0	200	75
7		400	0.6	1.2	1.8	6.2	12.8	17.4	12.2	16.0	32.2	155	95
8	100	550	0.4	1.0	2.0	5.0	10.8	11.4	14.4	17.0	38.0	168	90
9		700	0.4	0.8	1.6	3.0	4.0	9.6	8.4	14.2	57.8	184	83
10		400		1.6	6.6	10.0	9.8	20.2	15.6	18.4	18.2	128	118
11	150	550		0.2	2.4	10.8	13.0	21.8	13.0	16.6	22.4	135	109
12		700					5.0	24.0	17.6	21.8	31.4	166	91

TABLE 6.7 POWDER SIZE DISTRIBUTION OF THE VANED DISC ATOMIZED LEAD
 (Disc Speed = 19000 rpm, Disc Diameter = 32 mm, Vaned Number = 4)

Test No	Metal Flow Rate g/s	Liquid Metal Temp. °C	M E S H S I Z E μm								pan	Grain Finess Number	Mean Powder Size μm
			710	500	355	250	180	125	90	63			
1	50	400											
2		550											
3		700	1.2	2.0	4.0	6.8	9.2	19.0	13.4	16.4	28.0	146	102
4	75	400											
5		550	0.2	0.2	1.0	2.6	12.8	13.0	23.2	47.0	195	78	
6		700	0.6	1.4	3.2	10.8	12.6	22.6	12.6	35.8	165	91	
7	100	400	1.4	9.2	16.0	15.4	20.4	10.2	11.2	16.2	112	102	
8		550	0.2	1.2	3.0	5.2	12.2	10.6	17.0	50.6	195	78	
9		700	2.0	2.6	4.6	5.6	12.0	10.4	17.0	45.8	183	83	
10	150	400	0.2	0.4	9.4	21.6	17.8	23.4	11.4	10.6	7.2	93	159
11		550	0.4	1.6	8.8	17.8	23.4	14.8	15.2	20.0	131	116	
12		700	1.2	7.0	16.8	23.4	14.4	18.0	20.2		134	112	



○
 □
 △
 ○
 $Q =$
 9
 0

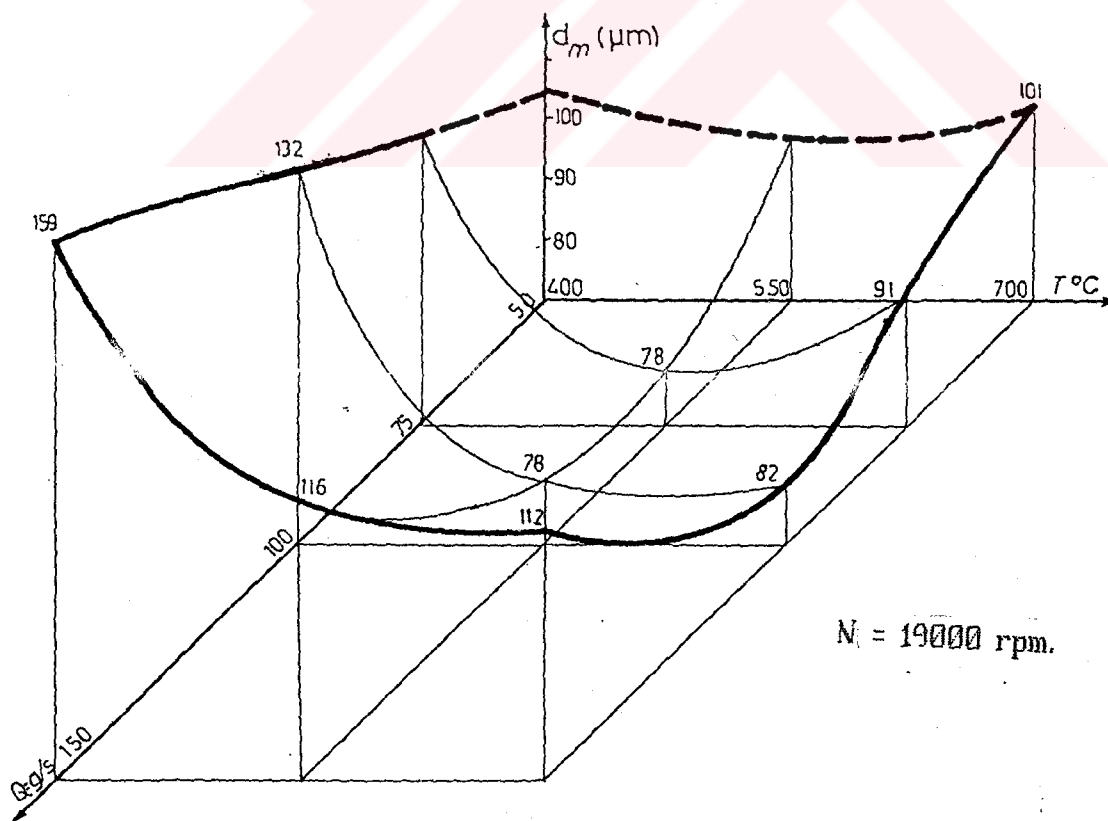


Fig.6.6 The Effect of the temperature and flow rate of the liquid metal on the powder size of the vaned disc atomized lead

Initially preheating of the vaned disc is not enough to prevent solidification of the liquid metal in the vane at low disc speeds. The atomization of lead at low speed, low flow rate and low temperature becomes unstable.

Fig.6.6(b) shows the variation of the mean powder size with respect to temperature and flow rate of the liquid metal. It is seen that the Fig.6.6(a) is similar to Fig.6.6(b).

The minimum powder size was determined as 75 μm at $N = 24000$ rpm, $T = 550$ $^{\circ}\text{C}$, and $Q = 75$ g/s. The particle size distribution is shown in Fig.6.7.

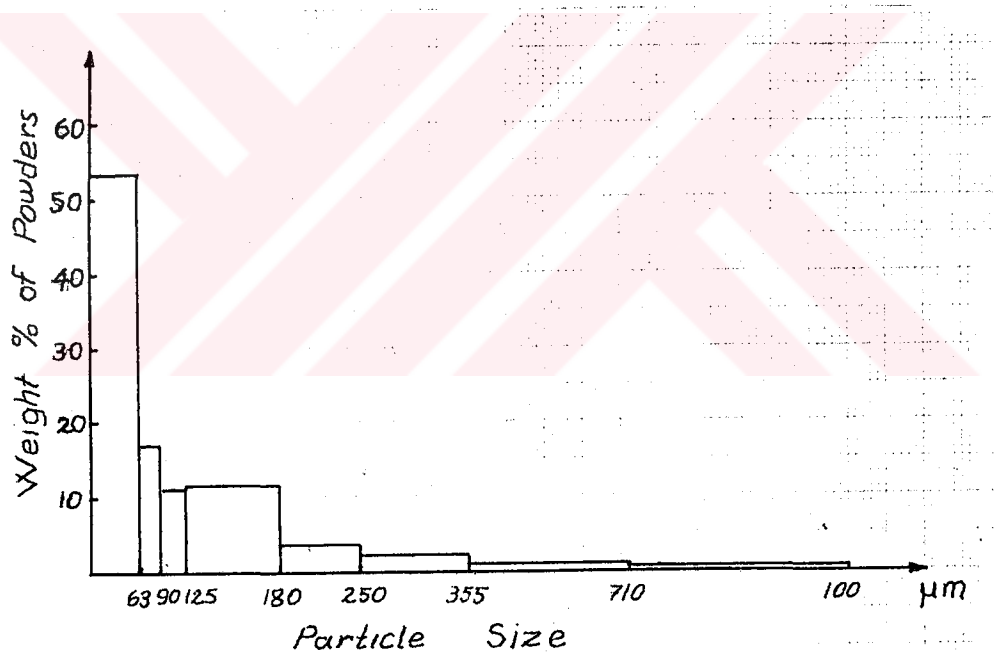


Fig.6.7 The Powder size distribution of the vaned disc atomized lead at the optimum conditions ($d_m = 75$ μm); $N = 24000$ rpm, $T = 550$ $^{\circ}\text{C}$, and $Q = 75$ g/s.

Cumulative weight percent versus particle size of the optimum condition of flat, cup and vaned disc atomizations of lead were plotted in log-log paper as shown in Fig.6.8.

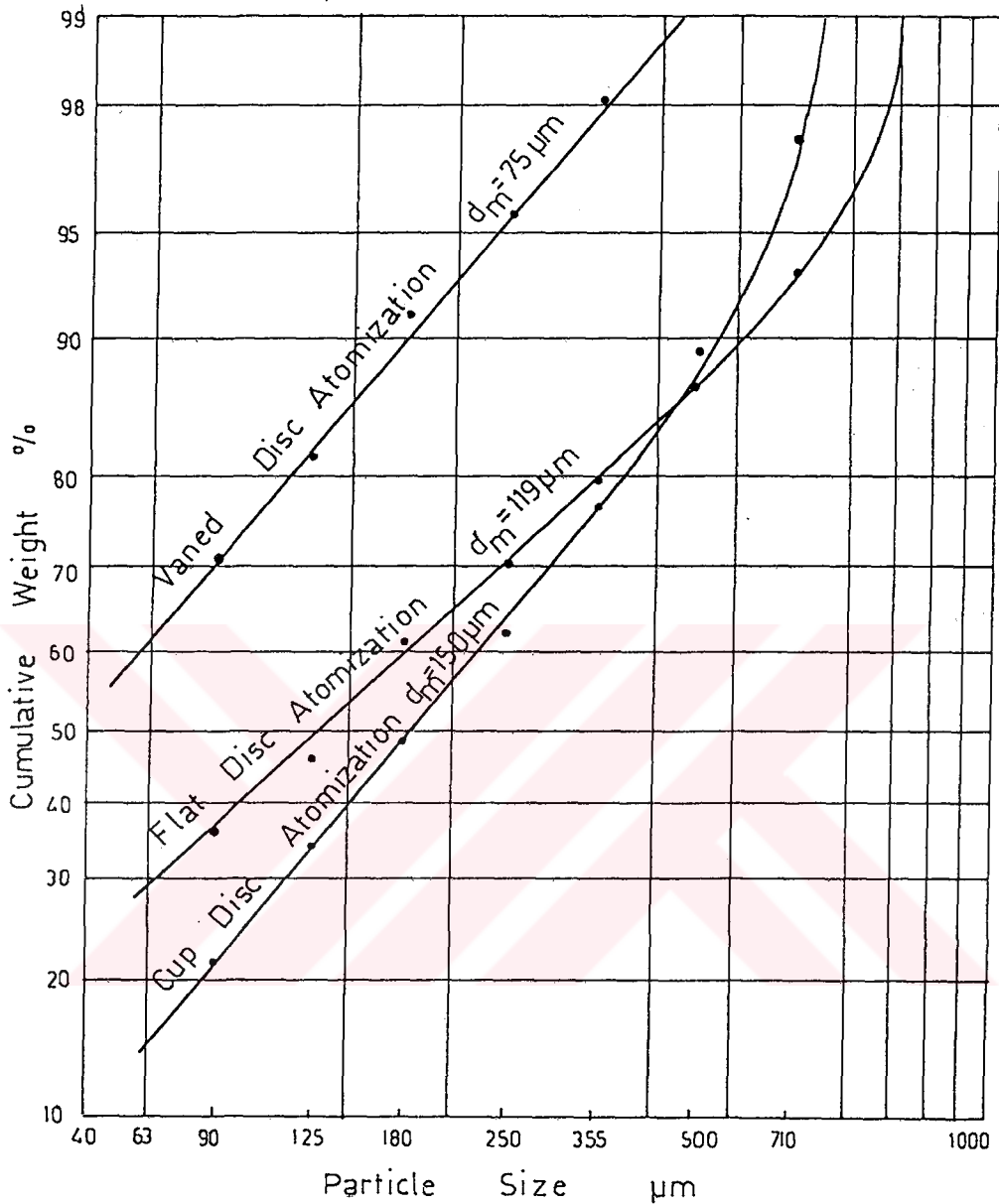


Fig.6.8 Cumulative weight percent distributions of the flat, cup shaped and vaned disc atomization of lead.

-It is seen that the graphs for the flat and cup shaped disc atomization are linear up to 400 µm. After that point linearity is break down. But, in vaned disc atomization, the graph is exactly linear. This means that the powder size distribution is normal distribution. The mean powder size of the vaned disc is about half of the flat and cup shape disc atomization.

6.4.2 Vaned Disc Atomization of Aluminum

Aluminum was atomized by three different sizes of vaned type atomizer discs (Fig.5.5). The metal flow rate was chosen as 50 g/s. Aluminum is a light metal and it has high viscosity and high surface tension. In centrifugal atomization low density, high viscosity and high surface tension make negative effects on the atomization. About 22 experiments were done with the various disc speeds and three different disc sizes.

The sieve analysis and the calculated mean powder size of each run were tabulated in Table 6.8. It is seen that the powders of aluminum are about three or four times coarser than the lead powders. Fig.6.9 shows the effects of disc speed, liquid metal temperature on the mean powder size at three different disc sizes. The two surfaces (Fig.6.9) produced by the disc diameter = 32 mm and 58 mm approximately parallel to each other. This means that the effect of the disc size on the powder size is linear for the condition of the experiments. It is seen that the mean powder size decreases, when the temperature of the liquid metal, and disc speed decreases.

The minimum powder size was obtained as 129 μm with the largest disc size (disc diameter = 82 mm) at 24000 rpm disc speed and 800 $^{\circ}\text{C}$ liquid metal temperature. The powder size distribution for this run was plotted in Fig.6.10.

Cumulative weight percent versus particle size distribution of the optimum condition of vaned disc atomized aluminum was plotted in log-normal probability paper as shown in Fig.6.11. It is seen that the graph is linear, this means that the distribution is normal.

Fig.6.12 shows the effect of the peripheral speed to powder size. It is seen that the variation of the mean powder size with respect to

TABLE 6.8 POWDER SIZE DISTRIBUTION OF THE VANED DISC ATOMIZED ALUMINUM

Disc Diam. mm	Disc Speed rpm *1000	Liquid Metal Temp. °C	M E S H S I Z E μm											Grain Finess Number	Mean Powder Size μm
			1000	710	500	355	250	180	125	90	63	pan			
31	15	800	11.0	26.8	28.5	15.4	8.3	4.0	3.6	1.2	0.8	0.4	30	600	
		900	14.5	18.3	24.5	16.0	11.0	6.1	4.5	2.3	1.2	1.2	33	540	
	24	750	2.4	10.6	26.3	22.6	16.7	10.3	6.1	2.2	1.7	1.1	43	385	
		800	2.3	9.8	24.9	21.4	17.7	10.6	7.0	3.1	2.1	1.1	46	350	
		850	3.0	9.0	23.1	19.2	16.8	12.3	10.1	3.7	2.1	0.7	47	330	
		900	1.2	8.9	24.2	24.8	18.1	10.6	6.4	2.6	2.0	1.2	46	350	
58	15	750	3.4	22.6	29.8	17.6	12.2	6.7	4.6	2.0	0.9	0.2	35	360	
		850	1.6	15.3	26.4	18.9	13.3	9.8	7.5	3.3	2.3	1.6	56	210	
	19	750	1.2	4.1	13.0	17.8	18.9	15.4	16.0	5.9	5.3	2.4	63	233	
		800	1.0	4.2	13.2	15.4	15.7	15.7	14.8	8.5	6.6	4.9	64	232	
		900	1.9	7.9	21.6	18.5	14.5	12.5	10.6	5.0	4.0	3.5	58	220	
	24	750		1.2	10.9	15.3	17.5	16.8	17.0	8.7	7.1	5.5	77	190	
		750		0.8	6.1	17.1	17.3	16.9	17.2	9.2	8.4	6.9	83	175	
		800	0.2	0.6	6.8	13.7	16.4	17.0	18.6	10.5	9.6	6.6	87	169	
		850	0.1	0.9	7.5	12.9	16.7	16.6	18.8	10.3	10.0	6.2	85	171	
		900	0.5	0.7	5.5	10.0	14.9	17.6	19.6	11.8	11.1	8.3	93	157	
82	24	750		2.4	3.0	7.0	13.0	17.0	23.0	12.5	12.5	10.0	101	149	
		800	0.1	0.7	3.2	5.2	10.8	16.8	20.7	13.9	13.9	14.7	114	129	
		850		1.1	2.2	5.6	10.7	17.6	21.7	13.6	15.1	12.5	111	134	
		900			1.0	6.9	11.3	16.7	23.2	15.3	13.2	11.8	110	135	

the disc speed for the disc diameters (31 mm and 58 mm) are linear with the same slope. This linearity breaks down with large disc diameter (83 mm).

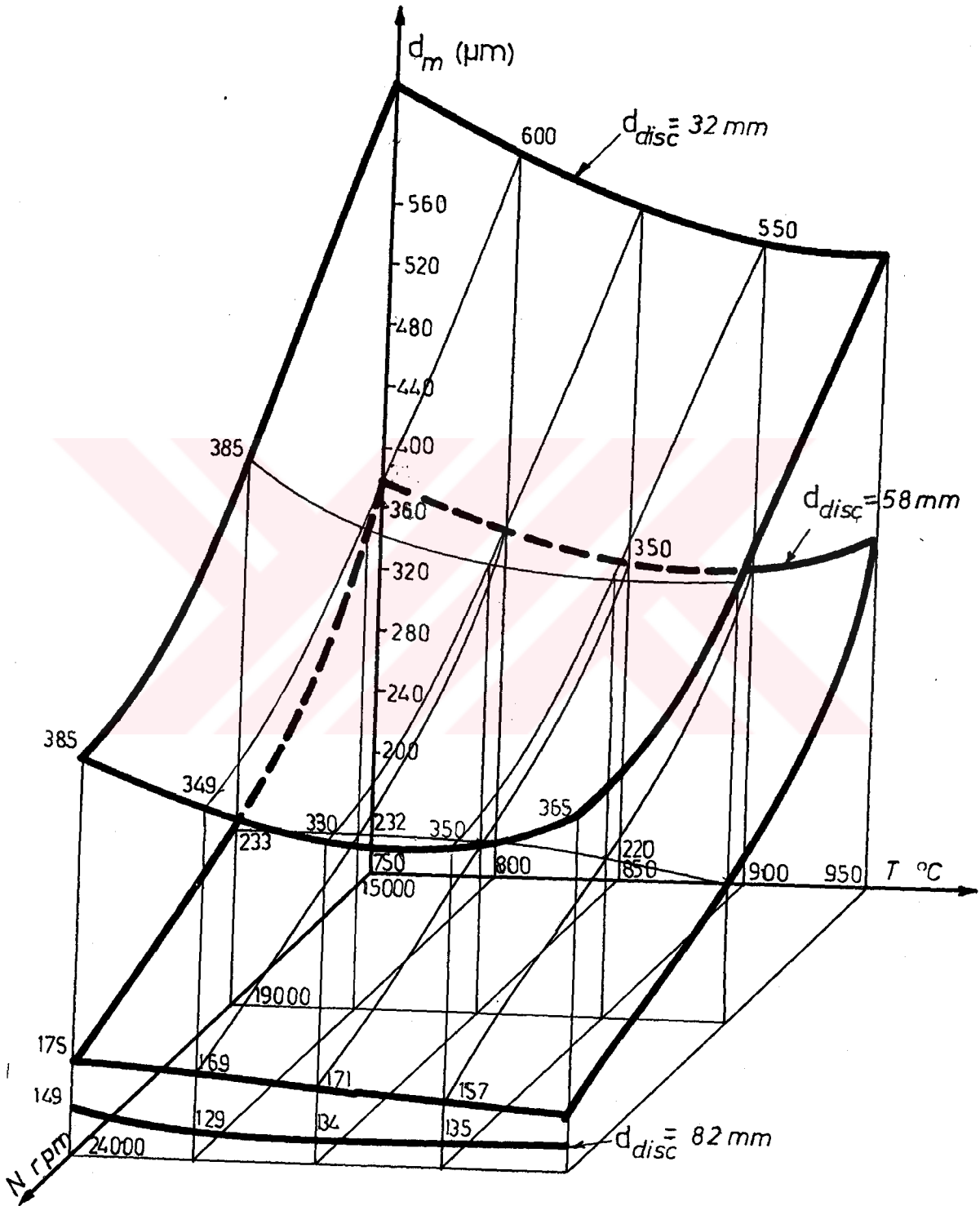


Fig.6.9 Effect of disc speed (rpm), liquid metal temperature ($^{\circ}\text{C}$), and disc diameter on the mean powder size (μm) in vaned disc atomized aluminum.

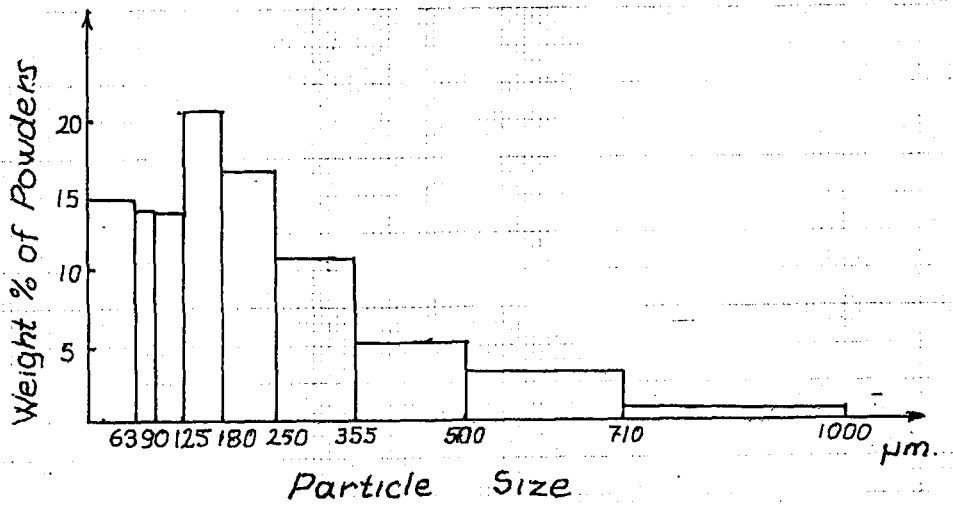


Fig.6.10 Powder size distribution of the Vaned Disc Atomized Aluminum

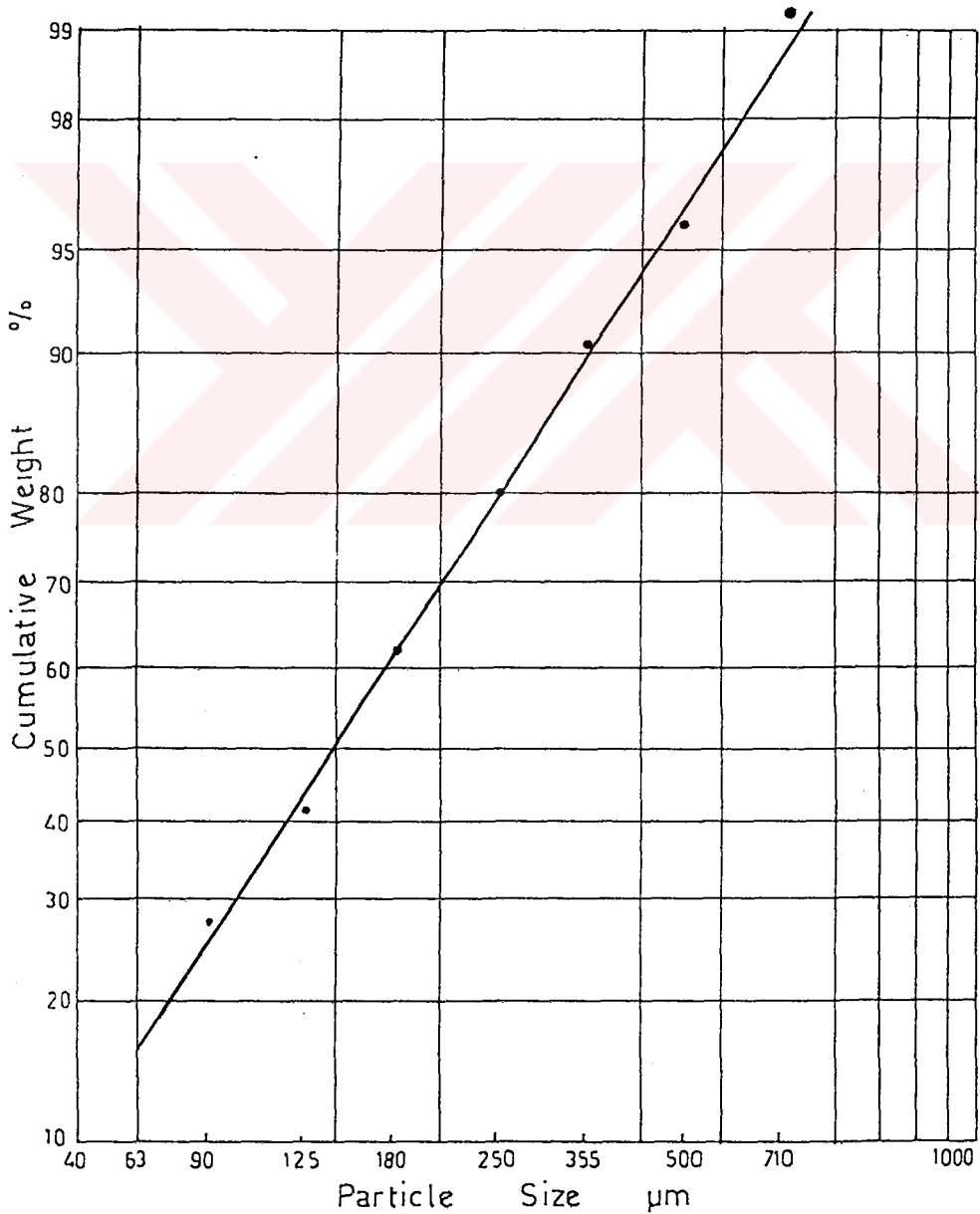


Fig.6.11 Cumulative weight percent distributions of the vaned disc atomized aluminum

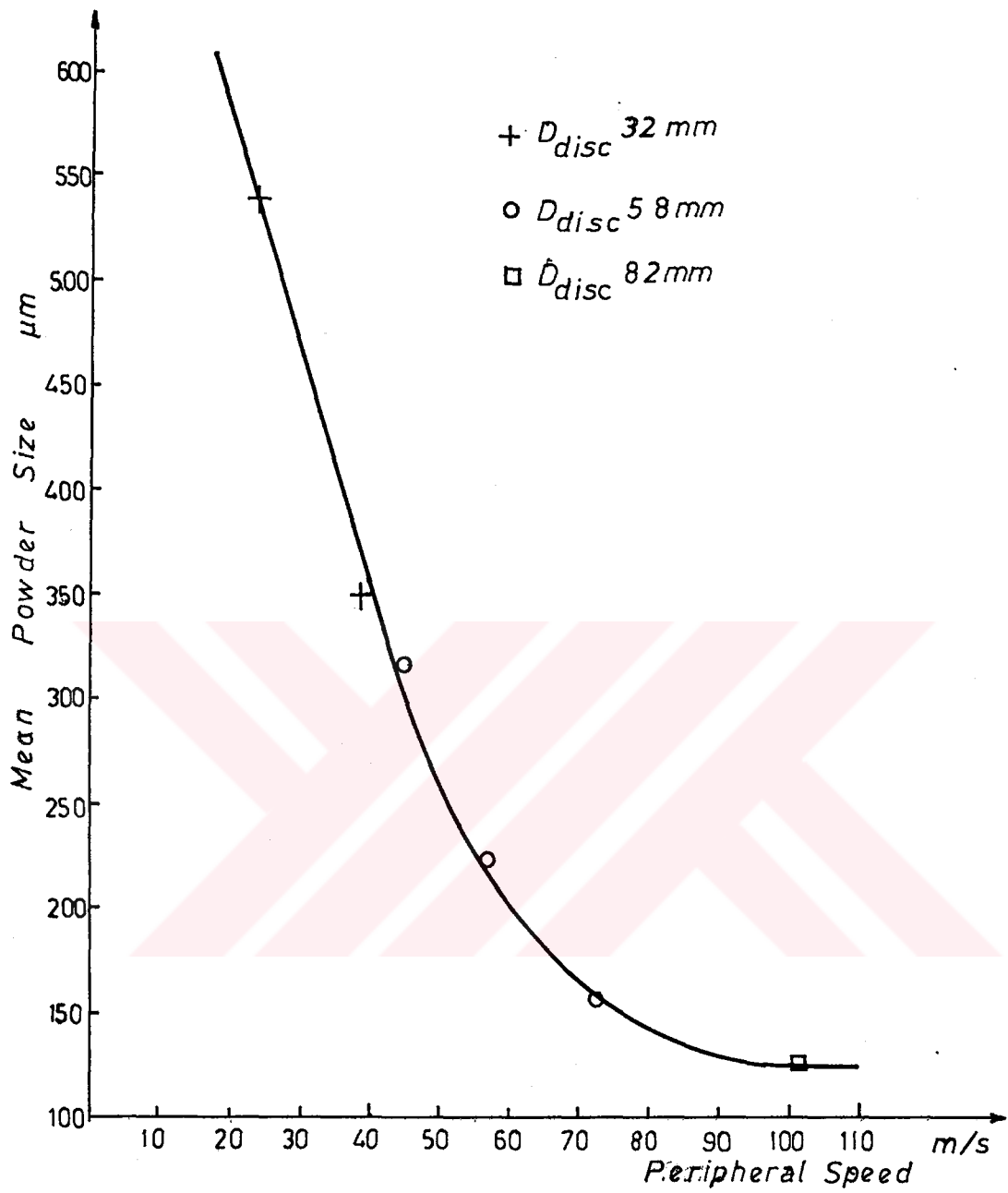


Fig.6.12 The effect of disc peripheral speed on the mean powder size of the atomized aluminum

6.4.3 Vaned Disc Atomization of Steel 8640

The condition of the flat disc atomization 12 % Mn steel were repeated in this experiment. The smaller size (32 mm) vaned disc was used at the speed of 24000 rpm. About 300 gr steel powder was produced.

The particle size distribution of the experiment was tabulated in Table 6.9. It is seen that the mean powder size is 122 μm . 13.6 % of the powders collected in the pan.

TABLE 6.9 POWDER SIZE DISTRIBUTIONS OF VANED DISC ATOMIZED STEEL 8640. (Disc speed = 24000 rpm, Liquid metal temp. = 1750 °C, Metal flow rate (approx.) = 200 g/s).

M	E	S	H	S	I	Z	E	μm		Grain	Mean
1000	710	500	355	250	180	125	90	63	pan	Fines	Powder
										Number	Size
											μm
0.2	1.6	0.6	6.0	11.4	28.6	19.2	18.8	13.6	124	122	

The powder size distribution was plotted as shown in Fig.6.13.

The cumulative weight percent of powders versus particle size distributions of flat disc atomized 12 % Mn steel and vaned disc atomized 8640 steel were plotted in log-normal probability paper as shown in Fig.6.14.

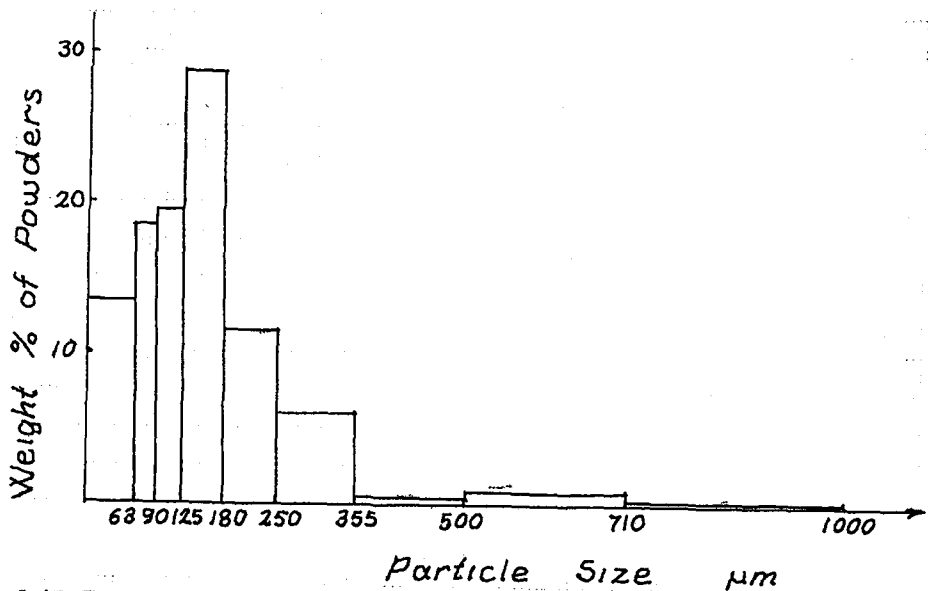


Fig.6.13 Powder size distribution of the vaned disc atomized steel 8640 ($d_m = 153 \mu m$) at $N = 24000 \text{ rpm}$, $T = 1750 \text{ }^\circ\text{C}$, $Q = 200 \text{ g/s}$

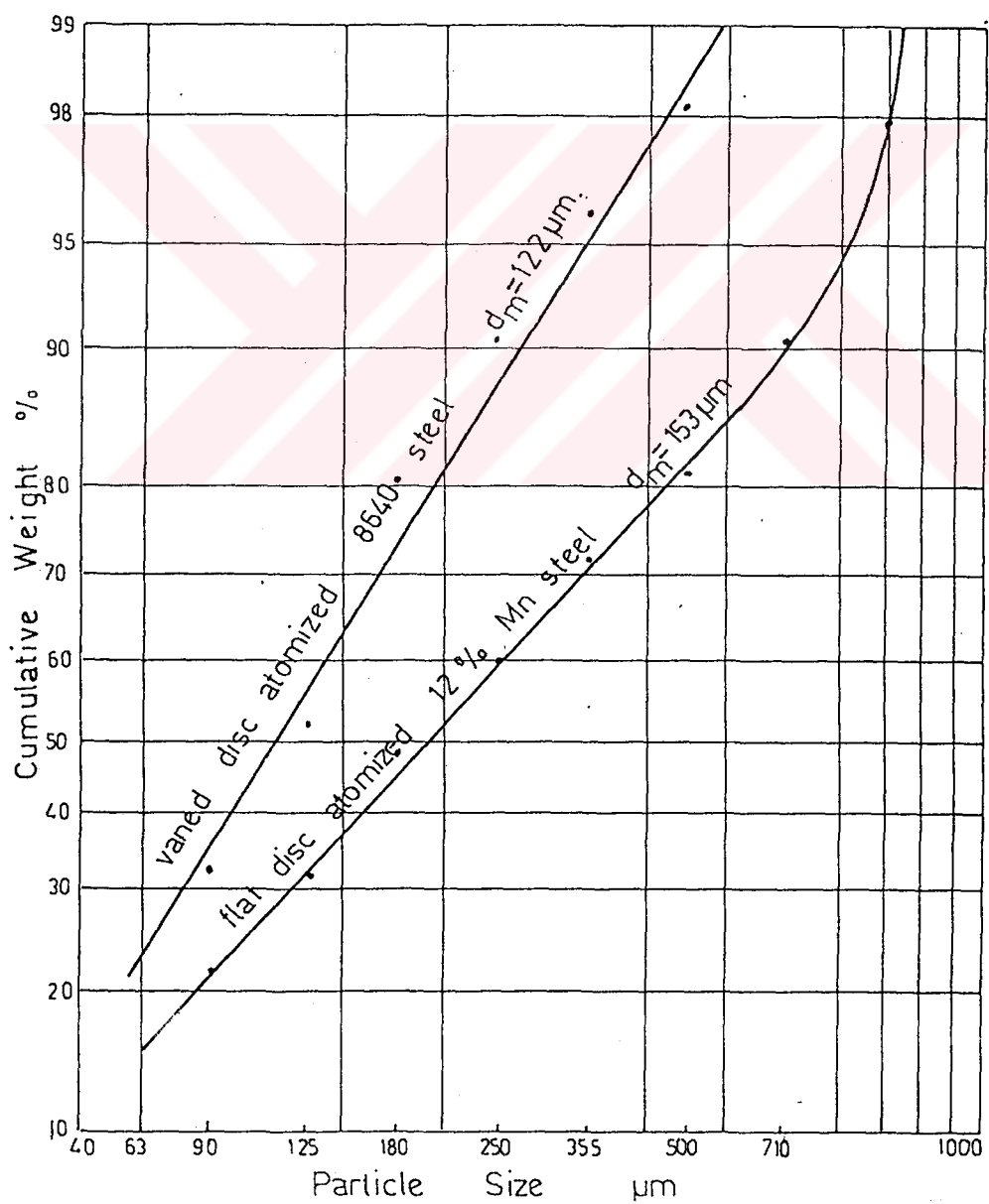


Fig.6.14 Cumulative weight percent distributions of the flat, and vaned disc atomized 12 % Mn steel and steel 8640

6.5 SHAPE AND MICROSTRUCTURAL ANALYSIS OF THE POWDERS

For each atomization condition, a few grams of powders were taken and mixed with polyester. This mixture was cold mounted. Each specimen was ground and polished by metallographic methods. The shape and microstructural analysis were examined by using a Leitz optical microscope with photographic facilities.

6.5.1 Shape Analysis of the Powders

The microscopic observation show that the shape of the powders are similar to water atomized powders for aluminum and lead. The complexity of the shapes was increased when the overheat temperature and the powder size increases. For the steel, since the degree of the over heat is low the shape of the powders are globular.

General views of transverse sections of aluminum powders, lead powders and steel powders are shown in Fig.6.15 to Fig.6.17 successively.

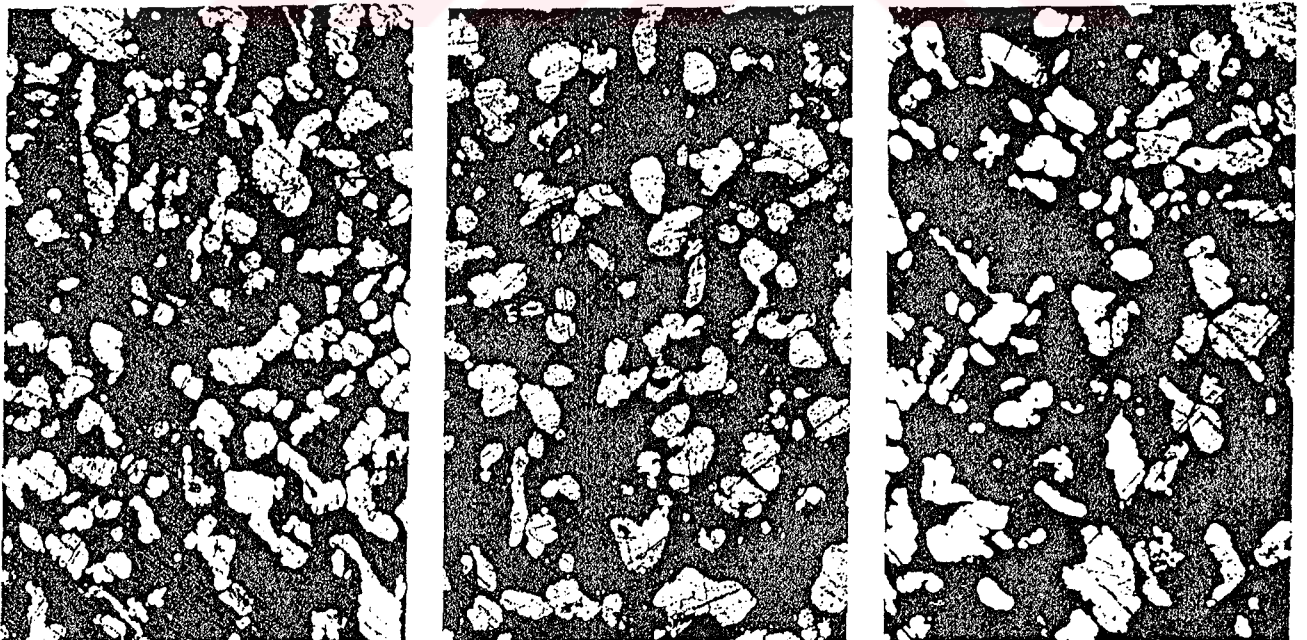
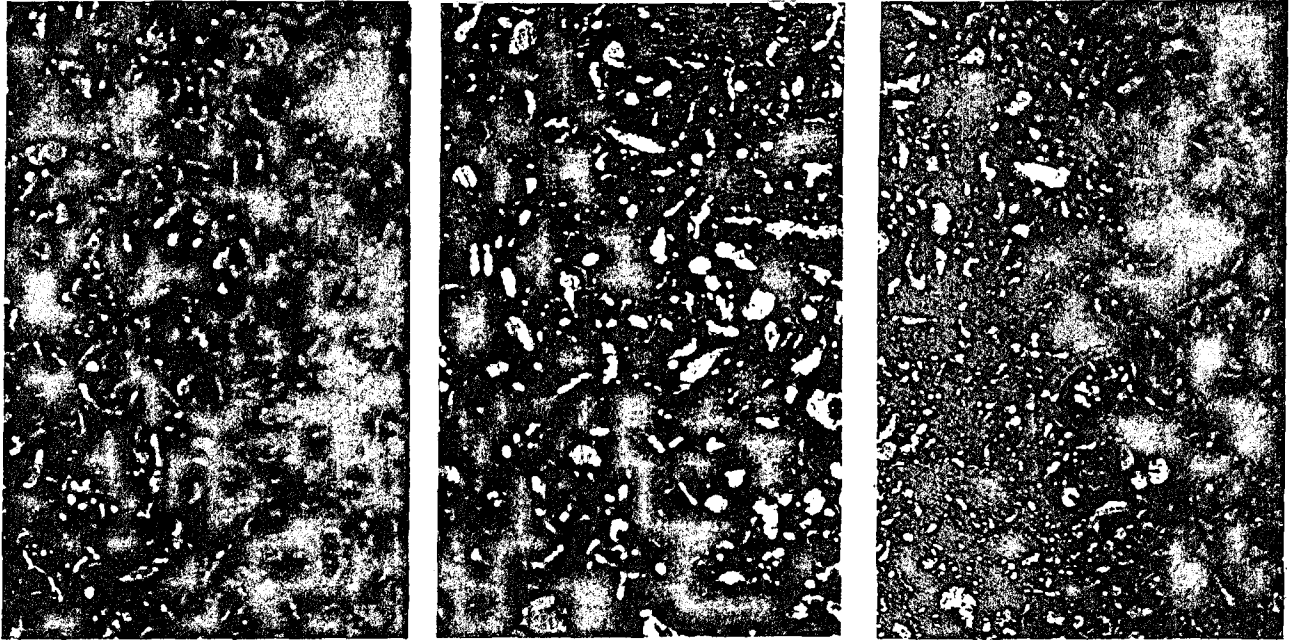
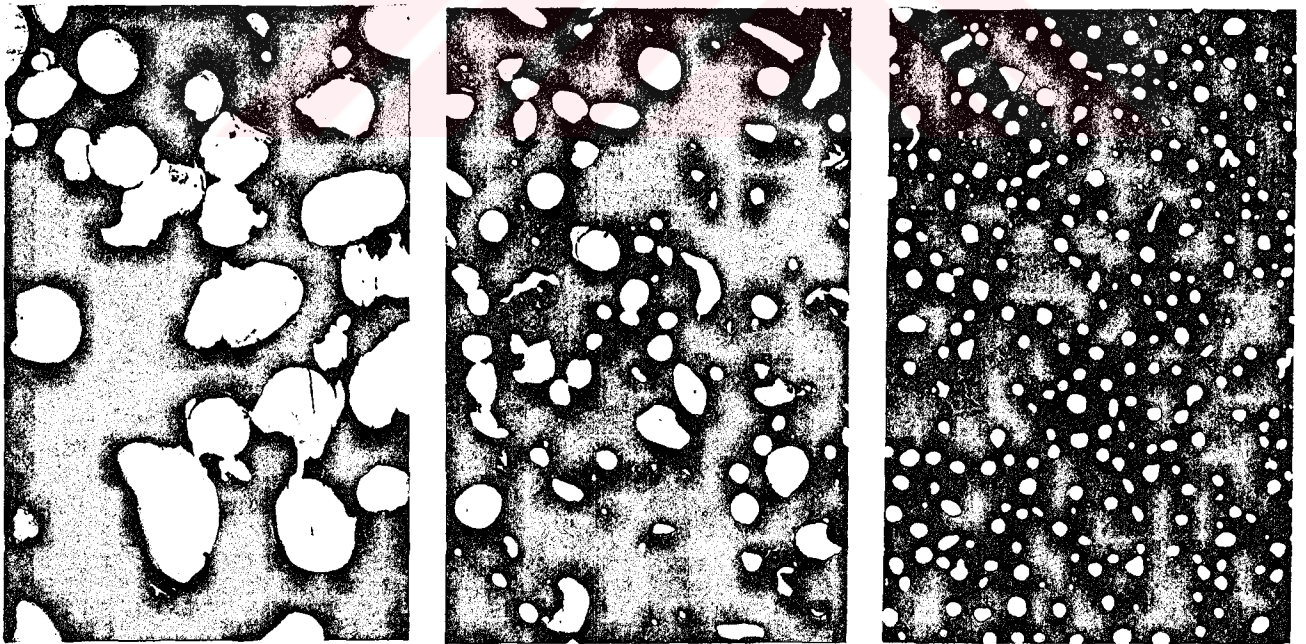


Fig.6.15 Transverse sections of aluminum powders . X50



X 50

Fig.6.16 Transverse sections of lead powders



X 200

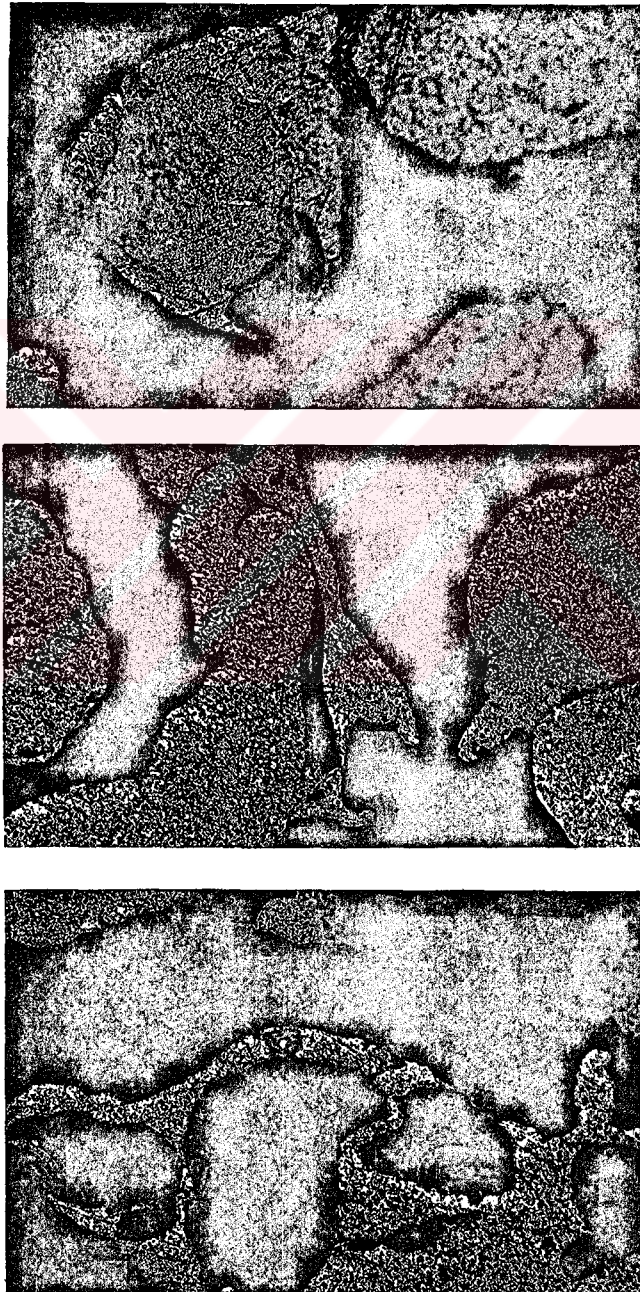
X 100

X 50

Fig.6.17 Transverse sections of steel powders

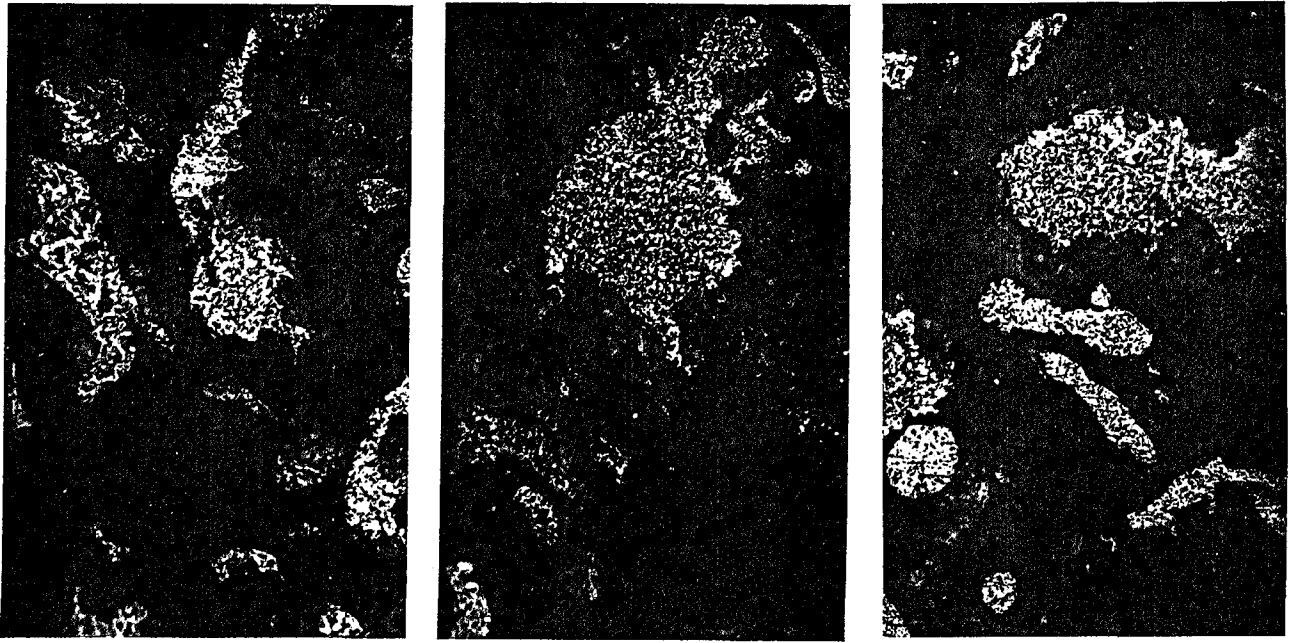
6.5.2 Microstructure of the Powders

Microstructural analysis of the powders were made by etching the specimens with suitable solutions and then examining them under the optical microscope. The grain size of the powders are very fine. Figs.(6.18, 19, 20,21) show the microscopic structure of the produced powders.



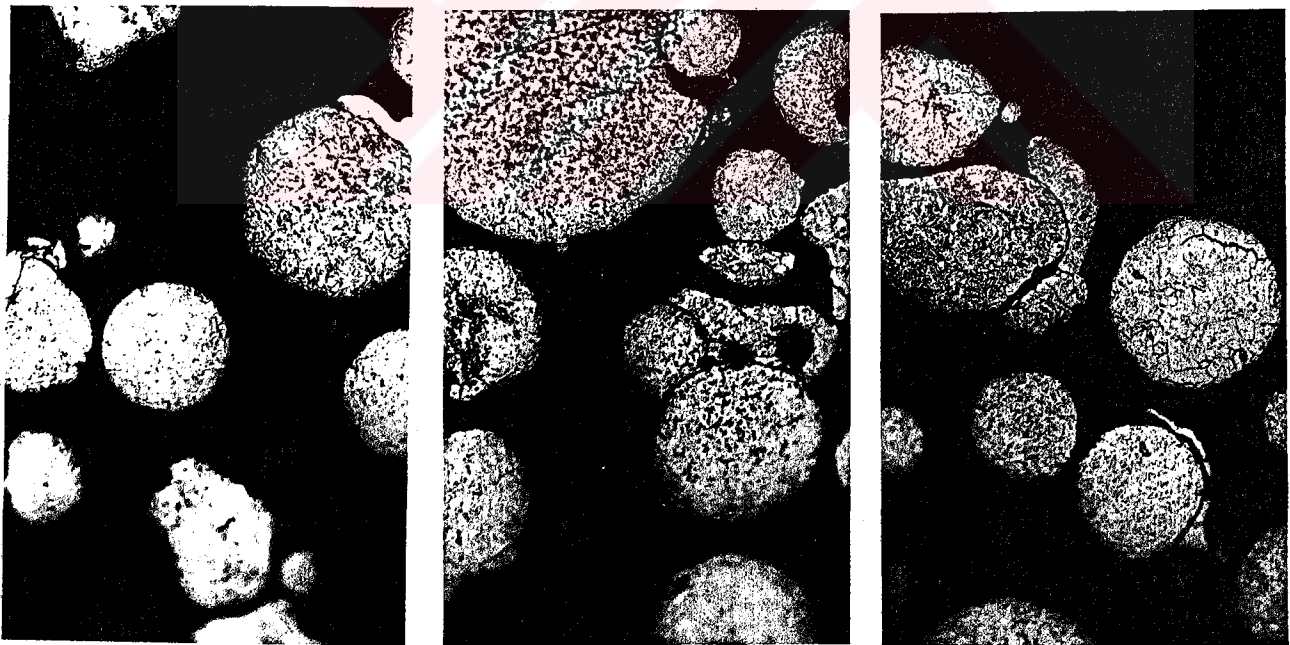
X 400

Fig.6.18 Microstructural views of aluminum powders



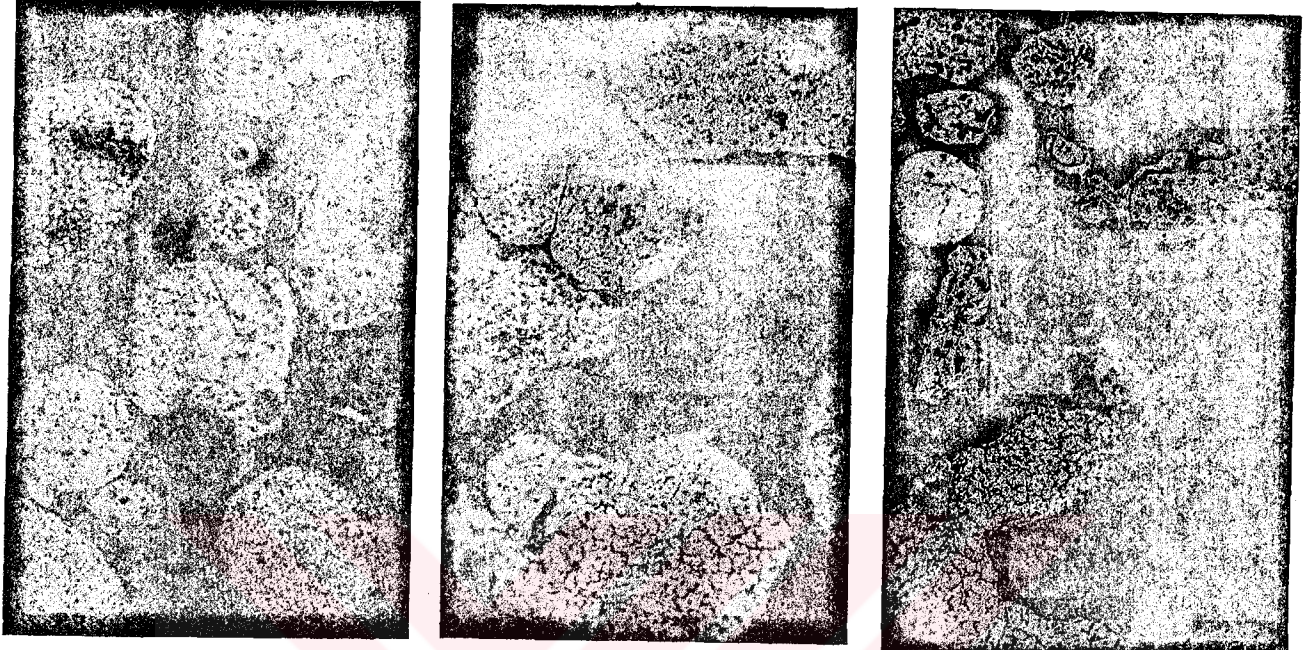
X 400

Fig.6.19 Microstructural views of lead powders



X 200

Fig.6.20 Microstructural views of steel 8640 powders



X 400

Fig.6.21 Microstructural views of 12 % Mn steel powders

6.6 SPECIAL FEATURES OBSERVED

6.6.1 Cavity

Vaned disc atomized aluminum powders contain cavities. The shape of these empty spaces are complex. Fig.6.22 shows general cross section of these types of powders.

When the size of the powders increased the number of empty spaces and the sizes of the cavities also increase as shown in Fig.6.23..

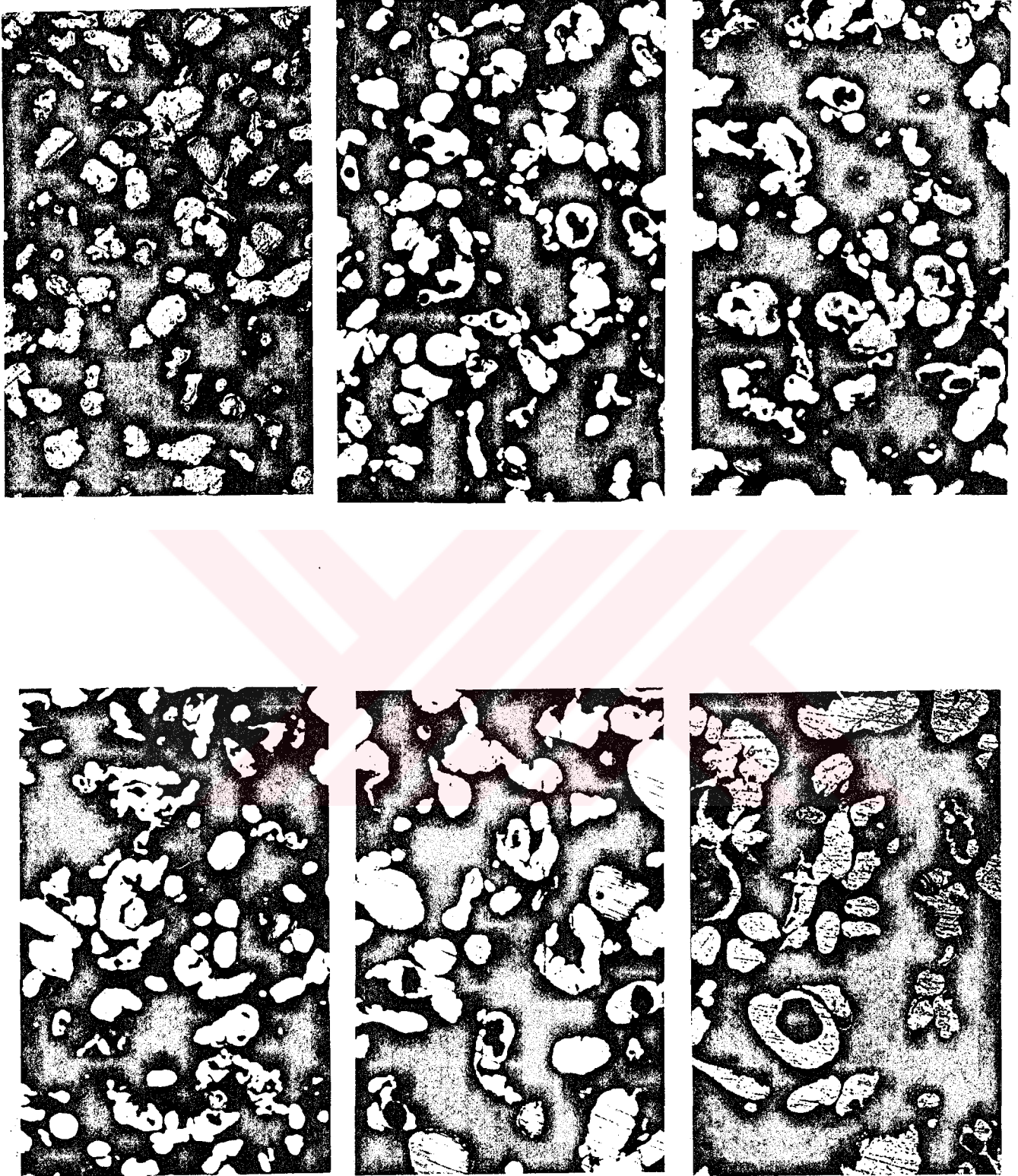


Fig.6.22 General cross sectional views of aluminum powders
contain cavities X 100

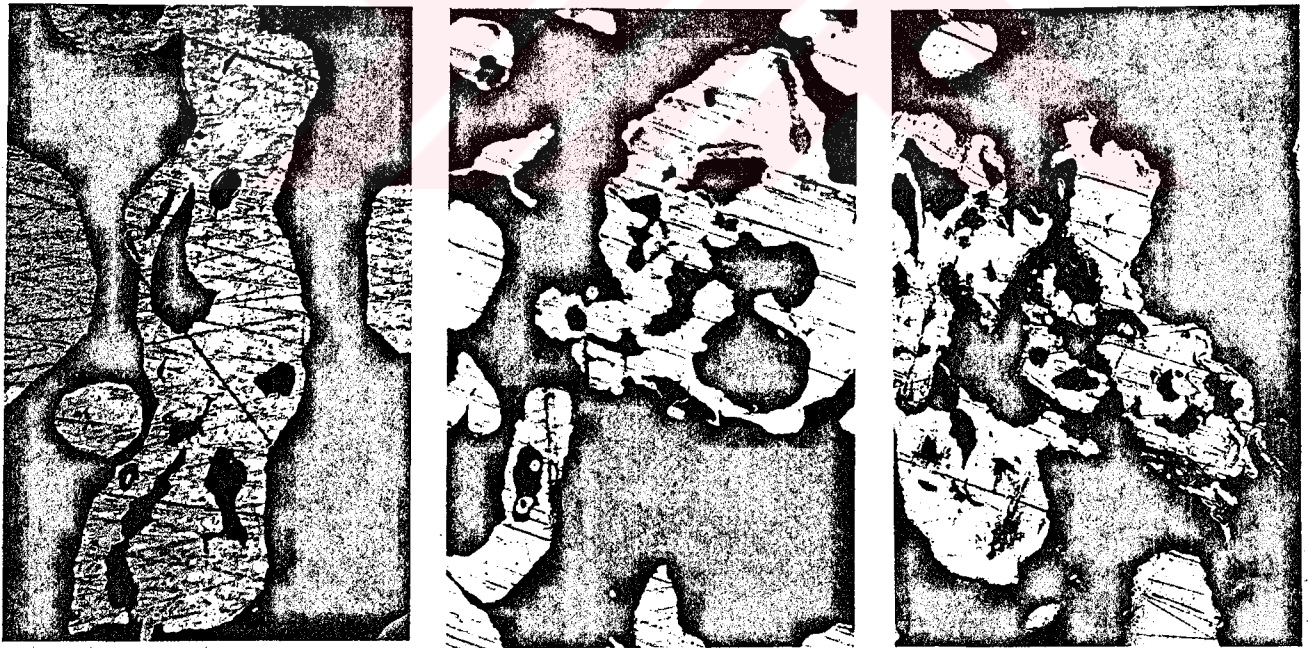
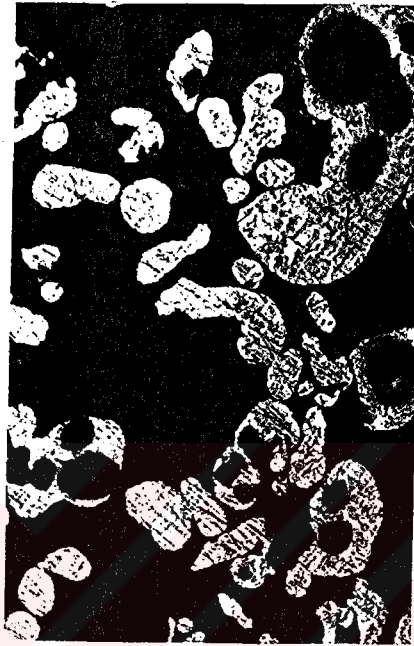


Fig.6.23 General cross sectional views of aluminum powders contain cavities X 200

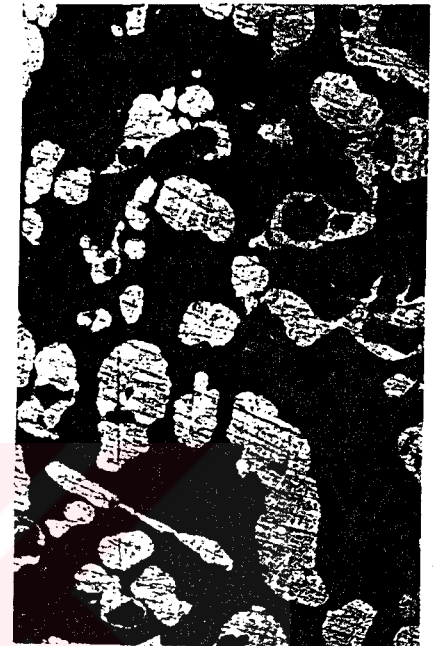
There are some spherical cavities in the powders. They must be created by separation of the bonded powders resulting from the collision of the particles during atomization. Fig.6.24 shows these types of cavities.



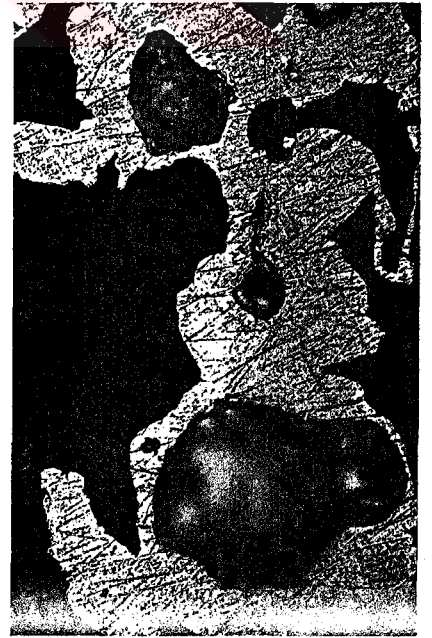
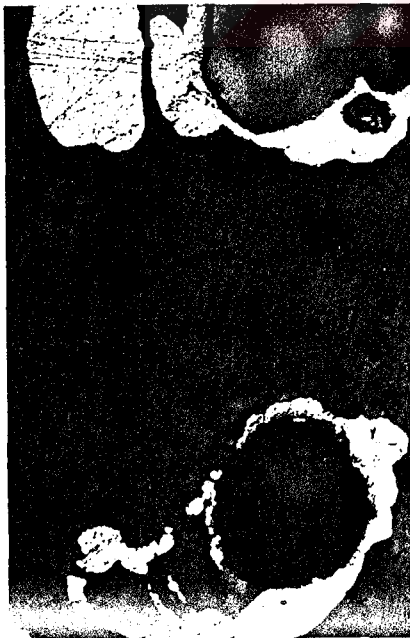
X 200



X 100



X 100



X 400

Fig.6.24 Cross sectional views of aluminum powders contain cavities created by separation of the bonded powders

6.6.2 Collisions

In the varied disc atomization due to the velocity differences of the droplets, collisions take place. Small droplets solidify quickly. They impact to large droplets which have not been solidified yet. As Fig.6.25 and Fig.6.26 show, sometimes these collisions can result with total encapsulation of the penetrating particle.

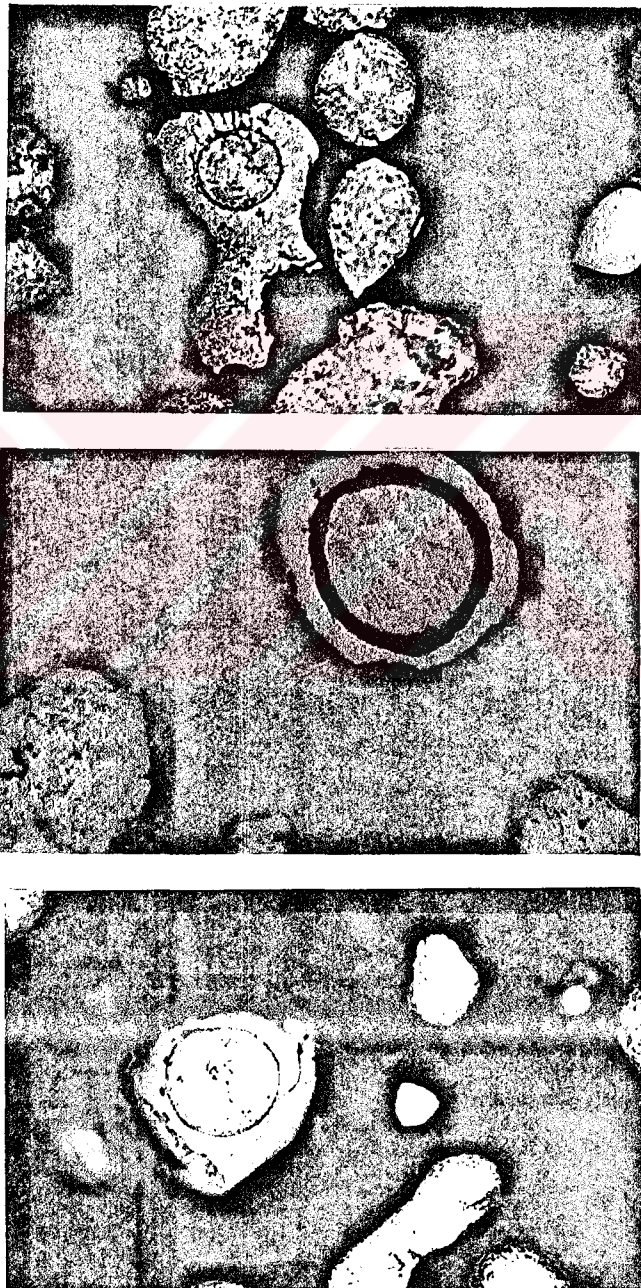


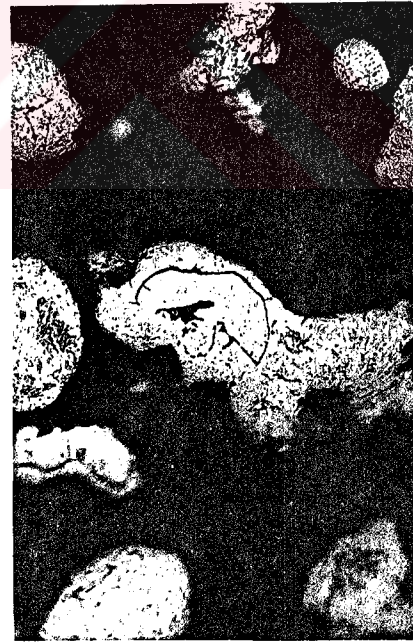
Fig.6.25 Encapsulation of the steel 8640 powders created by collision of the powders during the atomization X 200



X 200



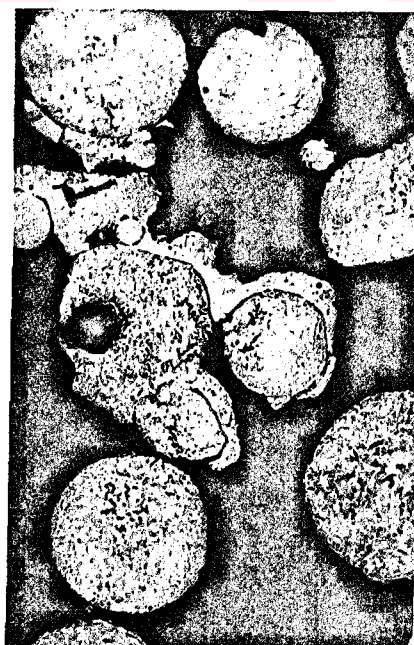
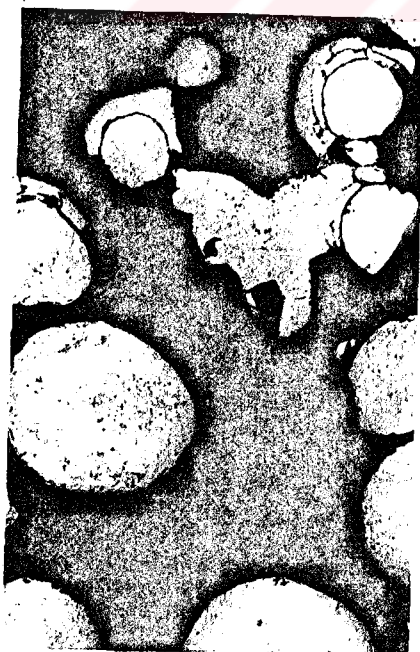
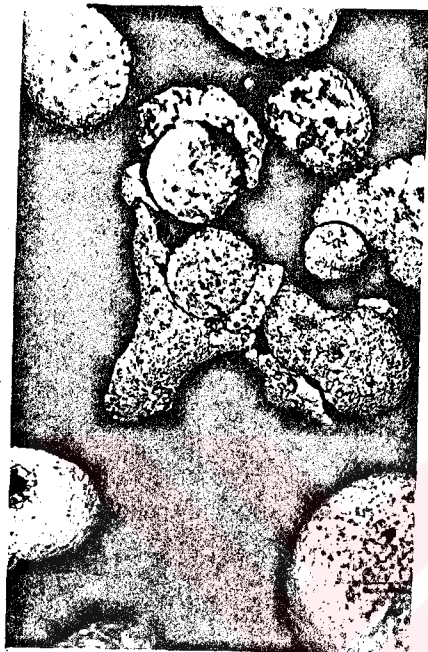
X 400



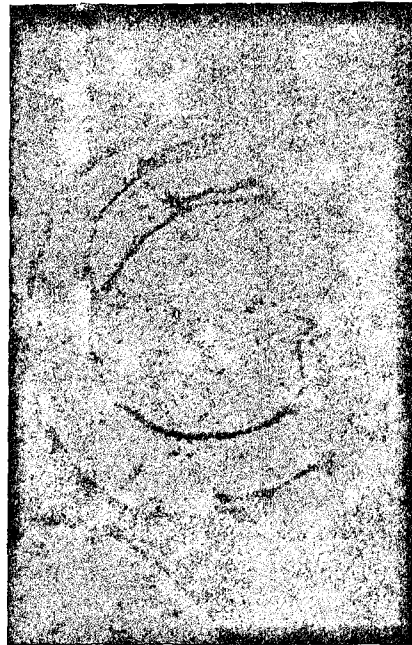
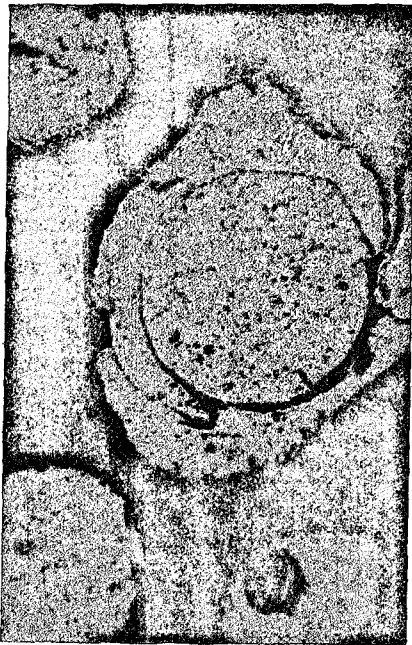
X 200

Fig.6.26 Encapsulation of the aluminum powders created by collision of the powders during the atomization

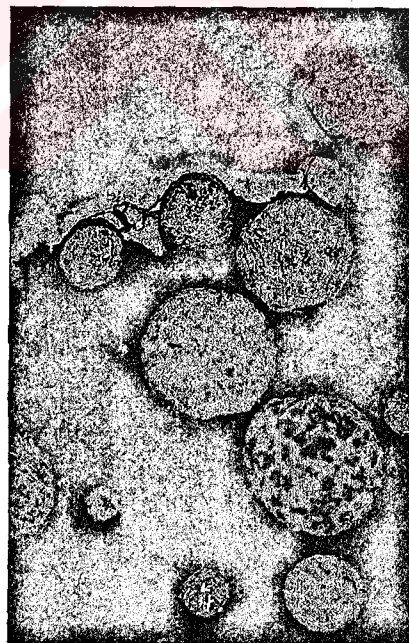
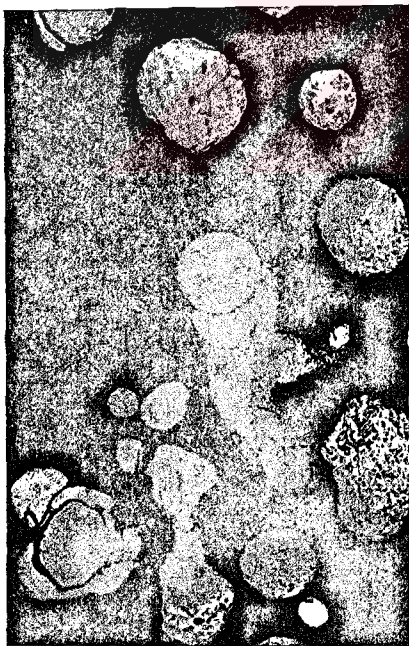
Sometimes collisions of more than two particles can take place. In these instances one or two of the particles (droplets) may not be totally solidified and total encapsulation may not occur as shown in Fig 6.27. Number of colliding particles can be as high as eight.



X 200



X 400



X 200

Fig.6.27 Various types of collisions observed in the steel
8640 powders

Fig.6.28 and Fig.6.29 show cracking in some powders and also holes through themselves produced due to collisions.

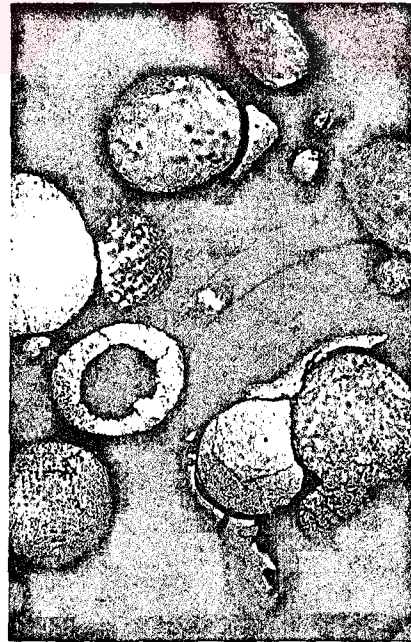
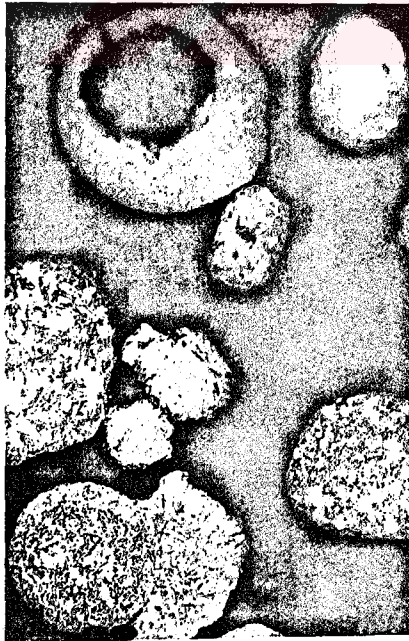
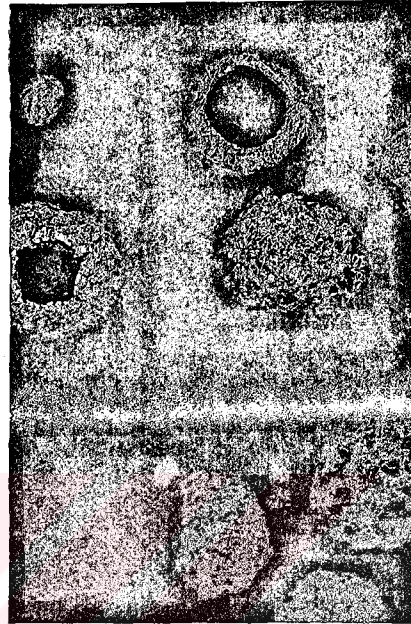
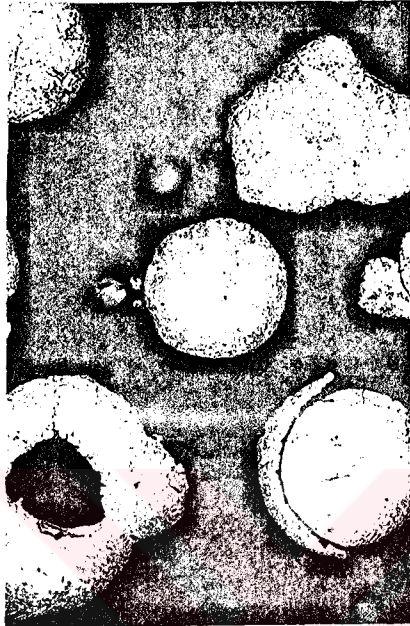


Fig.6.28 Transverse sections of steel 8640 powders holed through themselves produced due to collisions X 200

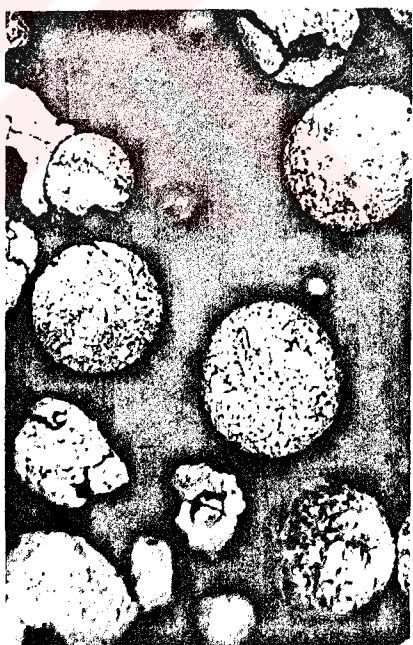
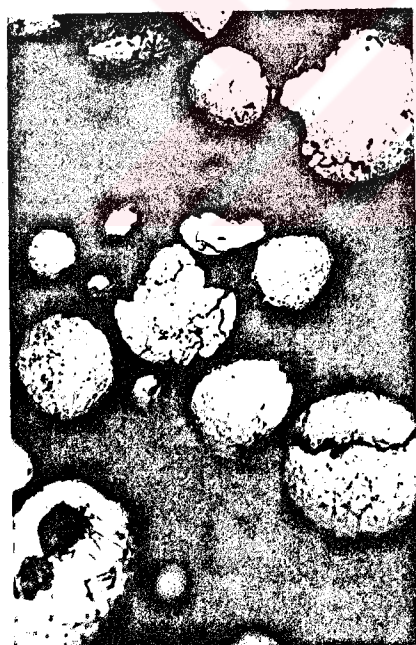


Fig.6.29 Transverse sections of steel 8640 powders cracked during the atomization X 200

6.6.3 Microhardnesses of Powders

LEITZ microhardness tester was used to determine the Vickers hardness of the steel powders. Six tests were made on the powders of steels. The measured values are tabulated in Table 6.10.

TABLE 6.10 MICRO HARDNESS TEST OF THE STEEL POWDERS
(Vickers Hardness: load $P = 100 \text{ g}$)

MATERIAL	T e s t n o:						Average
	1	2	3	4	5	6	
8640 Steel	1097	1018	946	1018	1097	1097	1050
12 % Mn Steel	401	342	373	383	380	401	380

CHAPTER 7

A) DISCUSSION

7.1 INTRODUCTION

As pointed out in previous chapters, the aim of this work was production of water atomized metal powders, being the most common metal powder used in P/M industry. Due to very high cost of high pressure water pump and accessories, research was diverted towards centrifugal atomization. Then, a unique design was made which used the principle of centrifugal atomization, but produced powders with characteristics of the water atomized powders.

In literature [39, 44, 47], metal powders by centrifugal atomization are produced by using a flat or a cup shaped disc. In this study, for the first time, the vaned disc geometry was introduced for the production of metal powders, by centrifugal atomization. The experimental results show that vaned disc can produce at much higher rates than the flat and cup shaped discs, the powders produced are much finer.

In this study, lead and aluminum are selected as the main metals for metal powder production. There are two important reasons for their selection:

(1) Economical reasons, melting and over heating of these metals are very easy.

(2) They offer opposing densities. Mass being the main parameter in centrifugal atomization. Towards the end of experiments, two different grades of steels are introduced just as trial runs.

In the following sections, performance of flat, cup shaped and vaned discs will be discussed, by paying special attention the characteristics of the powders produced.

7.2 FLAT DISC ATOMIZATION

Main experiments were done with lead, then a trial was performed with a 12 % Mn Steel.

In the flat disc atomization liquid metal was poured vertically on the surface of the disc. Liquid metal touches the disc at the center and, then it is centrifugally accelerated to high velocity before being discharged into cooling media. The liquid metal is uniformly distributed as a thin film from the center outwards becoming thinner while moving. Any volume of liquid metal follows a spiral path due to tangential and radial components of the forces created due to rotation: Tangential component being much bigger than the radial component.

The friction between the disc and the liquid metal is vital in atomization. If there is no friction, rotation of disc is not important, liquid will flow outward uniformly without making a spiral motion. The friction between the liquid metal and the disc surface is due to two different sources: viscosity of the liquid metal, and the surface roughness and type of the disc material.

At the contact area, disc is at a lower temperature than the solidification temperature of lead. So lead cools continuously on the contacting areas and becomes more viscous. Thus the speed of the liquid film touching to the disc is same as the disc speed. Velocity profile in the liquid film decreases toward upper portion of the film.

During experiments, the disc was heated to around 150 - 200 °C. This is below the melting point of the material. Therefore, the thin

film suddenly solidifies due to heat lost. For lead, when the preheated temperature of the disc is increased above 300°C, solidification does not take place. This means that the preheated temperature of the rotating disc must be 100°C higher than the melting point of the atomized material. Because of the safety of the system the preheated temperature of the disc was kept around 150 - 200 °C.

During the atomization the thickness of the solidified film was continuously increasing upto 2 - 3 mm. Then this plate was thrown away due to unbalance forces and vibration effect and some times the plate shear due to centrifugal force. Later, a new film grows on the disc surface and the same phenomenon repeats untill the end of the atomization. This is related with the temperature and flow rate of the liquid material and rotating speed of the disc. For high temperatures and high speeds (700 °C and 24000 rpm) about 20 % of the liquid metal solidified as a plate. This value increases upto 80 % , at the temperature of 400 °C and 19000 rpm disc speed. Below this speed plate formation increases to higher values. Therefore, the experiments were done above 19000 rpm and 400 °C.

During the atomization, the liquid metal flow over the solidified metal plate whose thickness changes with time. This means that the surface quality of the disc always changes. Since the solidification of the liquid metal on the disc surface takes place below the melting point of the atomized material, the surface roughness of the solid plate can be assumed same for all experiments.

Due to viscous action of the liquid, the rotational speed decreases parabolically down from the disc surface to the free surface of the liquid metal. Therefore the velocity of liquid while leaving the disc edge is much lower than the disc peripheral speed. This slippage of the liquid metal mostly related with the viscosity. Since the viscosity of the liquid metal decreases by increasing the temperature, the

powders become coarser when the temperature increases. The results of the flat disc atomization of lead (Fig.6.3) prove this relationship.

In the flat disc atomization, the liquid metal contact with the surface of the disc due to effect of the gravity force. If the centrifugal force of any volume of liquid metal is greater than the force that is produced from the viscosity, the surface tension and the friction, it separates from the disc surface. After this point disintegration of the liquid metal starts. The centrifugal force on a particle is also related with the density of the liquid metal. The atomization of the liquid metal starts at any point on the disc when the above condition is satisfied. If the energy at any point of the liquid is greater than the required minimum atomization energy, atomization will start at that point.

Minimum energy for atomization is the requirement to create new surface. The theoretical power (P_k) can be expressed [76,77];

$$P_k = A \sigma \quad (7.1)$$

where A = net average area created per unit time,

σ = surface tension.

This means that the liquid metal can be atomized not only at the outer edge but at every point of the disc. After the liquid metal separates from the disc surface, the disc can not impart the energy to the liquid metal. Therefore after certain disc speed the powder size does not change. It is seen from Fig.6.3.a and b that the variation of the rotating speed does not affect the powder size.

7.3 CUP SHAPED DISC ATOMIZATION

In cup shaped disc atomization the liquid metal (lead) contacts with the surface of the disc due to effect of gravity and centrifugal force. Since the inner surface of the disc is concave, the

centrifugal force increases the friction between the disc surface and liquid film. Because of this the slippage of the liquid metal on the cup shaped disc is very low when it is compared with the flat disc. During the atomization the liquid metal can not separate from the disc surface until the edge of the disc. The atomization starts at the edge of the disc. This increases the uniformity of the powder size distribution.

As Fig.6.4(b) shows, mean powder size is decreasing as the temperature increases. This is just opposite for the flat disc. In flat disc, at higher temperatures slippage was taking place due to reduction in viscosity. But with cup shape disc, slippage is prevented by the shape of the disc. Thus, as the temperature increases, viscosity and surface tension decreases. Decrease in viscosity can not cause slippage as explained above. Decrease in surface tension makes the atomization much easier, since the minimum energy for atomization is decreasing.

Mean powder size should be increasing as the flow rate increases. The values after 75 g/s obeys this relationship. At lower values, theoretically powder size should be decreasing. During experiments opposite took place. This should be due to cooling effect of the disc. Being much more affective at lower flow rates. The expected mean particle size should follow the dashed line.

At high speeds, the temperature and the flow rate are not effective as shown in Fig.6.6.b. Changes in viscosity and surface tension are not affective as the change in centrifugal force. Centrifugal force at these high speeds governs the atomization.

7.4 VANED DISC ATOMIZATION

Rotational speed of the liquid is few orders of magnitude bigger than the radial speed. Thus, liquid tries to rotate rather than more

outward on the disc. As shown in Fig.6.12 peripheral speed of disc varies from 24 m/s to 102 m/s. This peripheral speed produces centrifugal accelerations of 3600 g to 25000 g. So centrifugal component of the force on the liquid metal is incomparable with the gravitational force. As a result, liquid metal leaves the disc surface and accumulates on the vane surface. As shown in Fig.4.5.a, liquid film is parabolic and becomes thinner as approaching to the end of the vane. No slippage of liquid metal can take place since, vane is acting as a constrains. It prevents rotation of the liquid metal with the disc, and changes direction of the liquid metal by 90°.

With this kind of disc, controlling the experimental conditions were very much easier. Flow is virtually taking place in a chute. Changes in disc speed, flow rate and temperature have direct effects on the mean particle size. Experimental results are much more reliable and repeatable. Only problem relating to vaned disc is fan effect of the disc. Disc itself is working as a fan and sucking fresh air continuously. This cools the disc itself and the liquid metal which solidifies, after certain period of atomization in the disc. Thus, disc itself is blocked and becomes useless. Low flow rates and lower disc speeds are more dangerous. For lead atomization heating the disc to 300°C prior to atomization eliminated the blocking during our experiments.

Experimental observations as follows:

a) When the viscosity and the surface tension of the liquid metal is decreasing the powder size decreases. Since the viscosity and surface tension of a liquid metal decreases as the temperature is increasing, the powder size decreasing when the degree of the overheat temperature of the liquid material is increasing.

b) Because of no slippage occurring in the vaned disc the energy imparted to the liquid metal is proportional to the speed of the rotating disc. Therefore, the powder becomes finer when the disc speed is increased.

c) The powder becomes coarser when the film thickness of the liquid is increased. This means that, the powder size increases if the flow rate of the liquid metal is increased.

There are two important reasons for the deviation from the general rules, These are :

- 1) Solidification of the liquid metal during the atomization and
- 2) Fan effect of the vaned disc.

Solidification in the vaned disc taking place similar to that explained for the flat disc.

Because of the safety of the system the preheated temperature of the vaned disc is below the melting point of the material. A thin film on the vane surface solidify quickly due to heat loss. Then the liquid metal flow over the solidified film which the liquid metal flow over it is very high. This poor surface quality prevents the flow of the liquid metal through the vane. Therefore, radial speed of the liquid metal is low. This increases the duration of the contact of the liquid with the vane surface. Liquid metal becomes cooler and then surface tension increases which retards atomization.

But at the high temperatures and high flow rates the fan effect is very small.

The experimental results of vaned disc atomization of lead at 24000 rpm disc speed was shown as the three dimensional graph (Fig.6.3). It is seen that the powder size decreases by increasing the temperature and it increases with the increasing of the metal flow rate. The minimum average powder size was obtained as 75 μm at the high temperature (750°C) and low flow rate (75 g/s). At the low liquid metal flow rate (50 g/s), since, the film thickness of the liquid in the vane is very small the flow resistance of the liquid on the solidified film of the material is increased. Therefore the radial speed of the liquid metal decreases. The heat loss of the liquid metal increase since the duration of the contact of the liquid metal with vaned surface increases.

In the vaned disc atomization the speed of the disc is the most important parameter. It was seen that when the speed of the disc decreased to 19000 rpm the vane of the disc blocked suddenly at the low temperature (400 - 550°C) and low flow rate (50 - 75 g/s). For the other conditions, the variation of the powder size is similar to the first experiments. The minimum average powder size was obtained as 78 µm which is almost similar to the first one (75 µm).

In the vaned disc atomization of aluminum, three different sizes of disc were used. The experimental results were plotted as three dimensional graphs as shown in Fig.6.10. It was seen that all of the results of the experiments obey the theoretical rules.

Fig. 6.11 shows the effects of the disc size on the powder size.

7.5 SHAPE ANALYSIS OF THE POWDERS

In general, the shape of the powders produced by atomization is the function of the surface tension and the cooling rate. It is also related slightly with the powder size. The shape of the powder becomes complex if the powder size is increasing and it becomes spherical or globular if the powder becomes finer.

It was pointed out that the mean particle size of the powders depends upon:

- a) types of materials (density, melting temperature),
- b) degree of overheat temperature,
- c) rotating speed of atomizer disc,
- d) design of the disc, and
- e) metal flow rate,

For cup shaped and vaned disc atomization, the powder becomes finer when the overheat temperature and speed of the disc are increased, and metal flow rate, surface tension and viscosity of the liquid metal are decreased

Due to effect of the surface tension, the droplets try to reduce their surface area. This means that if a complex shaped droplet is kept at the liquid form in a certain length of time, the shape of the droplet changes to spherical form. If air or a gas is used as a cooling media, since it has low cooling rate the droplets stay enough time in the liquid form. Therefore, due to the effect of surface tension, the powders becomes spherical or globular shapes. Since the speed of the atomized particles are very high (30 to 100 m/s depending upon disc speed and disc diameter), at the beginning the friction and the drag force of the air also tend to change the shape to spheric. Because of these reasons if the air or a gas is used as the cooling media the shape of the powders become spherical or globular type.

If the cooling rate is increased the droplets solidfy quickly, therefore there is not enough time for making the droplets sphere. The effect of the surface tension on the powder shape decreased to low values when the cooling rate is increased up to a certain value.

If the cooling rate of the droplet is accelerated up to high values, the shape of the powder becomes too irregular due to high temperature gradient in the droplet. It is known that shrinkage is observed when any liquid is solidified. At high cooling rates, two phases which are liquid and solid can be observed at the same time. Because of these reasons the shapes of the powders become complex at high cooling rate.

In our system, liquid metal is atomized mechanically by means of centrifugal force and then cooled in water after flying about 10 cm in the air. Small droplets are solidifying while in flight in air, but large droples solidfy in water producing water atomized characteristics.

There are several collisions of the droplets and powders, which are observed in the vaned disc atomized aluminum and steel powders. In the vaned disc atomization the radial velocity component is much

smaller than the tangential component, release velocity approximates to the peripheral disc velocity. Since there is no slippage occurring in the vaned disc atomization, the release velocity of the various sizes of the powders are approximately the same and equal to tangential speed of the disc. Therefore, kinetic energy which imparted by th disc are related with the masses of droplets.

The drag force due to air resistance is acting opposite to the moving direction. The speed of powder various between 30 - 100 m/s. The effect of the drag force can be calculated analytically, assuming the shape of the powder as sphere. Since the diameter of the powders are very small (10 - 250 μm) the Reynolds Number at the speed of $V=30 - 100$ m/s for air is less than 100. Reynolds Number is inversely proportional to coefficient of drag force for spherical and cylindrical shapes. This means that the drag force to kinetic energy ratio of a particle decreases when the particle size increases. Therefore large particles moves faster than the small particles in air. On the other hand cooling rate of a droplet increases if the surface area to weight ratio is increased. So, smaller particles are solidifying earlier than larger particles (generally in air). As they are flying in air, large liquid droplets or partialy solidified mushy droplets reaches to small spherical powders and encapsulate them (Fig.6.25 and Fig.6.26). This is the most common collision type. Sometimes, the relative speeds between the two colliding mushy droplets + solid powder are so high that solid powder pierces through the dorplet like a bullet (Fig.6.28). But, in some cases solid powders penetrate into the mushy droplet but can not pierce through. They are trapped in them (Fig.6.27).

Fig6.29 shows that some powders are cracked. This is only observed in 8640 powders. This steel is a through hardening steel, and the cooling condition in the present set-up are very severe. Cooling rate as high as 10^8 $^{\circ}\text{C}/\text{s}$. are reported by Fischmeister and his Colliques during gas atomization[78]. In the Figure, it is observed that some

cracks are associated to collision. So, before entering into water, two solid powders must have been colliding at very high relative speeds. This collision would either cause cracks or produce damages in the powders. Later, during water quenching these damage could accelerate to produce crack. In some cracked powders no collision is observed. So, it must be only due to severe quenching conditions. As Table 6.10 shows microhardness of powders are very high.



CONCLUSIONS

1) The set-up designed and constructed produced powders with water atomized characteristics. Their shapes and mean particle sizes are very suitable for powder metallurgy applications.

2) In the case of lead atomization, minimum average powder sizes are : (a) Flat disc: 119 μm . (b) Cup shaped disc: 150 μm , and (c) Vaned disc: 75 μm .

3) In flat and cup shaped disc atomizations there are limiting values of metal flow rates varying with the type of the material. Above this value, the disc can not atomize the liquid metal due to severe slippage. This limit is 100 kg/hr for the flat disc and 120 kg/hr for the cup shaped disc atomization of lead.

But there is no such a limit for vaned disc atomization. The production rate of vaned disc atomization is 1000k g/hr for lead, 200 kg/hr for aluminum and 600 kg/hr for steel.

4) The set-up is very simple. Control of speed, temperature and metal flow rate are easy. For laboratory investigation of atomization, it is very adequate.

5) The efficiency of the system is about 30 % for flat disc, 35 % for cup shaped disc, and 70 % for vaned disc atomization.

6) In water atomization of elements like aluminum, explosion is taking place due to sudden exothermic reaction of water with the powder element. Since atomization is taking place by centrifugal forces, and initial cooling is in air, there is no explosion danger in the present set-up.

7) Small droplets generally solidifies in air and are spherical. Large droplets complete their solidification in water thus producing irregular shapes.

8) Many different collision types are observed: between liquid-solid, mushy droplet-solid, solid-solid.

9) In the case of 8640 steel atomization, resulting microstructure is very hard (about 1050 HV). Even crackings in the powders are observed. This shows that powders was super cooled.



FUTURE WORKS

1) The present set-up is suitable only for low melting point elements. Suitable tundish and a melting unit for high melting point elements should be added to the set-up.

2) Disc design should be further investigated: (a) disc shape, (b) disc material and (c) disc size.

3) Atomization at much higher disc speeds must be investigated (upto 100,000 rpm).

4) Powder characteristics should be further investigated. Shape analysis with SEM should be carried out. Microstructure of powders should be examined in better preparation condition and higher magnifications.

5) Water vortex can be replaced with different quenching media to obtain powders with different characteristics.

6) Atomization of various other elements can be tried at various overheats.

7) Further processing of the resulting powders should be investigated: Removal of oxides, grinding to obtain finer powders, etc.

8) Same set-up can be modified to suit rotating electrode atomization unit.

REFERENCES

- 1- Kuhn, H. A., and Lawley, A., Powder Metallurgy Processing, Academic Press, New York, U.S.A, 1978.
- 2- Beddow, J. K., Atomization, Heyden and Son. Ltd, London U.K, 1978.
- 3- Balke, C. C., Kents Mechanical Engineers Handbook, Wiley Engineering Handbook Series, New York, 1950, Section 19, pp.45-50.
- 4- Stevenson, R. W. "Cemented Carbides", Metals Handbook, Vol.7, Powder Metallurgy, 9th Edition, ASM, OHIO, U.S.A, pp.773-783.
- 5- Goetzel, C. G., "Cermets", ibid, pp 798-815.
- 6- Nadkarni, A. V., and Woodruff, J. R., "Electrical and Magnetic Applications", ibid, pp.624-645.
- 7- Snyder, J. J., "P/M Porous Parts", ibid, pp.696-700.
- 8- Arnold, N. A., "P/M Bearings", ibid, pp.704-709.
- 9- Ozsever, S., "P/M Friction Materials", ibid, pp.701-703.
- 10- Saritas. S., "Celik Toz Dovmecilik", ODTU Uygulamali Arastirmalar Dergisi, Vol.3, No.11, Ankara, 1985, pp.1-26.
- 11- Silbereisen, H., "Sintering and Economical Process for the Manufacture of Metallic Precision Parts, Proc. of Con., Non Machining Production Methods", VDI Education Centre, W. Germany, 1988.
- 12- Johnson, P. K., and Roll, K. H., "State of the P/M Industry and a Marketing Plan for the '80", Int. J. P/M and Tech., Vol.19, No.4, 1983.

- 13- Eloff, P. C., and Wilcox. L. E., "Fatigue Behaviour of Hot Formed Differential Pinion Gears, Mod. Dev. in P/M, Vol.7, 1973, pp.213-234.
- 14- Tsumuki, C., "Connecting Rods by P/M Hot Forging", *ibid*, pp.365-391.
- 15- Moyer, K. H., "The Effect of Preform Density on the Impact Properties of Atomized Iron P/M Forgings", *ibid*, pp.53-63.
- 16- Ishimaru, Y., Safto, Y. and Nishio, Y., "On the Properties of Ferrous Alloys", *ibid*, pp.441-449.
- 17- Kawakita, T., Onda, M., Kuroishi, N. and Iwaki, I., "Properties of Forged Super-high Density Sintered Steel", *ibid*, Vol.6, pp.349-356.
- 18- Pietrocim, T. W., and Gustatson, D. A., "Fatigue and Toughness of Hot Forged Cr-Ni-Mo and Ni-Mo Prealloyed Steel Powders", *ibid*, Vol.4, pp.431-439.
- 19- Brown, G. T., "Powder Metallurgy, Promises and Problems", 4th Eur. Symp. on P/M, Proc of Soc. Francais de Met., Paris, pp.96. 1975.
- 20- Bockstigel, G and Blande, C.A., "The Influence of Slag Inclusions and Pores on *ibid*, pp.21-42.
- 21- Bown, G. T., and Steel, J. A., "The Fatigue Performance of Some Connecting Rods Made by Powder Forging", P/M, Vol.16, No.32, pp.405-415. 1973.
- 22- Brown, G. T., and Steed, J. A., "A Comparision of the Mechanical Properties of Some Powder-forged and Wrought Steels", P/M, Nol.17, No.33, pp.157-177.
- 23- Hayness, R., P/M, Vol.13. No.26, pp.465-507. 1974.

- 24- Saritas, S., James, W. B, and Davies, T. J., "Influence of Preforging Treatments on Mechanical Properties of two Low Alloy Powder Forged Steels", P/M, No.3, pp.131-140. 1981.
- 25- Saritas, S., Usmani, F. H., and Davies, T. J., "Fatigue of Surface Treated Powder Forged Steels", Proc. of Heat Treatment '81, The Metal Society, London, U.K., pp.147-157. 1981.
- 26- Irmann. R., "Sintered Aluminum Temperatures", Metallurgia, pp.125-133. 1952.
- 27- Lyle, J. P. and Cebullah, W. S., "Fabrication of High Strength Aluminum Products From Powder", Powder Metallurgy For High-Performance Applications, Syracuse, U.S.A., pp.231-254. 1972.
- 28- Froes, F. H., Eylon, D., Wirth, G., and Smarsly, W., "Fatigue Properties of Hot Isostatically Pressed Ti-6AL-4V powders", Metal Powder Report, Vol.38, No.1, 1983, pp.36-41.
- 29- James, W. B., "Overview of High Density P/M Forming Process", Int. Con. Powder Metallurgy '84, Toronto, Canada, 1984.
- 30- Upadhyaya, G. S., "Powder Metallurgy in India", P/M Int., Vol.38, pp.223, 224, 1986.
- 31- Metals Handbook, 9th Ed. Vol.7, Powder Metallurgy, ASM, OHIO, U.S.A., 1984.
- 32- Klar, E., "Chemical Methods of Powder Production", *ibid*, pp.52-55.
- 33- Taubenblat, P. W., "Electrodeposition of Metal Powders" *ibid*, pp.71-77.
- 34- Singer, A. R. E., and Roche, A.D., "Roller Atomization of Molten Metals for the Production of Powders", Mod. Dev. in P/M, Vol.9, pp.127-140. 1976.

- 35- U.K. Patent 1 389 750, 1972.
- 36- Germany Patent. 30 19 047, 1980.
- 37- Beiss, P., "P/M Methods for Production of High Speed Steels", Metal Powder Report, Vol.38, No.4, pp. 185-194, 1984.
- 38- Small, S. and Bruce, T. J., Int. J. P/M, Vol.4, No.7, 1968.
- 39- Gummeson, P. U., P/M for High Performance Applications (Burke and Weiss Ed.) Syracuse, U.S.A., pp.231-254, 1972.
- 40- Brewin, P. R., Walker, P.I., and Nurthen, P.D., "Production of High Alloy Powders by Water Atomization", Powder Metallurgy, Vol.29, No.4, pp.281-285.
- 41- U.S.A. Patent 3 309 733.
- 42- Dunkley, J. J., "The Production of Metal Powders by Water Atomization" P/M int., Vol.10, No.1, pp.38-41, 1978.
- 43- Dunkley, J. J., and Palmer, J.D., "Factors Affecting Particle Size of the Atomized Metal Powders", Powder Metallurgy, Vol.29, No.4, pp.287-290.
- 44- Gummeson, P. U., "Modern Atomization Techniques", Powder Metallurgy, Vol.15, No.29, pp.67-94.
- 45- Michalke, M., and Scholz, W., "Production of Alloyed and Non-alloyed Iron Powder by Atomization of Melt, Vol.11, pp.5-9, 1970.
- 46- Nichiporenko, O. S., "Deformation and Atomization of Drops of Metal in Spray Draying for Powder Production", Doklady AN SSSR, Vol.195, No.5, pp.1062, 1083, 1970.

- 47-Patterson, R. J., "Rotating Disc Atomization", Metals Handbook, 9'th Ed. Vol. 7, Powder Metallurgy, ASTM, OHIO, U.S.A., pp. 45-48, 1984.
- 48-Roberts, P. R., "Rotating Atomization Process", *ibid*, pp. 39-42.
- 49-Fox, C. W., "Vacuum Atomization", *ibid*, pp. 43-44.
- 50-U.S.A. Patent 3 510 546.
- 51-Mizutani, T., Uga, Y., and Nishimota, T., "Investigation of Ultrasonic Atomization, Bull. JSME, Vol. 15, No. 83, pp. 620, 1972.
- 52-Sheikhaliev, M., and Popel, S.I., "Production of Metal Powders by Ultrasonic Atomization of Melts", Translated From Poroshkovaya Metallurgiya, Vol. 10, No. 250, pp. 18-24, 1983.
- 53-Richardson, F.D., and Jeffes, J.H.E., "The Thermodynamic of Substances of Interest in Iron and Steelmaking from 0° to 2400°C", J. Iron and Steel Inst., Vol. 160, pp. 261, 1948.
- 54-Allen, T., Particle Size Analysis, Chapman and Hall, London, 1968.
- 55-Standard Test Methods for Metal Powders and Powder Metallurgy, Products, MPIF, Princeton, U.S.A., 1985.
- 56-Hausner, H. H., and Mal, M. K., "Handbook of Metal Powder Metallurgy, MPIF, Princeton, U.S.A, 1982.
- 57-Handbook of Metal Powders, Arnold, N. A., 1968.
- 58-Masters, K., "Spray Draying", 2'nd, Ed. John Wiley & Sons, New York, 1972.
- 59-Marshall, W. R., Chem. Eng. Prog. Monograph Series, No. 2, 50, 1954.

- 60- Kurabayasi, T., Japan. Soc. Mech. Eng. Bulletin, 3, No. 11, 352, 1960.
- 61- Adler, C. R., and Marshall, W.R., Chem. Eng. Prog., 47, 515, 601, 1951.
- 62- Bauer, H., and Kruger, R., Verfahrens Technik, 3, No. 3, 107, 1969.
- 63- Philipson, K., Aerosol Sci., 4, 51, 1973.
- 64- Frazer, R. P., Eisenklam, E. P., and Dombrowski, N., Brit. Chem. Eng., 2, No. 9, 196, 1957.
- 65- Lapple, C. E., Henry, J.P., Blake, D. E., Atomization- A Survey and Critique of the Literature, Stanford Research Inst., Menlopark, Calif., U.s.a., 1967.
- 66- Dombrowski, N., and Munday, G., Biochemical and Biological Eng. Science, Vol 2, Ed. Blekebrough, Chap. 16. 209, 1968.
- 67- Master, K., Straarup, O., Brit. Patent 1 331 708, 1973.
- 68- Bar, P., Doctorate Dissertaion Technical College, Karlsruhe, Germany 1935.
- 69- Walton, W. H., Prewett, W. C., Proc. Phys, Soc., 62B, 341,1949.
- 70- Hege, H., (a) Chemie-Ing.-Tech., 36, No. 1, 52 1964
- 71- Oyama, Y.,Endou, K., Chem. Eng. Tokyo, 17, 256, 275, 1953.
- 72- Friedman, S.j., Gluckert, F. R., and Marshall, W.R., Chem. Eng. Prog., 48, No.4, 181, 1952.
- 73- Rao, P., "Shape and Other Properties of Gas Atomized Metal Powders, Ph.D. Dissertation, Dept. Chem. Eng. Drexel University,

Philadelphia, Pennsylvania.

74-Rao, P., M. S. Thesis, Dept. Chem. Eng., Drexel University, Philadelphia, Pennsylvania

75-Grandzol, R. J., "Water Atomization of 4620 Steel and Other Metals, Ph.D. dissertation, Dept. Chem. Eng., Drexel Univ., Philadelphia, Pennsylvania.

76-Giffen, E., Muraszew, A., Atomization of Liquid Fuels, London: Chapman and Hall 1953.

77-Seltzer, R., and Marshall, W. R., Chem. Eng. Prog., 46, 10, 501, 1950.

78-Fischmeister, H. F., Orerskii, A. D., and Olsson, L., "Solidification Structure of Gas-atomized High Speed Steel Powders". Powder Metallurgy Group Meeting, 28, 1980.

T. C.
WIKSEKOGRETIEM KURUUM
Dokumentasyon Herkesi